

Dottorato di Ricerca in  
**MECCANICA E SCIENZE AVANZATE DELL'INGEGNERIA**

Curriculum 3 - Meccanica Applicata

Ciclo XXVII

SETTORE CONCORSUALE DI AFFERENZA  
09/A2 Meccanica Applicata alle Macchine

SETTORE SCIENTIFICO DISCIPLINARE  
ING-IND/13 Meccanica Applicata alle Macchine

**A NEW TEST RIG FOR IN-VITRO EVALUATION  
OF THE KNEE JOINT BEHAVIOUR**

TESI DI DOTTORATO DI  
Margherita Forlani

COORDINATORE  
Chiar.mo Prof. Ing. Vincenzo Parenti Castelli

RELATORE  
Chiar.mo Prof. Ing. Vincenzo Parenti Castelli



## ABSTRACT

The evaluation of the knee joint behavior is fundamental in many applications, such as joint modeling, prosthesis and orthosis design. In-vitro tests are important in order to analyse knee behavior when simulating various loading conditions and studying physiology of the joint.

A new test rig for in-vitro evaluation of the knee joint behavior is presented in this paper. It represents the evolution of a previously proposed rig, designed to overcome its principal limitations and to improve its performances. The design procedure and the adopted solution in order to satisfy the specifications are presented here.

Thanks to its 6-6 Gough-Stewart parallel manipulator loading system, the rig replicates general loading conditions, like daily actions or clinical tests, on the specimen in a wide range of flexion angles. The restraining actions of knee muscles can be simulated when active actions are simulated. The joint motion in response to the applied loads, guided by passive articular structures and muscles, is permitted by the characteristics of the loading system which is force controlled. The new test rig guarantees visibility so that motion can be measured by an optoelectronic system. Furthermore, the control system of the new test rig allows the estimation of the contribution of the principal leg muscles in guaranteeing the equilibrium of the joint by the system for muscle simulation. Accuracy in positioning is guaranteed by the designed tibia and femur fixation systems, which allow unmounting and remounting the specimen in the same pose.

The test rig presented in this paper permits the analysis of the behavior of the knee joint and comparative analysis on the same specimen before and after surgery, in a way to assess the goodness of prostheses or surgical treatments.

**Keywords:** knee behavior, test rig, static analysis, dynamic analysis, human joint test, test rig design.



---

# INDEX

ABSTRACT .....	1
INDEX.....	3
CHAPTER 1. INTRODUCTION.....	7
CHAPTER 2. BACKGROUND .....	10
2.1 KNEE ANATOMY AND PHYSIOLOGY .....	10
2.1.1 TERMINOLOGY.....	11
2.1.2 ANATOMY .....	13
2.1.3 KNEE REFERENCE SYSTEM .....	26
2.1.4 KNEE MOTION.....	32
2.2 KNEE TESTS.....	34
2.2.1 UNLOADED MOTION TESTS .....	35
2.2.2 LOADED MOTION TESTS .....	35
2.2.3 SIMULATING MOTION OR MOVEMENT? .....	37
2.2.4 LOADS AND MOVEMENTS IN DYNAMIC TESTS .....	37
CHAPTER 3. OVERVIEW OF AVAILABLE TEST RIGS.....	42
3.1 KNEE SIMULATORS .....	42
3.1.1 OXFORD KNEE RIG.....	43
3.1.2 EVOLUTIONS OF OKR.....	44

---

3.1.3	PURDUE KNEE SIMULATOR: MARK II .....	48
3.2	ROBOT-BASED KNEE TESTING SYSTEMS .....	50
3.2.1	EARLIER MACHINES .....	51
3.2.2	SERIAL RIGS .....	52
3.2.3	DECOUPLED RIG.....	57
3.2.4	PARALLEL RIGS .....	58
3.3	TEST RIG BASED ON CABLE-DRIVEN LOADING SYSTEM .....	62
CHAPTER 4.	TECHNICAL SPECIFICATIONS OF THE NEW TEST RIG .....	67
4.1	RANGES OF MOTION AND LOADS .....	67
4.2	OTHER REQUIREMENTS .....	70
CHAPTER 5.	DESIGN OF THE NEW TEST RIG .....	71
5.1	OVERALL DESCRIPTION OF THE MACHINE STRUCTURE.....	71
5.2	TIBIA LOADING SYSTEM.....	72
5.2.1	DEFINITION OF THE ACTUATION SYSTEM.....	74
5.2.2	IDENTIFICATION OF THE BEST CONFIGURATION.....	79
5.2.3	CONTROL OF THE LOADING SYSTEM.....	119
5.3	FIXATION SYSTEMS.....	121
5.3.1	FEMUR FIXATION SYSTEM.....	121
5.3.2	TIBIA FIXATION SYSTEM .....	126
5.4	FLEXION ROTATION SYSTEM .....	129

---

---

5.4.1	ACTUATION OF THE PORTAL.....	130
5.5	MUSCLE SIMULATION.....	132
5.5.1	EXTENSOR MUSCLE SIMULATION.....	132
5.5.2	FLEXOR MUSCLE SIMULATION.....	135
5.5.3	MUSCLE CONTROL SYSTEM.....	136
CHAPTER 6.	DISCUSSIONS AND CONCLUSIONS.....	138
REFERENCES	.....	142
ANNEX 1.....	.....	147
ANNEX 2.....	.....	148
ANNEX 3.....	.....	150



# CHAPTER 1.

## INTRODUCTION

The evaluation of the kinetostatic and dynamic behavior of the human knee has attracted the attention of a great amount of researchers all around the world. Indeed, it is essential for the definition and validation of biomechanical models, for the design and assessment of prostheses and orthoses, and for the planning of surgical treatments and rehabilitation strategies [1,2]. Furthermore, the comparison between behaviors recorded on intact, damaged and subjected-to-implant joints are important to evaluate the goodness of some medical practices and/or devices [3,4,5]. Many tests to measure the response of the joint undergoing various loading conditions have been performed both in vivo and in vitro. In particular, in-vitro tests permit an accurate measurement of the motion pattern, but they require a complex system to replicate the external and muscular loads. Loading conditions, indeed, have to be measured in vivo firstly and then carefully reproduced on specimens during in-vitro tests by a dedicated rig. Similarly, muscular actions can be imposed or evaluated.

Several devices for in-vitro knee tests have been proposed in the last few decades to replicate the in-vivo loading conditions. According to their design philosophies, they can be grouped in Knee simulators (KS) [6] and robot-based knee testing systems (RKTS) [7]. The KS try to mimic the motion in a physiological way, by replicating the ankle and hip joints. Different levels of test accuracy can be reached with different versions of KS [6,8,9], but complex and flexion-dependent loading conditions can hardly be applied. Conversely, RKTS appear less physiological, since they completely block one bone of the joint and apply motion (loads) to the other one, and they measure loads (motion) at the same time. They are based on serial [3,10] or parallel [11,12] architectures. Main limitations of the RKTS are the impossibility to reach high angles of flexion/extension of the knee and the difficulty in replicating the flexion-dependent loading history typical of the principal daily activities.

Aside from this classification, a test rig was developed by the author's research group in the last years [13] which foresees the movement of the knee as the result of two combined actions: i) the rotation of the femur about a fixed axis, and ii) the movement of the tibia due to applied loads. This test rig is capable to apply to the joint a load variable as function of the flexion angle. Some in vitro tests were performed with the test rig. Albeit good results have been obtained, some limitation have been identified especially regarding to the loading system and the range of knee flexion.

The purpose of this research is the development and design of a new test rig able to realize in-vitro tests of the knee kinematics and dynamics, overcoming the principal limitation presented by the available machines. The purpose of the new rig is to apply loads and measure the knee motion. In particular, the rig, must be able to apply loading conditions that simulate typical daily actions, like walking, squat and sit-to-stand, i.e. loading conditions that are variable with the kind of task and are functions of the knee flexion angle. While applying loads, the rig must guarantee six degrees of freedom (six DOF) to the knee, i.e. six DOF to the relative motion between tibia and femur. Furthermore, the rig must guarantee the simulation of the muscular actions.

In this work, the result of the study and the design process of the new rig dedicated to in-vitro knee tests is presented. The first key feature of the machine is the possibility to impose the flexion angle by rotating the femur about an axis fixed to the frame, while the tibia is left free to move in the six DOF. Loads simulating the daily activities are applied to the tibia, by a 6-6 Gough-Stewart platform actuated by stepper motors and ballscrews. Extensor muscle forces are simulated via a cable connected to a electromechanical actuator via a system of pulleys. Flexor muscle forces are simulated by imposing an equivalent system of forces via the tibia loading system. The control system allows the estimation of forces that muscles have to exert in order to equilibrate the applied loads simulating daily activities.

The knee principal anatomical and physiological characteristics are reported in Chapter 2, as their analysis has been a fundamental step in order to correctly identify the specification of the rig. A deep literature review on rigs developed by other research groups has been performed in order to understand the principal strengths and

limitations of these machines and is reported in Chapter 3. The new rig technical requirements are listed and discussed in Chapter 4. The functional analysis and adopted design solutions are presented in Chapter 5. In particular, after an overall description of the rig, each functional group is presented in detail. A wide part of Chapter 5 is dedicated to the loading system, which is the core of the machine and was designed by means of an iterative procedure made up of several steps. Finally, the result of the design is discussed in Chapter 6, and its strengths and weaknesses are highlighted.

A comment on Chapter 5 is in order. Each section is dedicated to the design of a functional group. The choice of analysing each functional group appears natural when the purpose is to explain how each singular group is designed with a specific purpose, i.e. to meet a certain technical requirement. Nevertheless, it is worth noting that many interconnections among the functional groups are present, since each group is often involved in satisfying also other specification than the one it is design for. Thus, in Chapter 5 many connections are underlined between the sections, in order to understand the overall way of operation of the rig.

## CHAPTER 2.

# BACKGROUND

### 2.1 KNEE ANATOMY AND PHISIOLOGY

The knee is the intermediate joint of the lower limb which allows the end of the limb to be moved towards or away from its root or, in other words, allows the distance between the trunk and the ground to be varied [13]. This joint allows the thigh to change his relative position to the leg.

The principal movement allowed by the knee is the so-called flexion, but it also allows smaller movement along and about other directions.

From the mechanical point of view the knee is a compromise which sets out to reconcile two mutually exclusive requirements:

- i) to have great stability in complete extension, when the knee is subjected to severe stresses resulting from the body weight and the length of the lever arms involved;
- ii) to have great mobility after a certain measure of flexion has been achieved, essential for completing active tasks like running.

In this section a complete description of the human knee will be furnished. First of all, the anatomical reference systems and the biomechanical terminology will be introduced. Then, the structures that guarantee the mobility and stability of the joint will be analysed under both the anatomical and physiological points of view. Indeed, the study of their behavior, or the comparison of their behavior with that of prostheses, is the main purpose of the designed machine test. A full understanding of the knee physiology is essential to define the specification of the rig.

### 2.1.1 TERMINOLOGY

To allow the description of the human knee and its movement, a reference system needs to be defined and some terminology needs to be known. Some general definitions are provided in the following, which allow describing the structures composing the joint. After that, a proper convention to describe motion, based on the anatomical characteristics of the joint bones, is presented.

Given the large number of DOF possessed by the human body, the first definition that ought to be provided is that of a reference position. This is known as anatomical position (Figure 2.1) and is that with the body erect, with the upper limbs at the sides, the head, eyes and hand palms facing forward, i.e. in the direction of progression (anterior), the lower limbs fully extended, and the feet together and in complete contact with the soil [14].

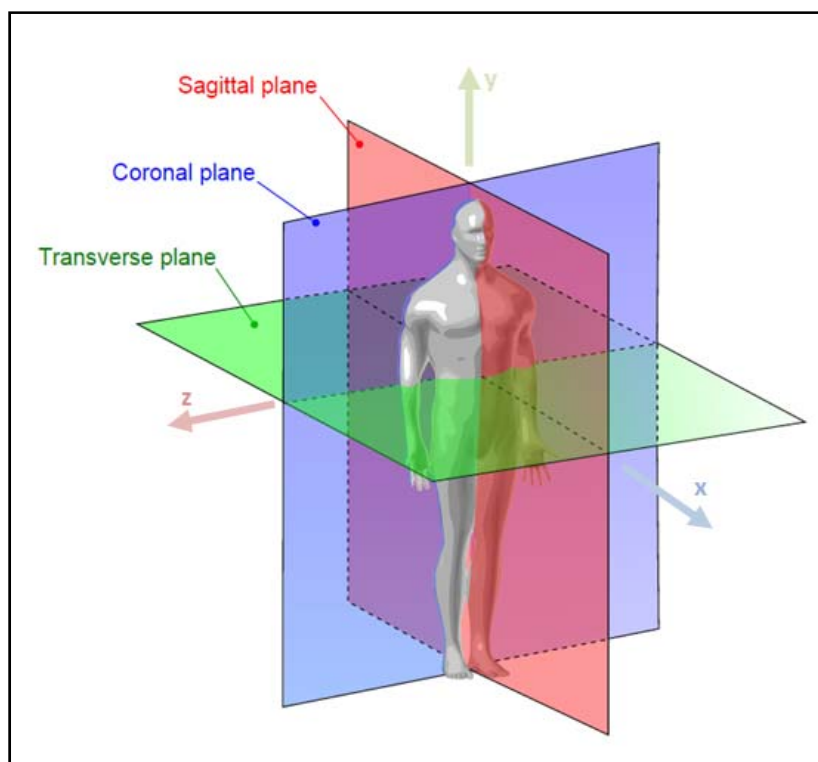


Figure 2.1 Relevant terminology used in anatomy: principal axis and planes.

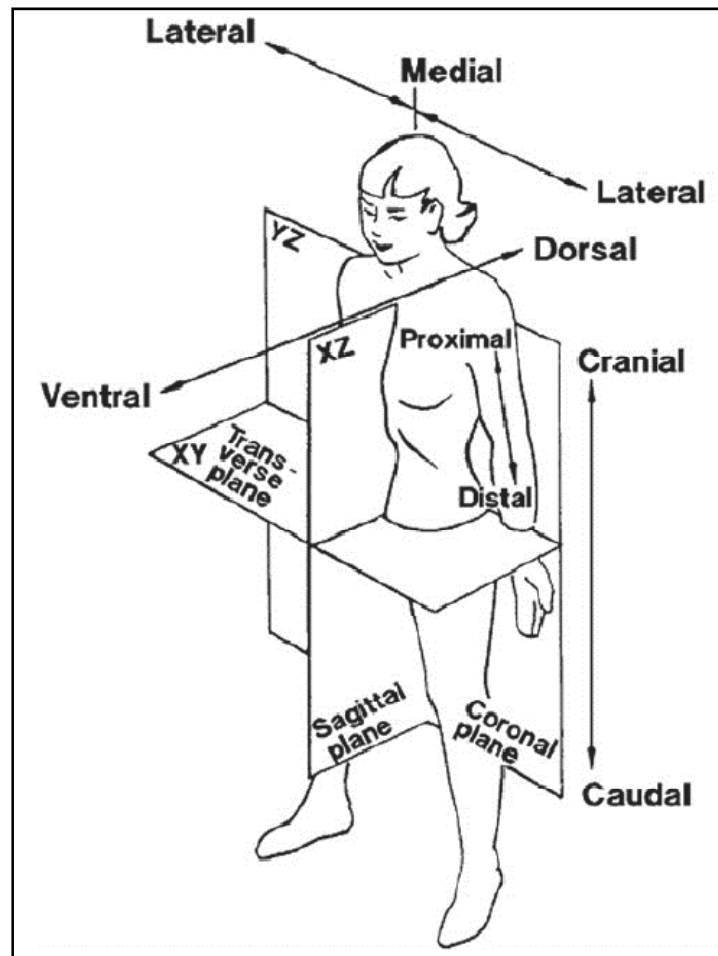


Figure 2.2 Relevant terminology used in anatomy: principal planes.

In addition, three Cartesian axes are usually defined in anatomy [14] (Figure 2.1):

- y-axis, generally vertical (parallel to the field of gravity) and pointing upwards;
- z-axis, perpendicular to the y-axis and pointing in the right direction;
- x-axis, perpendicular to both the y and z axes and pointing in the anterior direction.

These axes, in turn, allow for the definition of three anatomical planes [14](Figure 2.1):

- transverse or horizontal (axial) plane, perpendicular to the y-axis;
- sagittal or medial plane, perpendicular to the z-axis and parallel to gravity; it divides the body in its right and left parts;
- coronal or frontal plane, perpendicular to both the planes above.

Finally, the following terminology is used in order to refer the relative position of two different body parts, namely A and B (Figure 2.2) [15]:

- proximal (distal), when part A is closer to (farther from) part B's centroid;
- medial (lateral), when part A is closer to (farther from) part B's sagittal plane;
- superior (inferior), when part A is above (below) part B;
- anterior (posterior), when part A is in front of (behind) part B.

## 2.1.2 ANATOMY

### 2.1.2.1 BONES AND ARTICULAR STRUCTURES

The knee joint connects and permit motion between two body segments: the thigh and the shank. It involves mainly three bones: femur, tibia and patella. In addition, the fibula articulates with the tibia which is important since it hosts the insertion of some ligaments.

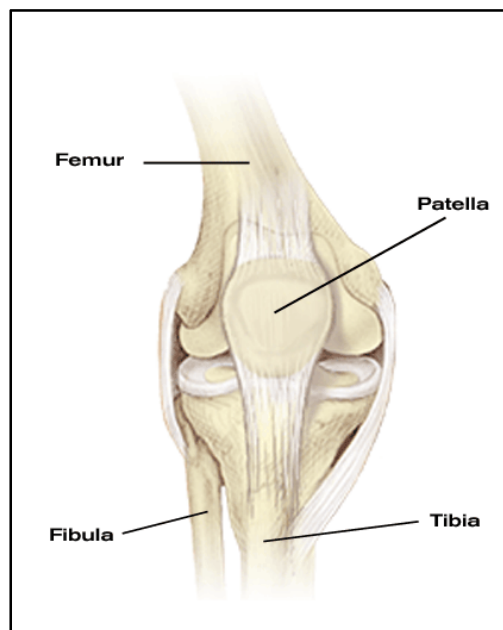


*Figure 2.3 Bones constituting the knee.*

Femur, tibia and fibula are long bones, while patella is a sesamoid bone. The main articulation of the knee happens between the distal surface of the femur and the proximal surface of the tibia. Furthermore, the posterior surface of the patella articulates with the distal anterior surface of the femur.

The most visible movement of the knee is the relative rotation about a medio-lateral axis of the tibia with respect to the femur. This rotation is associated with other movements with a smaller range.

### THE FEMUR

The femur is the longest and heaviest bone in the body, its length varies from one fourth to one third of that of the body [16]. When a subject is in the standing position, the femur transmits weight from the hip bone to the tibia located at its extremities.

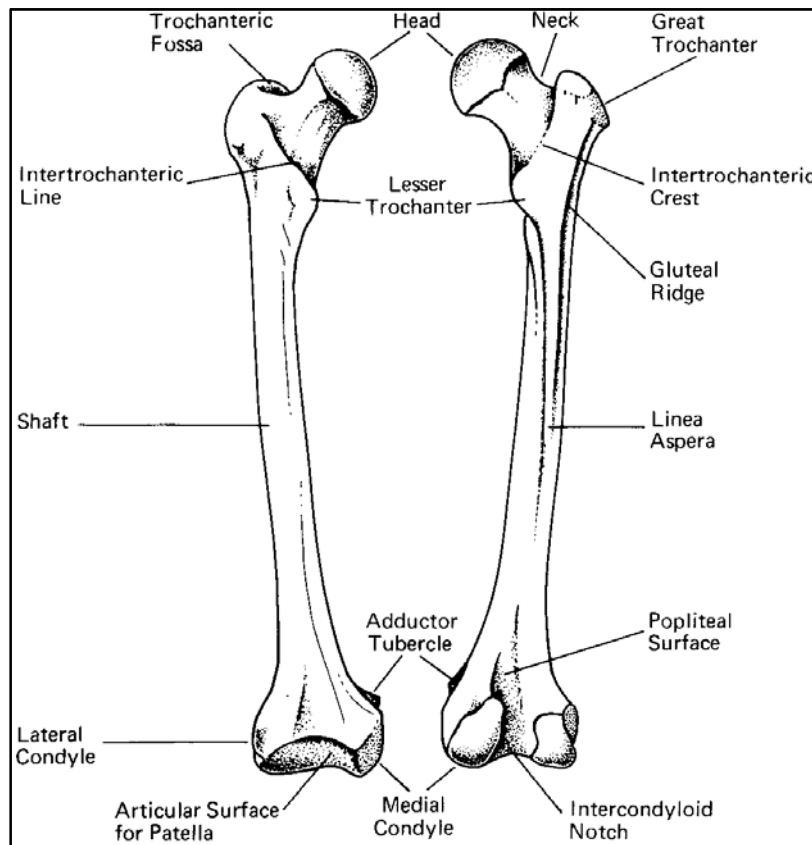


*Figure 2.4 Anterior and posterior views of a right femur.*

The superior extremity of the femur consists of a head, a neck, and two trochanters (Figure 2.4). The inferior end consists of two condyles. The shaft of the femur connects superior and inferior parts of the bone.

The head of femur faces superiorly, medially and slightly anteriorly and it articulates with the acetabulum in order to generate the hip joint. The femoral neck develops laterally and distally, ending in the trochanters. The plane of the neck, followed medially, usually lies anterior to that of the femoral condyles (anteroversion of femoral head), and the two planes form an angle of about  $15^\circ$  [16].

The shaft of the femur, which is convex anteriorly, presents anterior, medial and lateral surfaces. Despite its geometrical complexity, in the present work it will be considered as a cylinder of diameter coinciding with that of its central region. A reference value of 26 mm, obtained from the literature [17], will be assumed for such quantity.

Finally, the two condyles are convex and, at first instance, it is possible to say that they represent two segments of a pulley, in both their inferior and anterior parts, since they articulate both with tibia and patella. Condyles are convex both in anteroposterior and transverse planes. Medial and lateral condyles are not strictly identical: their long (i.e. anteroposterior) axes converge anteriorly and diverge posteriorly, as shown in Figure 2.5. In addition, the medial condyle is narrower and juts out more than the lateral condyle. The curvature radius is not constant for each of the condyles. In the sagittal plane, it increases postero-anteriorly until a certain point (point *t* in Figure 2.6) and then decreases to form the articular surface with patella. The position of the centre of curvature is not constant, but changes together with the change of radius. The two condyles are continuous anteriorly but separated inferiorly and posteriorly by the intercondylar fossa (Figure 2.5).

On their anterior aspects, the condyles form the patellar surface, which comprises a wider lateral and a narrower medial part; this articulates with corresponding facets on the patella. The most prominent part of the medial condyle is the medial epicondyle; similarly, the lateral condyle presents the lateral epicondyle, near which are the origins of the lateral head of the gastrocnemius and the popliteus.

---

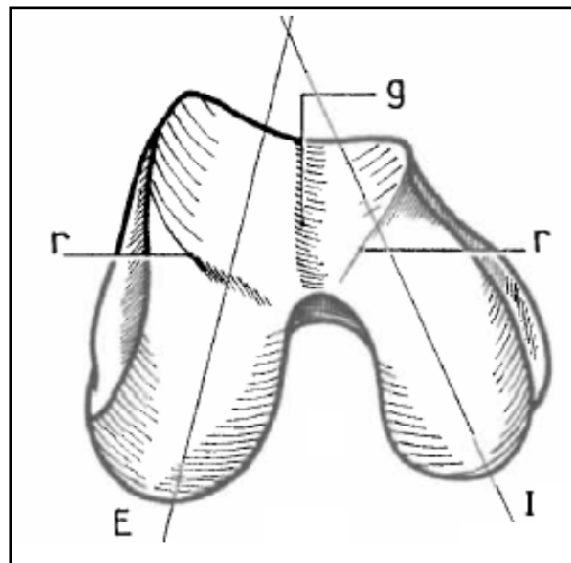


Figure 2.5 Coronal view of the knee: the direction of the two condyles converge anteriorly [13].

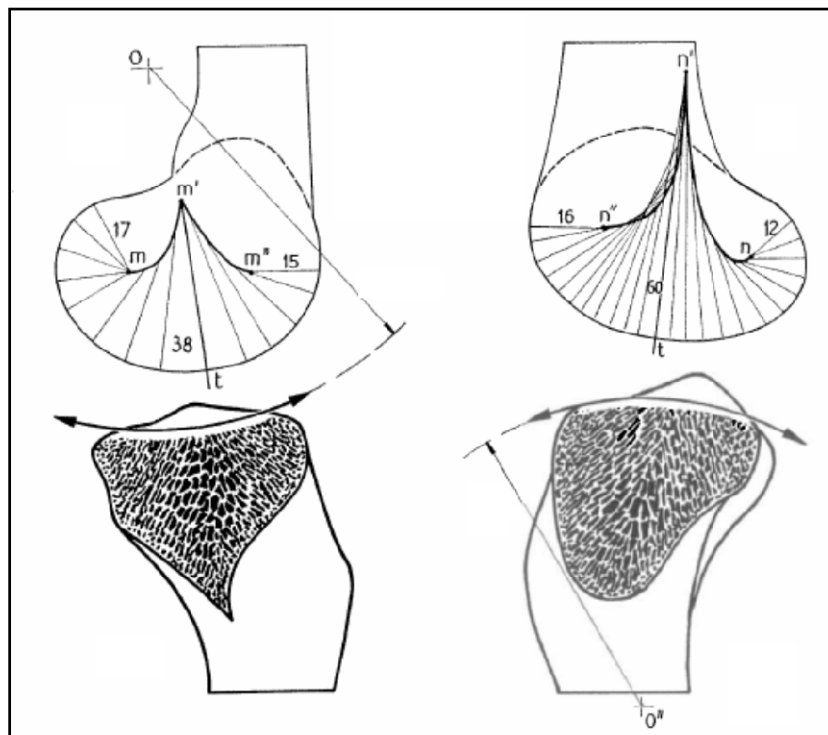


Figure 2.6 View of the medial (left side) and lateral (right side) condyles: the variable radius of curvature is represented [13].

## THE TIBIA

The tibia measures about one fourth to one fifth of the length of the body [15] and, when a subject is in the standing position, it transmits the weight from the femur to the foot, to which is connected via the ankle joint.

The superior end of the tibia is expanded for articulation with the inferior end of the femur so as to form a plateau (Figure 2.7). The inferior part of the tibia is expanded for articulation with the talus and the fibula at the ankle joint. Proximal and distal extremities are connected by the shaft of the tibia.

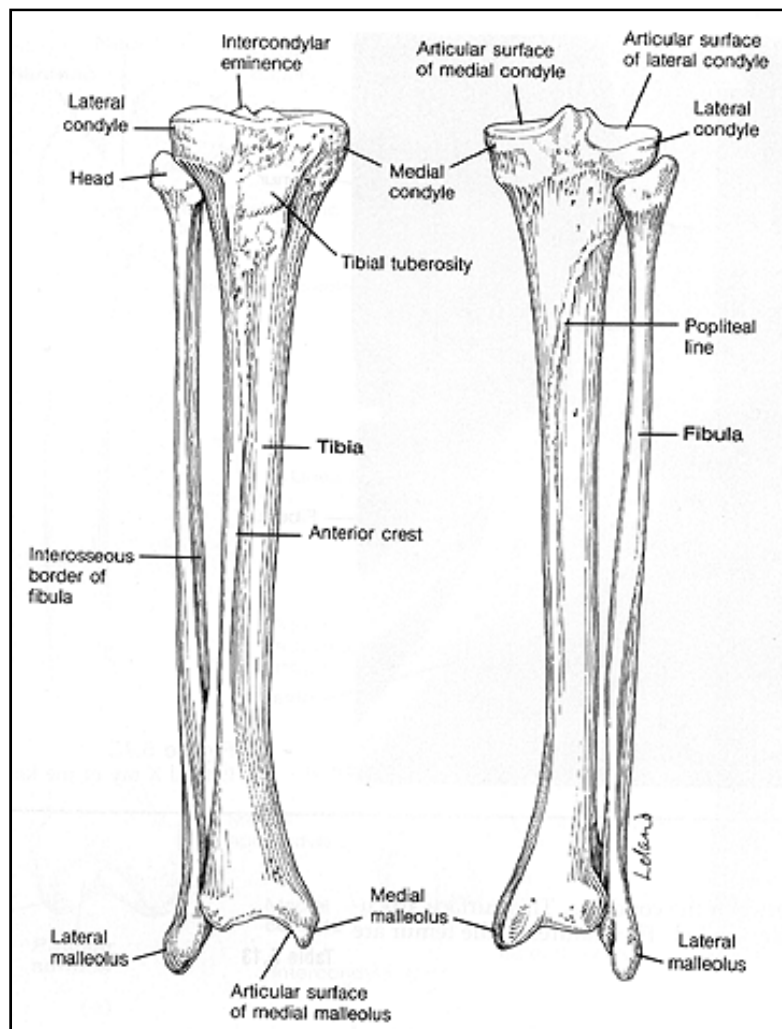
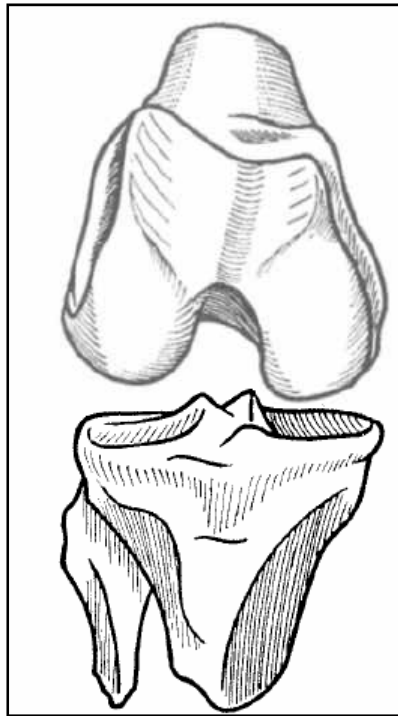


Figure 2.7 Anterior and posterior views of a right tibia and fibula.



*Figure 2.8 Anterior view of the tibia articulating with the femur [13].*

The superior plateau consists of medial and lateral condyles, and a tuberosity is found anteriorly at the junction with the shaft (Figure 2.8). The superior end of each condyle articulates with the corresponding femoral condyle; the inferior aspects of the lateral condyle presents posteriorly a circular facet for the head of the fibula.

The two condyles of the tibial plateau articulates with the condyles of the femur described above. The radii of curvature are different and the surfaces are not congruent (Figure 2.6). They are separated by a blunt eminence running anteroposteriorly, which is lower at the extremities and presents a higher middle part that is coupled with the femoral notch and behaves as a pivot. The condyles are both concave in the frontal plane but they appear very different if their anteroposterior profile is examined: the medial condyle is concave superiorly, while the lateral condyle is convex. As a result, more stability is registered at the medial condyle, while the lateral one is unstable and the stability depends more on the ligaments.

The inferior end of the tibia presents an anterior surface, a lateral surface ending in the fibular notch (allowing articulation with the lower end of the fibula), a posterior surface grooved by the tibialis posterior and flexor digitorum longus tendons, a medial surface running onto the distal prolongation of the tibia (medial malleolus), and an inferior surface which articulates with the talus. Note that the talus also articulates with the lateral surface of the medial malleolus. Values reported in the literature for the distance between the tips of the two malleoli are about 62 mm in males and 53 mm in females [17]. It should also be noted that the line connecting the two tips forms an angle of about  $10^\circ$  in both genders with the horizontal direction [17].

When viewed superiorly, the shaft of the tibia appears twisted, as if the upper end were rotated more medially than the lower [15]. The angle of tibial torsion (usually  $15\text{-}20^\circ$ ) is that between a horizontal line through the condyles and one through the malleoli. The shaft of the tibia has medial, lateral, and posterior surfaces that are separated from one another by interior, interosseous, and medial borders. A view of the unregular cross section of a left tibia is depicted in Figure 2.9.

A study on the relation between stress fractures and the tibial bone width [19] reports approximately equal medio-lateral and antero-posterior widths at about 8 cm above the ankle joint in the subjects considered for the study; the measured width is of 26.9 mm.

## FIBULA

The fibula is the slender, lateral bone of the leg and it does not bear weight [16]. It articulates with the tibia superiorly and with the talus inferiorly, and is anchored in between to the tibia by the interosseous membrane (Figure 2.7).

The superior end, or head, articulates with the posteroinferior aspect of the lateral condyle of the tibia; it is on the same level as the tuberosity of the tibia. The head is prolonged superiorly into an apex (styloid process) posterolaterally (Figure 2.7).

The shaft of the fibula has a roughly triangular cross section, although the surfaces and borders vary considerably.

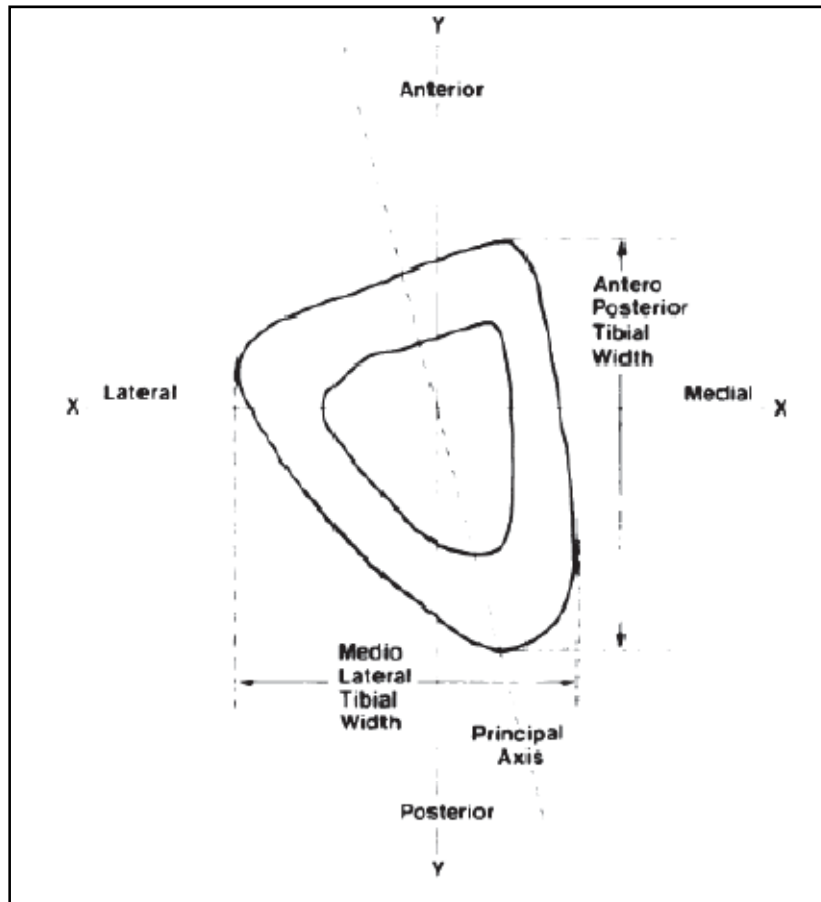


Figure 2.9 Cross section of the human tibia: irregular shape can be noted [19].

The inferior end of the fibula, or the lateral malleolus, is more prominent, more posterior and extends about 1 cm more distally than the medial malleolus [15]. It articulates with the tibia and with the lateral surface of the talus; the talus fits between the two malleoli. Posteromedially, a malleolar fossa gives attachment to ligaments; posteriorly, a groove on the lateral malleolus is occupied by the peroneal tendons.

## PATELLA

The patella is a triangular sesamoid bone embedded in the tendon of insertion of the quadriceps femoris muscle (Figure 2.3). The superior border of this bone is the base of the triangle, and the lateral and medial borders descend to converge at the apex. The patella can be moved from side to side when the quadriceps is relaxed; a part of the

quadriceps tendon covers the anterior surface of the bone and is continued, as part of the patellar ligament, to the tuberosity of the tibia. The patella articulates on its posterior side with the patellar surface on the condyles of the femur. The articular surface of the patella comprises a larger, lateral facet and a smaller, medial one [16].

### 2.1.2.2 LIGAMENTS

To help providing the stability of the knee joint, it is contained in the joint capsule and equipped with ligaments. The shape, length, orientation and properties of the knee ligaments affect the joint kinematics. The purpose of the present section is to review the knee ligaments having a crucial role in knee motion; thus only some of the knee ligaments will be considered here. In particular, two groups of ligaments will be described in the following: the cruciate and the collateral ligaments. The former, namely the anterior and the posterior cruciate ligaments (ACL and PCL, respectively) are interwoven and are located in the center of the knee joint while the latter, namely the medial and lateral collateral ligaments (MCL and LCL, respectively) are parallel to each other and are attached to the medial and lateral sides of the knee (Figure 2.10).

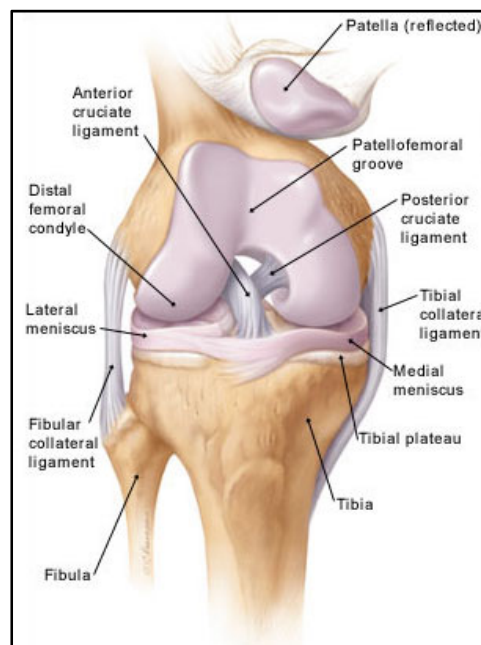


*Figure 2.10 Knee passive structures.*

## THE CRUCIATE LIGAMENTS

The cruciate ligaments account for a considerable amount of overall knee stability. They lie in the centre of the joint, contained in the intercondylar notch. They take their name from the fact that they cross each other somewhat like the lines of the letter "X", and have received the names of anterior and posterior from the position of their attachments to the tibia [13].

The ACL is an intracapsular and extrasynovial structure. It inserts medially in the anterior intercondylar fossa of the tibia and runs superiorly and posteriorly to the medial aspect of the lateral femoral condyle. The PCL is inserted in the posterior part of the posterior intercondylar fossa of the tibia and runs obliquely medially, anteriorly and superiorly to be inserted both in the intercondylar notch and on the medial condyle of the femur. The cruciate ligaments are the primary structures that act to constraint anteroposterior stability of the joint. In particular, the ACL constitutes a primary constraint of the anterior tibia translation. The PCL acts as a drag during the gliding phase of motion and resists posterior translation of the tibia. In addition, the PCL it prevents hyperextension of the knee and prevents the femur from sliding forward during weight bearing.

Furthermore, the cruciate ligaments have a very important role in guiding the unloaded motion of the joint [2].

## THE COLLATERAL LIGAMENTS

The collateral ligaments strengthen the knee in its medial and collateral aspects. They are therefore responsible for the transverse stability of the knee during extension. Medial and lateral collateral ligaments run in vertical direction from the femur to the tibia and fibula on medial and lateral side respectively.

The MCL arises from the medial femoral condyle and extends inferiorly to insert on the tibia about 2.5 cm below the joint line [19]. The MCL provides primary valgum stability to the knee joint and is intimately adherent to the medial meniscus. The LCL origins from the outer surface of the lateral condyle and inserts below to the lateral side of the

head of the fibula. The LCL provides lateral stability to the knee against varu and external rotation forces, and it has no attachment to the lateral meniscus.

Both ligaments become taut during extension and slackened during flexion [13], so their restraining role is exerted mainly when the knee is extended.

#### THE PATELLAR LIGAMENT

In addition to the four ligaments considered above, the central portion of the quadriceps tendon is usually referred to as patellar ligament, thus making a fifth ligament participating in knee motion. Such ligament originates on the apex and adjoins margins of the patella and the rough depression on its posterior surface, while it is connected to the tuberosity of the tibia below; its superficial fibers are continuous over the front of the patella with those of the tendon of the quadriceps femoris.

The patellar ligament is strong, flat and its length is about 8 cm [19]. Its importance for knee functioning is clearly related to the action of the quadriceps femoris.

### 2.1.2.3 MUSCLES

After describing the passive structures, i.e. the bones with their articular surfaces and the most important ligaments, which stabilise the joint and guide the tibio-femoral motion, attention is now moved on the muscles that allow for knee movement during physiological activities.

A high number of muscles can be observed in the human leg (Figure 2.11); a thorough description should then analyse separately those in the thigh and those in the leg, and classify them according to their anatomical position (anterior, medial and posterior muscles in the thigh, and anterior, lateral and posterior in the leg). However, the intent of this section is only to present the most outstanding muscles involved in knee flexion during normal daily activities.

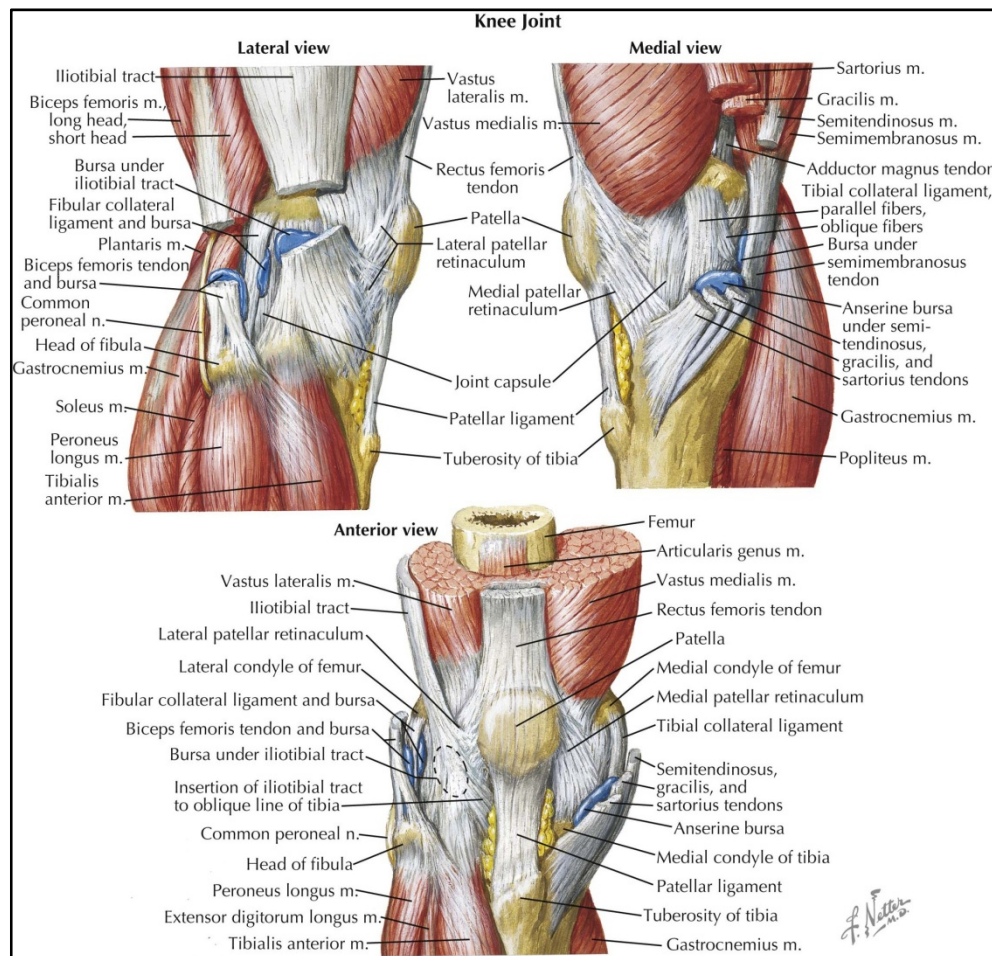


Figure 2.11 Muscles of the human leg [21].

## THE EXTENSOR MUSCLES OF THE KNEE

The quadriceps femoris is the principal extensor muscle of the knee. It lies in the anterior part of the thigh, together with iliopsoas and the sartorius. When the knee is flexed (even a small flexion angles) it counteracts gravity, thus it is very strong: it can exert a force superior to 1,5 bodyweight. The quadriceps, as indicated by its name, consists of four muscle bellies, which are inserted by a common tendon on the anterior tibial tuberosity. Three out of the four muscles, namely the vastus intermedius, the vastus medialis and the vastus lateralis are monoarticular, are monoarticular, while one, namely the rectus femoris, is monoarticular.

The four muscles converge in the extensor tendon which embeds patella and inserts in the tibial tuberosity anteriorly. The presence of the patella increases the effect of the quadriceps, since it increases the distance between the principal axis of rotation of the knee and line of action of the force exerted by quadriceps. Thus the presence of the patella generates a longer arm, that allows obtaining a higher moment with the same force, than the one that would be obtained without the patella.

While the three monoarticular muscles contribute only to knee extension, the rectus femoris is also responsible for hip flexion, i.e. the movement of bringing the anterior part of the hip close to the trunk. Usually, the vastus medialis is a bit stronger than the vastus lateralis, thus preventing the lateral dislocation of the patella. Anyway, the resultant force of the quadriceps is directed along the axis of the femur.

#### THE FLEXOR MUSCLES OF THE KNEE

The principal flexor muscles of the knee are positioned in the posterior part of the thigh. They are the hamstring (namely the bicept femoris, semitendinosus and semimembranosus), the three muscles inserted in the medial aspect of the tibia (namely the gracilis, sartorius and semitendinosus) and the popliteus.

All these muscles are biarticular, except for the monoarticular bicept femoris and the popliteus, so they act on knee flexion and hip extension.

In particular, the hamstring are those that furnish the higher contribution to flexion. Their efficiency strongly depend on the position of the hip. When the hip is flexed, they undergo a stretch, thus their efficiency as knee flexor increases. When the hip is fully extended, they show a relative lengthening, loosing some of their efficiency. In this conditions, the monoarticular muscles have a more relevant role on knee flexion, since the position of the hip does not influence their efficiency.

In addition to the muscle lying in the posterior part of the thigh, muscles in the posterior part of the shank help in flexion: they are the gastrocnemius and the soleus. The gastrocnemius is more superficial while the soleus is more deep. Their tendon originate in the posterior part of the femoral condyle and converge in the calcaneal tendon which

inserts into the back and inferior surface of the calcaneus. Thus they are biarticular muscles. According to some authors [13], their primary role is in plantar flexion, but they also contribute to the knee stabilization, as antagonist muscles of the quadriceps. Furthermore, they participate in knee flexion during locomotion.

### *2.1.3 KNEE REFERENCE SYSTEM*

Once defined the anatomy of the joint and before describing its motion, it is necessary to define a system to quantify the motion parameters, i.e. define the relative position between two bodies of the knee at different instants. The most commonly used in biomechanics is the joint coordinate system proposed by Grood and Suntay (G&S) in 1983[22], and applied at the knee joint. This system allows the description of the pose of one bone of the joint with respect to the other through six parameters (three rotations and three translations) that are independent on the order they are considered.

The definition of this joint coordinate system consists in three steps:

- i) The description of the shape of each body, with respect to a Cartesian reference frame fixed to the same body;
- ii) The definition of the three axes of the joint coordinate system (JCS), along which motion can be described independently from the order of rotations/translations;
- iii) The location of the translation reference point.

According to G&S proposed procedure[22], the three axes of the JCS are defined in a way that one is coincident with an axis of the femur, one is coincident with an axis of the tibia and the third one is the common perpendicular to the other two. With an accurate choice of the axes, the description of motion in terms of angles and displacements is very similar to that provided by clinicians.

With reference to the tibia, an interesting movement is the rotation of the tibia about its longitudinal axis, rotation that is almost null if the knee is fully extended but can noticeably increase if one of the knee is flexed. So one of the axes of the tibia reference system is chosen coincident with the longitudinal axis of the tibia, i.e. the axis that passes midway between the two intercondylar eminences proximally and through the

centre of the ankle distally. This axis is named as the  $z$ -axis of the tibia coordinate system  $S_t$ . The centre of the Cartesian coordinate system  $S_t$  is the midpoint between the centres of the tibial plateau. The tibial  $y$ -axis is the anterior axis of the tibia, which runs from the origin of the reference system. Its direction is defined as the cross product of the fixed axis with a line connecting the approximate center of each tibial plateau. The tibia  $x$ -axis is defined by completing the right hand coordinate system. It is positive to the right, so it is directed laterally for the right knee and medially for the left knee.

With reference to the femur, the interesting movement is the flexion/extension movement, i.e. the rotation about the mediolateral axis. The  $x$ -axis of the femur reference system  $S_f$  is chosen in a way to replicate this rotational axis. The femur frontal plane must be defined to identify the  $x$ -axis. This plane contains the femoral mechanical axis and is oriented so that the most posterior points of the two femoral condyles are equidistant from the plane. The femoral mechanical axis is defined as the axis that connects the center of the femoral head proximally with the point most distal point on the posterior surface of the femur, midway between the medial and lateral condyles. This axis is coincident with the  $z$ -axis of the femur. The  $x$ -axis is so defined as lying on this plane and being perpendicular to the femur mechanical axis. The  $y$ -axis is perpendicular to the frontal plane.

Once defined the two Cartesian reference system, the joint coordinate system is define by choosing two of their axes: one on the femur and one on the tibia. For physiological reasons, the  $x$ -axis is chosen on the femur reference frame, since it is directly connected to knee flexion/extension; this axis corresponds to the axis  $e_1$  of the JCS. For the same reasons, the  $z$ -axis is chosen on the tibia reference frame, since it is connected to the interesting internal/external rotation of the tibia, and represents the axis  $e_3$  of the JCS. The third axis,  $e_2$ , is defined as perpendicular to the two previously defined.

The relative joint rotations between bones are represented by the angles:

$\alpha$ : flexion (+) / extension (-) – rotation about  $e_1$

$\beta$ :  $\pi/2$ +adduction (+) /  $\pi/2$ -abduction (-) for the right knee – rotation about  $e_2$

$\gamma$ : external(+) / internal(-) rotation for the right knee – rotation about  $e_3$

Translations are presented as the components of a vector which is directed from femoral to tibial origin. The three components of position vector with respect to the base vectors  $e_1, e_2, e_3$  of the JCS are the three joint translations, independently from the sequence they are performed.

The three elements that represent the three translations along the JCS axes are defined as:

$q_1$ : medial-lateral tibial translation along  $e_1$

$q_2$ : anterior-posterior tibial translation along  $e_2$

$q_3$ : distraction-compression along  $e_3$

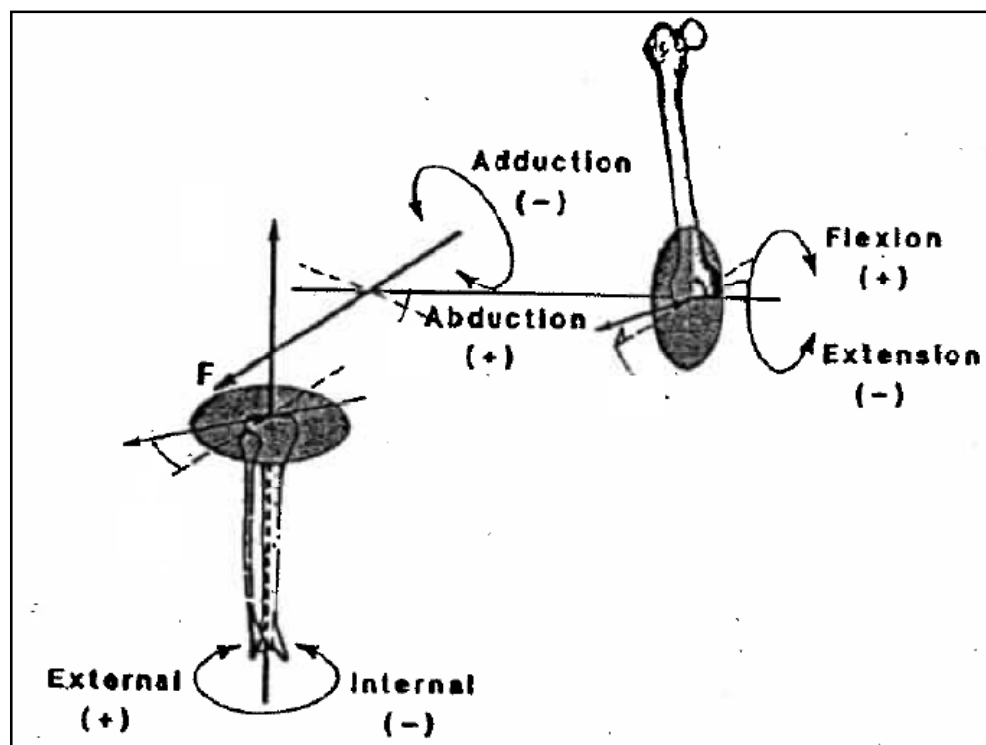


Figure 2.12 Grood and Suntay Joint Coordinate System [22].

## KNEE BONES RELATIVE POSITION

Once the single bone reference systems and the joint coordinate system have been defined, the motion of the joint can be accurately described using the parameters.

First of all, it is necessary to analyse the relative pose of the bones when they are at full extension, which is the reference position to describe motion. If considering the whole leg, i.e. thigh and shank together, the mechanical axis of the lower limb is defined in physiology as the axis that connects the centre of the femoral head (i.e.. the centre of the hip) with the centre of the knee and the centre of the ankle (midway between malleoli). This axis is not vertical in the frontal plane, but it reveals a mean inclination of  $3^\circ$ : it is directed medially if moving from the hip to the ankle, as shown in Figure 2.13 [13]. The inclination depends on the wideness of the hips, so strongly depends on anatomy and gender. This mechanical axis is roughly coincident with the longitudinal axis of the tibia, but not with the axis of the femoral shaft, since the femoral neck and head overhang the shaft itself. Thus, a further inclination of about  $6^\circ$  results between the femoral shaft and the leg longitudinal axis [13]. The angle between tibial and femoral axis, thus, varies between  $170$  and  $175^\circ$ .

If this angle increases until  $180$ - $185^\circ$ , i.e. the center of the knee moves laterally with respect to the mechanical axis of  $10$ - $20$  mm, pathological genu varum (commonly called bow-leggedness, Figure 2.14b), is diagnosed on a subject. If the angle decreases until  $165^\circ$ , i.e. the centre of the knee moves medially of  $10$ - $20$  mm, genu valgum (commonly called knock knee, Figure 2.14a) is diagnosed.

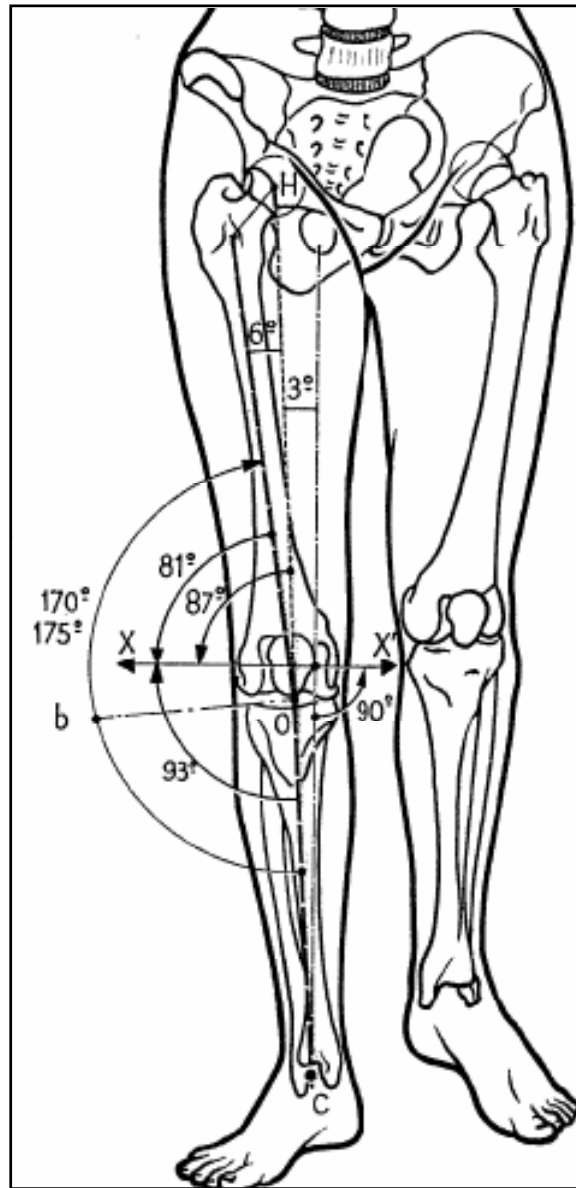


Figure 2.13 Position of the bones at knee reference position [13].

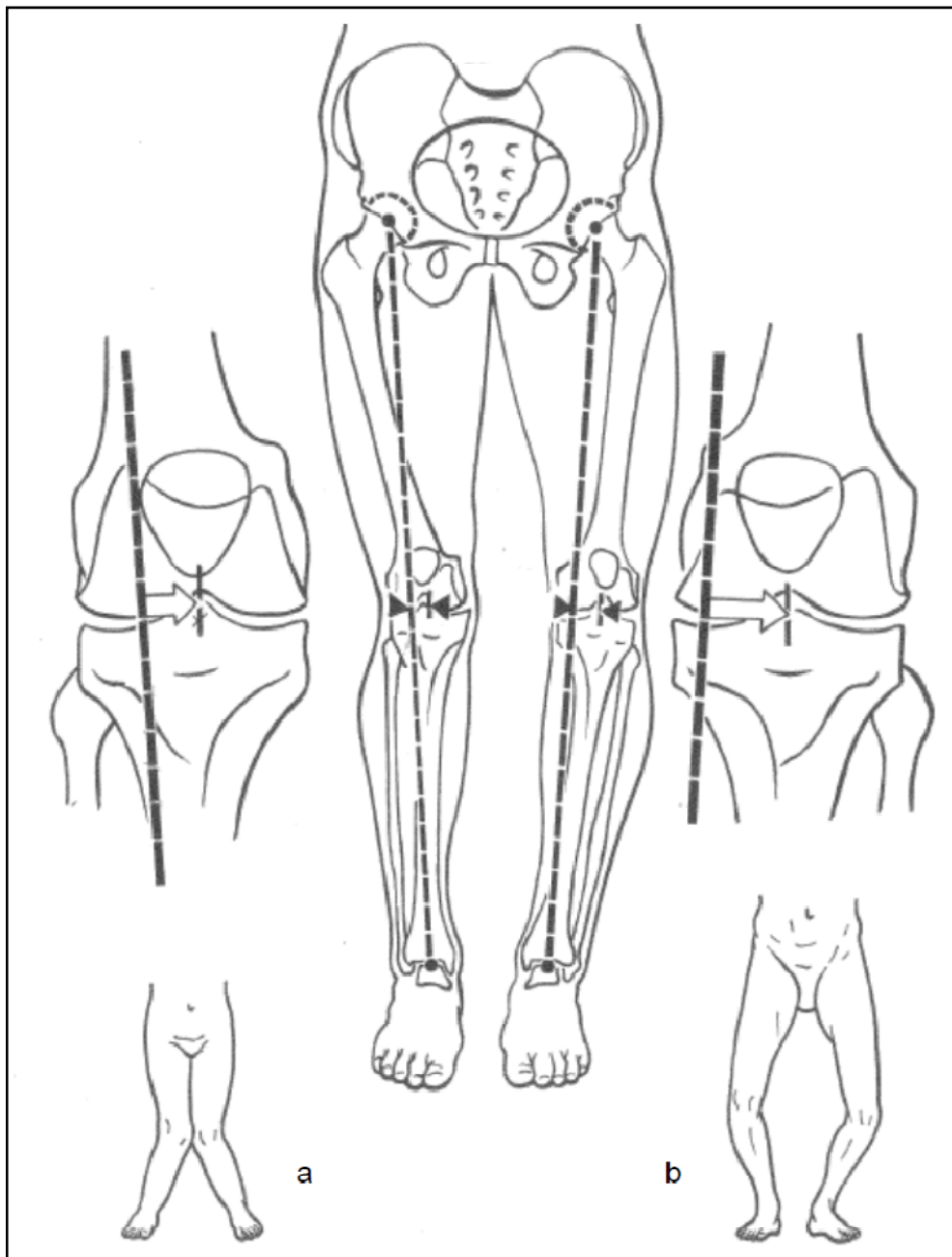


Figure 2.14 Genu valgum(a) and genu varum(b) (adapted from [13]).

## 2.1.4 KNEE MOTION

The information on the reference system and on the reference position permits the description of the range of motion of the knee. Each single motion parameter is analysed in the following.

### 2.1.4.1 KNEE ROTATIONS

#### FLEXION/EXTENSION

As already mentioned in previous sections, the main rotation of the knee is the one about the  $e_1$  axis of the above defined reference system. Considering the reference position the one that foresees the axis of the leg in line with that of the thigh seen in the sagittal plane, the following range can be described:

- i) passive extension (also said hyperextension):  $5^\circ$  to  $10^\circ$  can be reached;
- ii) active flexion:  $140^\circ$  can be reached with the flexed hip and  $120^\circ$  can be reached with the extended hip;
- iii) passive flexion:  $160^\circ$  can be reached with flexed hip.

#### INTERNAL EXTERNAL ROTATION

Motion in the transverse plane is influenced by the joint flexion angle [23]. With the knee in full extension, rotation is almost completely restricted by the interlocking of the femoral and tibial condyles. Nonetheless, the range of possible rotation increases as the knee is flexed, reaching its maximum at  $90^\circ$  of flexion, when external rotation can range from  $0^\circ$  to approximately  $45^\circ$  while internal rotation can range from  $0^\circ$  to approximately  $30^\circ$  [23]. Normal ranges of rotation Beyond  $90^\circ$  of flexion, instead, the range of internal and external rotation decreases, primarily because the soft tissues restrict rotation [23]. It is worth noting that these ranges are permitted if tibial rotation is imposed, but are not physiological during motion.

When considering the internal/external rotation, also the physiological internal/external rotation associated with the flexion angle must be taken into account. When the knee is

---

extended, indeed, the foot is laterally rotated, while when the knee is flexed, the foot is medially rotated. Passing from full extension to full flexion, though, an internal rotation of the tibia occurs with respect to the femur.

#### ABDUCTION-ADDUCTION

As for the internal rotation, ab/adduction is affected by the amount of joint flexion. In fact, full extension of the knee precludes almost all motion in the frontal plane[23]. Passive abduction and adduction increase with knee flexion up to 30°, but each reaches a maximum of only a few degrees [23]. When the knee is flexed beyond 30°, instead, motion in the frontal plane again decreases because of the limiting functions of the soft tissues [23].

### 2.1.4.2 KNEE TRANSLATION

In the following, translation parameters are discussed. It is important to note that information referring to the knee displacements is often scarce and, when it is available, conflicting data are reported by different authors. The amount of translation, indeed, is strongly dependent on the reference point for describing it, whose movement is subjected to the pure translation and the motion due to coupled rotation. So small differences in the definition of the reference point result in big differences in the translation parameters.

#### ANTERO-POSTERIOR TRANSLATION

Antero-posterior translation occurs during flexion. Belvedere et al. [24] considered the translation of the center of the tibial plateau in the femoral reference frame, and observed that it only moved posteriorly in the full 0°-140° F-E rotation range. The mean measured range was of 25.8±5.9 mm and mostly occurred within the first 70° of flexion [24].

#### COMPRESSION-DISTRACTION TRANSLATION

Data dealing with the knee compression-distraction range of motion are not very common in the literature; again, the author herein refers to those reported in [24]. In

---

particular, only compression (proximal) translations were observed, with an average value of  $23.8\pm 3.3$  mm.

#### MEDIAL-LATERAL SHIFT

Finally, also data regarding the knee medio-lateral (M-L) translation range of motion are not very common in the literature; thus the approach adopted herein will be, once again, that outlined in the previous sections. In particular, still referring to [24], only medial translations were observed, with an average value of  $4.8\pm 2.8$  mm. However, the authors claim that such values are quite large, so that a comparison with other values available in the literature for in vitro tests is sought. Nonetheless, values used for comparison are of 5 mm for the mean M-L translation in the  $0^\circ$ - $100^\circ$  flexion range (obtained by Wilson et al. in 2000 by means of an electromagnetic tracking system [24]), and of 2.7 mm in the  $0^\circ$ - $90^\circ$  range (obtained by Li et al. in 2007 by means of a robotic system [24]); therefore, the value reported in [24] can be herein considered as an upper boundary for the quantity of interest.

## 2.2 KNEE TESTS

Several tests, with different level of complexity, have been performed in the last decades. The need of different kinds of test arises to address the need of considering the behavior of different structures. In particular, when replicating the passive motion only the role of some passive structures (mainly articular surfaces and ligaments) in guiding the joint behaviour can be analysed. Clinical tests are performed in order to assess damages in joint structures that constraints the motion of the joint. Dynamic tests involve all the joint structures: bones and articular surfaces, ligaments, tendons and muscles. In this sense, dynamic tests are also the most complete ones. In this section, the different tests will be analysed more in detail, in order to better understand the specification required to the test rig.

### *2.2.1 UNLOADED MOTION TESTS*

The evaluation of the behavior in unloaded conditions consists in the measurement of the relative pose of the tibia and the femur at each knee flexion angle, when virtually no loads are applied to the joint.

The passive motion of the knee exhibits one degree of freedom [2], i.e. the values of 5 motion parameters depend on the value of one independent parameter. In particular, the knee passive motion is a three-dimensional motion function of the knee flexion. The passive motion of the knee is analysed by relatively moving the tibia and the femur, at the same time trying not to apply loads.

### *2.2.2 LOADED MOTION TESTS*

As for the loaded motion, a large number of different loading conditions can be considered. They can mainly be divided in static and dynamic tests.

#### STATIC TESTS

The most commonly realised static tests are the so called clinical tests and consist in applying a static force (moment) along (about) one physiological axis of the joint to one bone of the joint, while the other bone is kept fixed. They are usually performed by orthopaedists on patients in order to assess any damage in the joint structures. The three most common clinical tests are known in the literature as the drawer, the internal/external rotation and the abduction/adduction tests.

With reference to the Grood and Suntay joint coordinate system [22] defined in Section 2.1.3, the drawer test, which is showed in Figure 2.15a, is performed by blocking the femur and, at a fixed flexion angle, by applying a force to the tibia directed along the posterior/anterior direction (i.e. the  $x$ -axis of  $S_t$ ). The internal/external rotation test, which is showed in Figure 2.15b, is performed by blocking the femur and, at a fixed flexion angle, by applying a torque to the tibia directed along the distal/proximal direction (i.e., the  $y$ -axis of  $S_t$ ). Finally, the abduction/adduction test, which is showed in

Figure 2.15c, is performed by blocking the femur and, at a fixed flexion angle, by applying a torque to the tibia directed along the posterior/anterior direction (i.e. the  $x$ -axis of  $S_t$ ). These tests are repeated at different flexion angle values.

Other static tests can be performed on a knee by applying each desired static loads. Nevertheless, the described ones are the most common and useful for injuries diagnosis.

### DYNAMIC TESTS

Dynamic tests are the most complex and complete ones, since they foresee the simulation of the complete joint function, including muscles, during the performance of dynamic tasks. The loading conditions measured on a living subject during daily activities are replicated on the specimen, both in terms of forces exchanged with the system and forces exerted by muscles. Usually, loading conditions replicate common daily activities: walking, sit-to-stand and squat are the most common ones. Dynamic tests on specimens are based on data recorded on living subjects performing the analysed activities. In particular, ground forces, i.e. forces exchanged between the foot and the ground, can be measured thanks to a force platform. Muscle activation patterns can be recorded via electromyographic signals. Joint motion can be recorded by using different techniques, like skin markers, intracortical pins, MRI and fluoroscopy. Measured loads (measured movement) are (is) replicated on the joint, whilst the consequent movement (loads) is (are) measured.

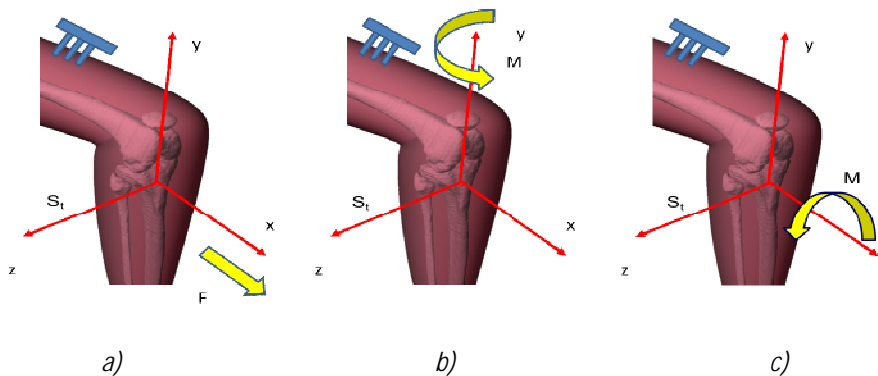


Figure 2.15 Clinical tests executed on the knee: a) anterior/posterior drawer; b) internal/external rotation; c) ab/adduction test.

### *2.2.3 SIMULATING MOTION OR MOVEMENT?*

All the above mentioned loaded tests can be performed in two ways: by imposing a certain path of motion and measuring the forces necessary to obtain it or by imposing the forces and measuring the motion.

Tests where motion is imposed are usually chosen when forces exerted by the different structures are calculated. In particular, they are often performed when all the structures are intact and then cutting some of the restraining structures. The different measured loads, and thus the different loads calculated for each structure, permit to determine which motions are resisted by each structure and the relative importance of the structures[25]. They have been applied to discern the functions of each ligament or even parts of ligaments. When these tests are executed, a stiffness approach is used.

Tests where loads are imposed and displacements are evaluated are more similar to those realised by clinicians and are useful to evaluate the sensitivity of knee laxity to injuries or perturbation of the knee normal conditions (for example, a prosthesis implant). When these tests are executed, a flexibility approach is used.

As it will be seen in the next chapter, both the approach have been used by many researchers and different solutions have been proposed for the utilized test rig, according to the tests necessity. For the purpose of our analysis, the flexibility approach is used. The evaluation of the behavior of the knee when prostheses are implanted is one of the purpose of the tests that will be performed with the test rig. In particular, the stability of prostheses can be tested by comparing the motion measured when the same loads are applied.

### *2.2.4 LOADS AND MOVEMENTS IN DYNAMIC TESTS*

A literature research has been performed in order to understand the wrenches (i.e., a vector whose components are forces and moments) that are applied to the knee joint when daily activities are performed and the consequent motion.

The most common activities realised during the day, and so the most frequently analysed ones, are sit-to-stand, squat and walking. Several papers have been published in which loads and motion of volunteers were measured while they performed the above mentioned tasks. Literature has been analysed and the most complete in terms of reported data and description of the test condition have been taken as reference for the design of the new test rig. The reported data include both the ground reaction forces, the relative pose between the foot and the ground and among the leg segments.

In the following, each test will be analysed in order to define the requirements for the test rig. The angles between long axis of the leg segments have been determined from the literature and/or from other considerations, together with the measured forces. In particular,  $\alpha$  represents the flexion angle of the knee,  $\beta$  represents the angle between the long axis of the foot and the ground and  $\theta$  represent the angle between the tibia and the ground.

In particular, results of ground reaction forces and knee flexion angle measured while volunteers performed squat have been reported by Guess et al. [26]. In Figure 2.16 forces and angles have been represented as a function of the flexion angles. As it is possible to see, the performed squat was not deep; this permitted the volunteers to keep their heels on the ground. The angle  $\beta$  was thus calculated as half the flexion angle and the angle  $\theta$  was computed as the complementary angle of  $\beta$ .

Results in terms of ground reaction forces and knee flexion angles measured while volunteers performed sit-to-stand have been reported by Hirsfeld et al. [27]. Forces and are reported in Figure 2.17 as a function of the flexion angle. Angles  $\beta$  and  $\theta$  were computed as for the squat.

Finally, results in terms of ground reaction forces and joint angles have been presented by Anderson and Pandy [1]. Forces and angles are reported in Figure 2.18 as functions of the percentage of the gait cycle. As reported in Figure 2.18 only a portion of the gait cycles has been considered and it is composed by an extension and a following flexion of the knee. Indeed, the considered portion of the task is that were the highest loads

---

are measured. In Figure 2.19 the behavior of the angle  $\alpha$  is reported for all the gait cycle and the most relevant instants of motion are emphasised, as to allow the reader which part of motion has been considered in Figure 2.18.

From the data reported, it can be noted that the vertical one is the highest of the GRF components for all the tasks. In particular, the highest GRF were measured during walking. It could be expected, since it is the only task that sees a leg standing the whole weight, while during squat and sit-to-stand the weight is borne by both legs.

From the same figures, it can be observed that the range of variation of the angles is wider during squat and sit-to-stand than during walking. The different tasks, indeed, allow the evaluation of the knee in different flexion conditions. Finally, it must be noted that if the shank is perpendicular to the ground, the vertical component of GRF is approximately along the leg longitudinal axis. If a smaller angle is formed by the shank and the ground, the vertical component results inclined with respect to the leg longitudinal axis, thus generating a higher flexion/extension moment at the knee. The smaller angles between the shank and the ground are those measured during squat. For these reasons, all the different loading condition and daily actions are necessary to evaluate the knee behaviour, since each of them allows the consideration of different aspects.

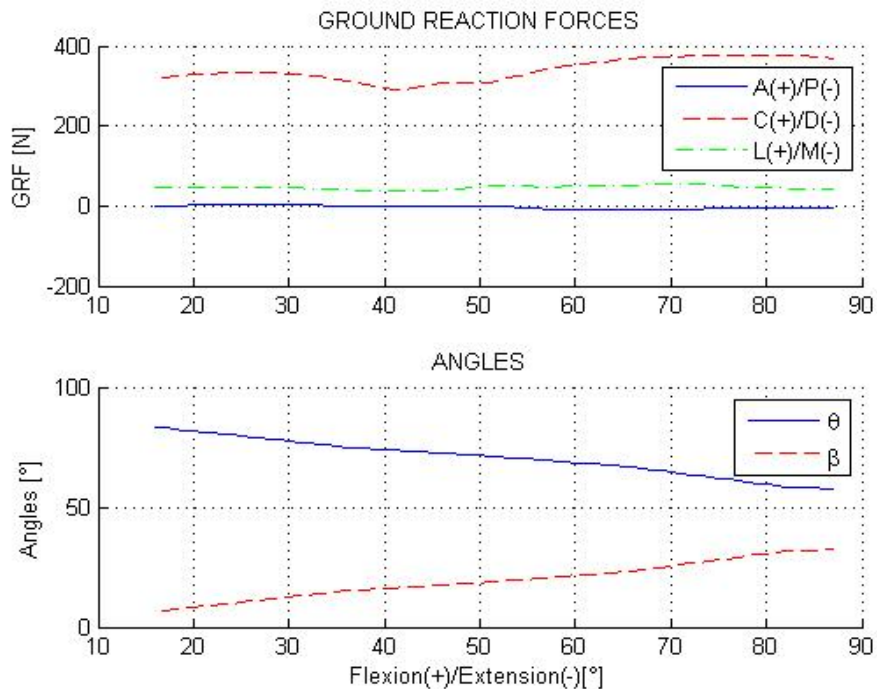


Figure 2.16 Loads and joint angles during squat. Loads are reported in [26] and angles are computed.

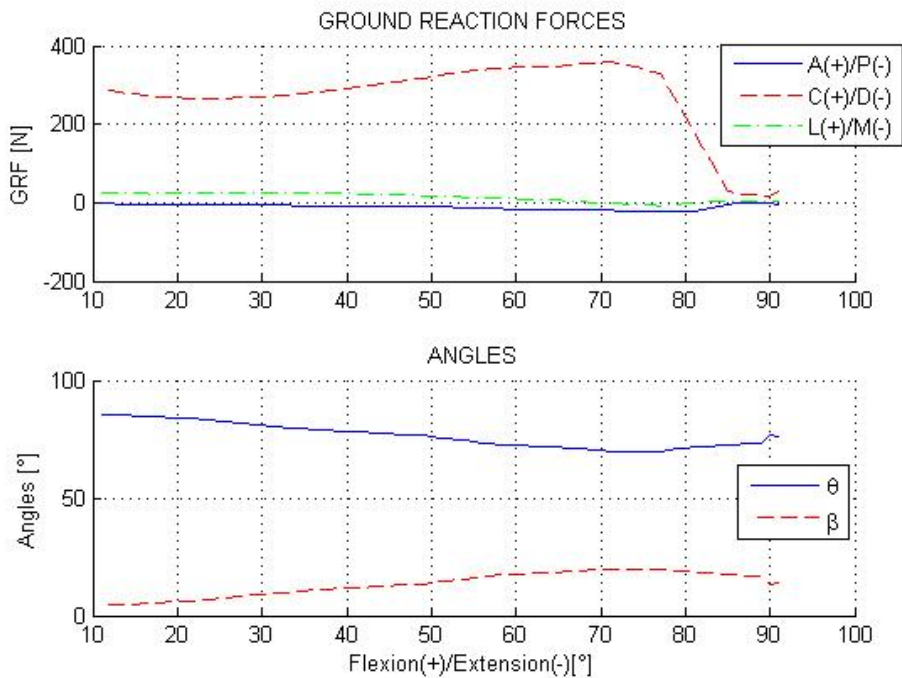


Figure 2.17 Loads and joint angles during sit-to-stand. Loads are reported in [27] and angles are computed.

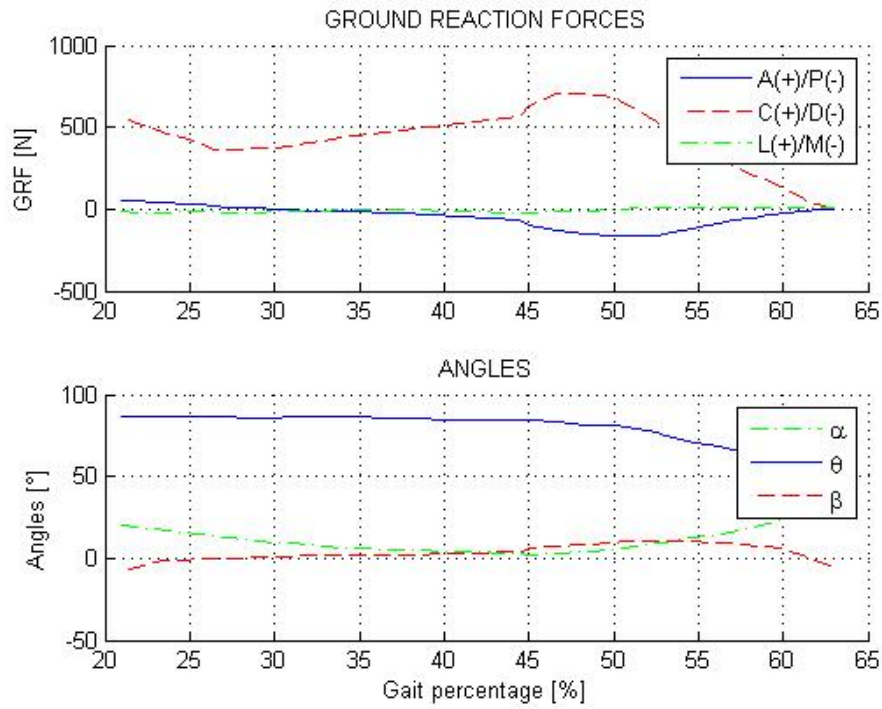


Figure 2.18 Loads and joint angles during walking. Loads and angles are reported in [1].

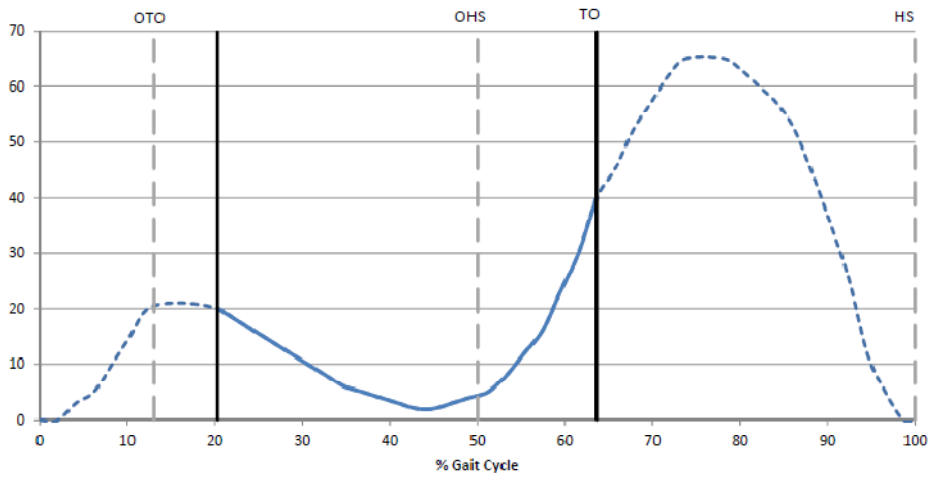


Figure 2.19 Knee flexion angle during the gait cycle: OTO: opposite toe off; OHS: opposite heel strike; TO: toe off; HS: heel strike. The part in which the knee is involved in bearing loads goes from HS to TO.

## CHAPTER 3.

# OVERVIEW OF AVAILABLE TEST RIGS

In the last decades, a big amount of attention has been devoted to the development of test rigs dedicated to the in vitro evaluation of the knee movement and to the replication of the movement itself or of the forces measured on in vivo subjects. As discussed in Section 2.2, indeed, tests are executed with different purposes. At the same time, different features are required to the test rigs in order to execute the different tests. In this chapter an overview of the machines developed to address different needs will be provided.

According to their architecture, the knee rig can be grouped in Knee Simulators (KS) and Robotic Knee Testing Systems (RKTS). Machine belonging to the first group are generally designed in order to replicate the kinematic chain of the lower limb and perform tests in more physiological conditions than RKTS. Different machines belonging to each group will be analysed in the following.

### 3.1 KNEE SIMULATORS

The rigs belonging to the first group are designed and built with the effort to replicate the kinematic chain of the lower limb from the hip to the ankle. These rigs are usually load controlled, and the external loads are typically applied to the specimen via the hip and ankle joints. Muscular loads are simulated at different level of complexity and their loads are directly applied to the bones. They are usually adopted when tests focused on the motion measurement have to be performed.

### *3.1.1 OXFORD KNEE RIG*

The most common device of this group is the Oxford Knee Rig[6], built in its first version by O'Connor and his colleagues in 1978 in order to study different kinds of knee arthroplasties. It was used to simulate knee flexion-extension under the action of loads, while measuring the relative motion of the tibia and femur. The first version of the OKR presents three main elements: the hip assembly, the ankle assembly and a vertical sliding couple (Figure 3.1). The hip assembly is connected to the femur and has two sets of rotary bearings that allow two rotations of the femur, namely flexion/extension and ab/adduction. The axes of these two bearings intersect at the centre of the hip. The ankle assembly is connected to the tibia and has three sets of rotary bearings that allow the spherical motion of the tibia around the ankle centre. The centre of the ankle is posed directly under the centre of the hip, vertically. A vertical slide, composed of bearing running on two vertical rods, allows the vertical translation of the hip assembly, and so permits the flexion of the knee. A mass is hanged at the hip assembly, to simulate human weight. A force is applied to quadriceps tendon, in order to simulate the action of quadriceps and to balance the external load during flexion. The test rig is used to measure the relative movement of the tibia and femur, during flexion, under the action of an external load, i.e. the simulated human weight, and the simulated action of the quadriceps muscles. It has been proven that the described geometry allows a knee specimen its six DOF natural movement [6]. So the complete six-DOF motion can be replicated and measured by using this rig. Although the six DOF are guaranteed, the hip and ankle assemblies do not really replicate the physiology of the human hip and ankle joints. The hip joint, indeed, is very similar to a spherical joint, thus allowing also internal/external rotation of the femur that is not permitted by this test rig.. Another limitation of the rig is the reduced range of knee flexion, which is 90°. Furthermore, the application of general loads required for the simulation of daily activities is not possible with this rig: only a constant load can be applied at the hip joint and variable force can be applied at the quadriceps.

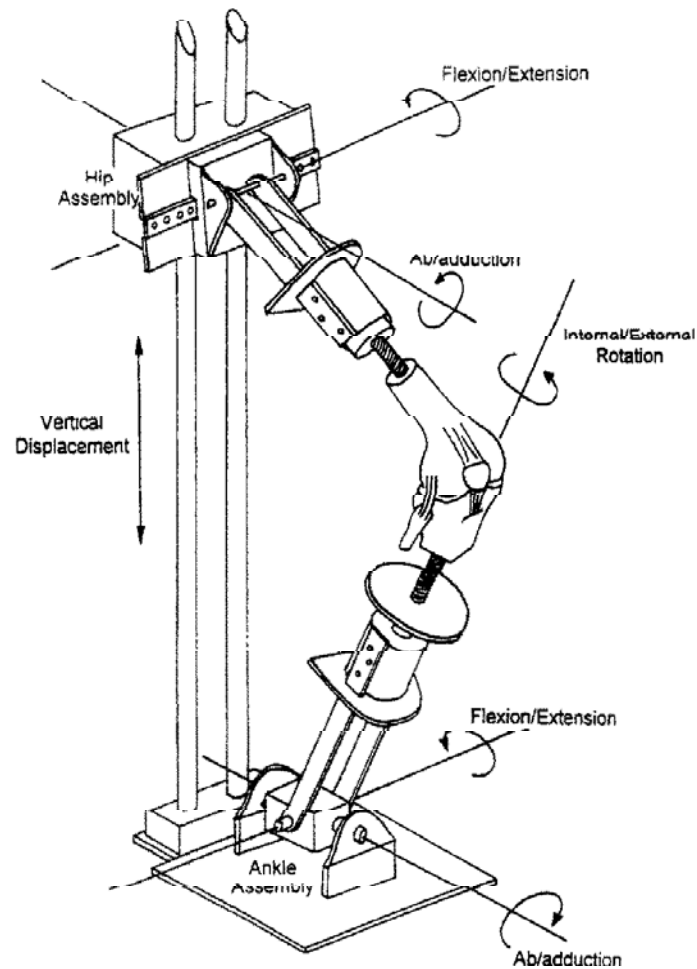


Figure 3.1 The Oxford Knee Testing Rig. In figure the two rotations at the hip assembly and the three rotations at the ankle assembly are shown, together with the vertical displacement of the hip assembly [6].

### 3.1.2 EVOLUTIONS OF OKR

Many test rigs have been built as evolutions of the rig described above, trying to overcome its principal limitations.

Yildirim et al. [8] built a refined version of the rig reported in Figure 3.2. The hip joint is simulated with a spherical bearing, so that the three physiological DOF, i.e. the three rotations, are allowed to the femur with respect to the frame. The ankle joint is simulated with a connection that permits the rotations of the tibia about its longitudinal

---

axis, i.e. allows tibia internal/external rotation, and about an axis fixed to the frame, coincident with the intermalleolar axis, i.e. the flexion/extension. Furthermore, the tibia fixation system allows a physiological limited range of rotation about an anterior axis, i.e. the ab/adduction rotation. Similar to the original version, the hip joint is connected to a sliding plate that moves along two vertical rods, simulating the knee flexion. The human weight is simulated by hanging a mass to the vertical plate. The action of quadriceps is simulated by applying a variable force to the quadriceps tendon with a stepper motor that slides together with the hip joint. Furthermore, the action of the hamstring muscles is simulated via two extension springs connected to the posterior tibia and to the femur fixture. The version of the machine presented by Yildirim et al. [8] represents an evolution of the original OKR, based on the same architecture, but able to realise more physiological in vitro experiments. The hip and ankle assemblies, indeed, allow more physiological couplings and the simulation of the hamstring with a variable force represents an improvement in the replication of in vivo conditions. A flexion angle of 135° can be reached with this machine.

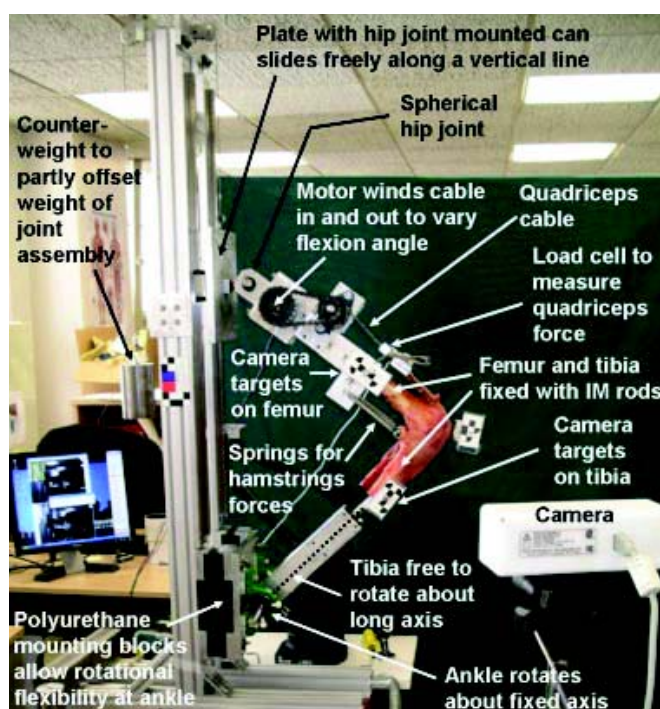
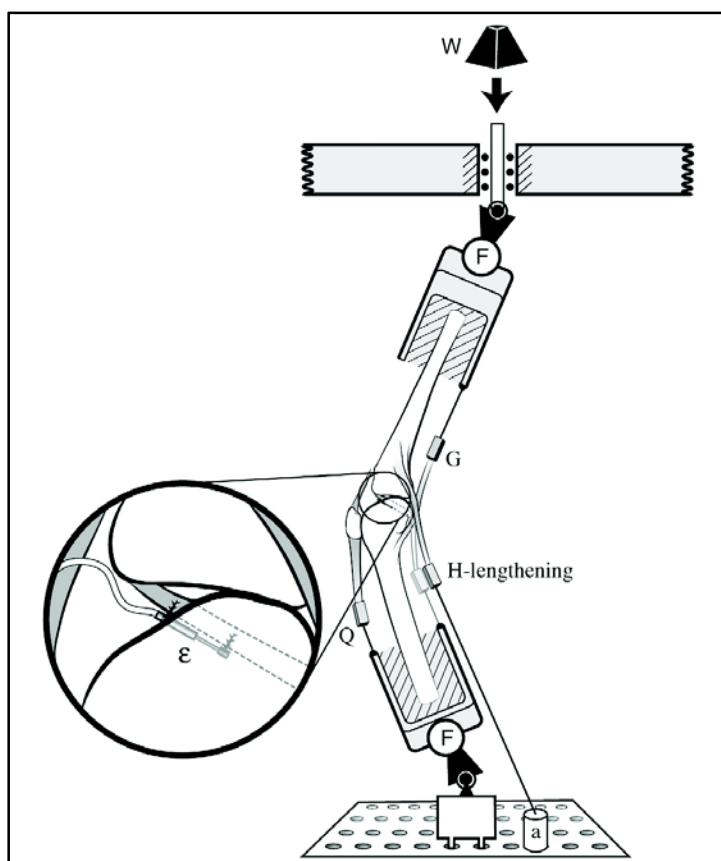


Figure 3.2 The so called crouching up-and-down machine used by Yildirim et al. [8] to apply continuous flexion-extension to the knee.

A similar architecture was utilised by Withrow et al. [5] to test the effect of varying hamstring tension on the anterior cruciate ligament when an impulsive load is applied causing knee flexion. The test rig is reported in Figure 3.3 and presents two spherical joints at the hip and at the ankle. Once again, the flexion is guaranteed by a sliding couple between the frame and the hip assembly. In this version, in addition to femur, both hamstrings and gastrocnemius are simulated thanks to a system of wires and springs. This system reveals to be cumbersome and complex, but this did not represent a limitation for the purpose of the above-mentioned test, since no deep knee flexion was required. In addition, the system does not allow imposing a desired variable force at the simulated posterior muscles.



*Figure 3.3 Schematic of test setup, showing the knee mounted for testing as well as the applied loading ( $W$ ) and three-axis load cells ( $F$ ). Three of the five cables representing pre-impact tensions in the quadriceps ( $Q$ ), medial and lateral hamstring ( $H$ ), and medial and lateral gastrocnemius ( $G$ ) muscle-tendon units are also visible. to measure the relative strain ( $e$ ) [5].*

A more refined version of this rig is the Tuebingen knee simulator used by Wünschel et al. [4] and reported in Figure 3.4. As many other simulators, it guarantees the 3 rotations at the hip joint plus its vertical translation and the three rotations at the ankle joint. A variable weight is simulated at the hip via a linear actuator. Muscles are described with greater accuracy in this version of the rig: 3 actuators are used to simulate the quadriceps muscle and 2 actuators to simulate the semimembranosus and the biceps femoris, in order to respect their lines of action in vivo. This machine allows controlling and simulate the different muscles in an accurate way, since different loads can be applied along different lines of action. During the tests described in the reference paper, indeed, a constant force has been assigned to the posterior muscles, while a variable force has been applied to quadriceps, in order to guarantee the equilibrium. The range of flexion (from 20 to 110°) of this machine appears to be limited: neither full extension nor deep flexion can be analysed. This limitation does not permit to replicate the common daily activities with this machine.

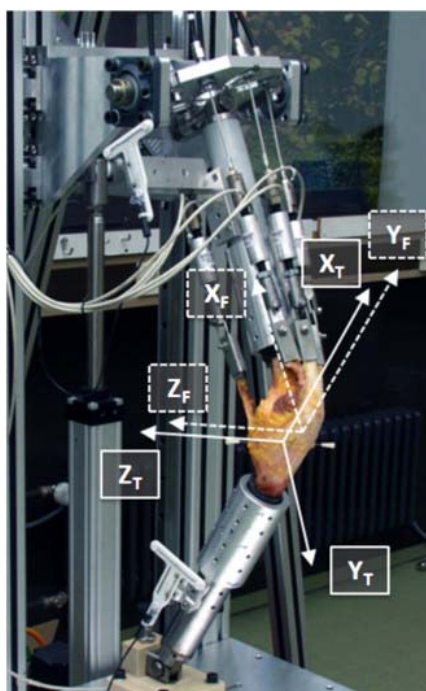
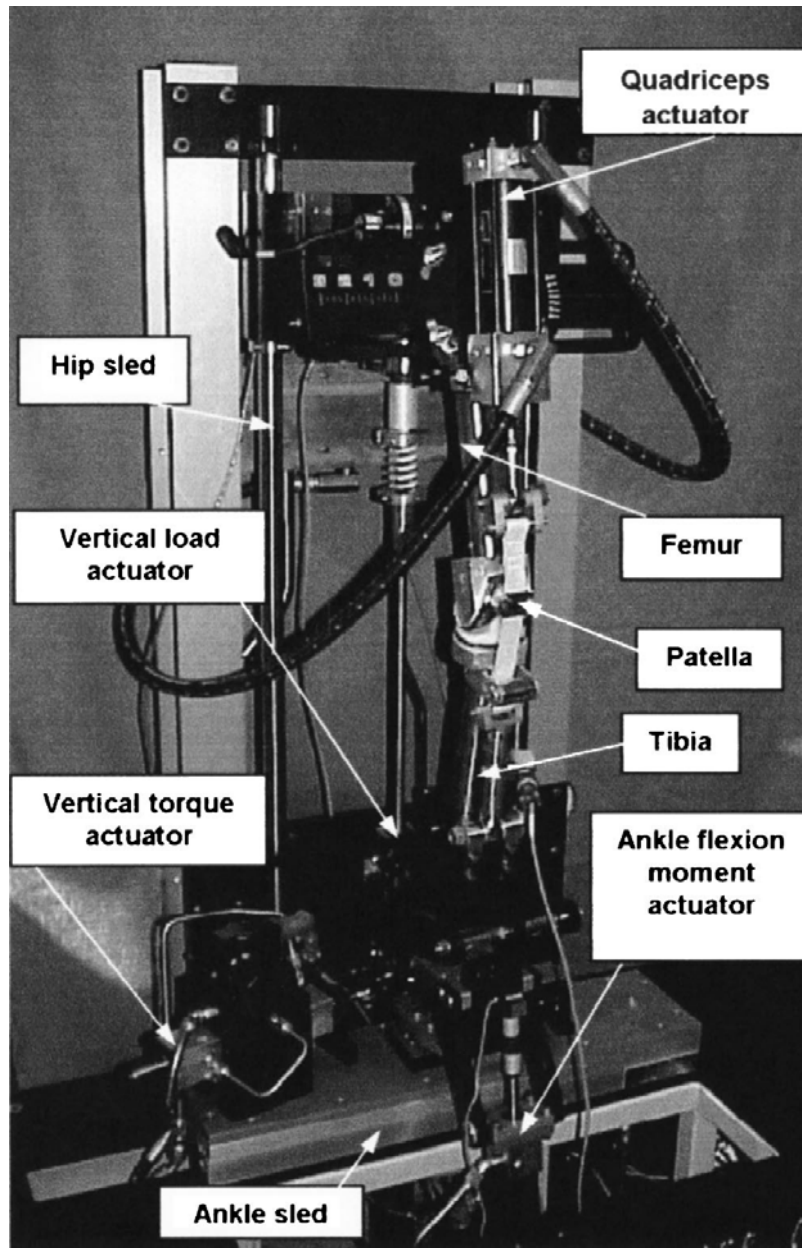


Figure 3.4 Experimental set up of the Tuebingen knee simulator with the actuators to simulate muscular loads [4].

### *3.1.3 PURDUE KNEE SIMULATOR: MARK II*

In the evolution of the OKR discussed in the previous section, only a vertical load could be applied as an external load. Some machines offer the possibility to apply other loads at the hip or at the ankle joint, to create a more accurate three-dimensional loading simulation. Two of the more common loads applied to the joint are tibial adduction/abduction and internal/external torques, as described in Section 2.2.2. The Purdue Knee Simulator Mark II [9] is one of the above mentioned rigs. As shown in Figure 3.5. This knee simulator has an architecture similar to that of the OKR, but the bones are substituted by two links that simulate the bones themselves; the tested knee or prosthesis is mounted on the links. The six DOF are obtained at the knee by allowing two DOF at the hip and four DOF at the ankle. Vertical translation and flexion/extension with respect to the sled are allowed to the hip. Flexion/extension and ab/adduction are allowed to the tibia at the simulated ankle joint; furthermore, rotation about a vertical axis (that results in a combined rotation, with a component of internal/external) and medio/lateral translation are allowed between tibia and frame. The weight is simulated via a vertical actuator that acts on the hip sled and the quadriceps force is simulated via another actuator fixed to the femur. To better simulate physiological loading conditions, a medio/lateral force can be applied between the sled and the frame and two moments can be applied between the tibia and the sled; in particular, a moment about the vertical axis and the other one about the ankle flexion/extension axis. The 5 actuators are used to replicate the internal loads at the knee joint calculated during common daily activities. In particular, internal forces at the knee are taken from the literature (according to different approaches of calculation) and are applied to the joint as a function of the flexion angle. Four actuators (vertical and medial/lateral forces, internal/external and ankle flexion/extension moments) are controlled in load and the quadriceps actuator is controlled in position, to smooth the flexion/extension cycles. The knee flexion angle is approximately calculated as double the measured hip flexion angle. The load history is applied as a function of the measured angle. In the reference paper, only a walking task is performed on the knee and no information are given about the maximum reachable flexion angles.

To the purpose of applying flexion-dependent loads, the measure of the angle between tibia and femur is necessary. The measurement reveals tricky with this kind of machine and requires some approximations, as, for example, a relationship between the knee angle and the hip angle, which can be measured more easily.



*Figure 3.5 Photography of Purdue Knee Simulator: Mark II [9].*

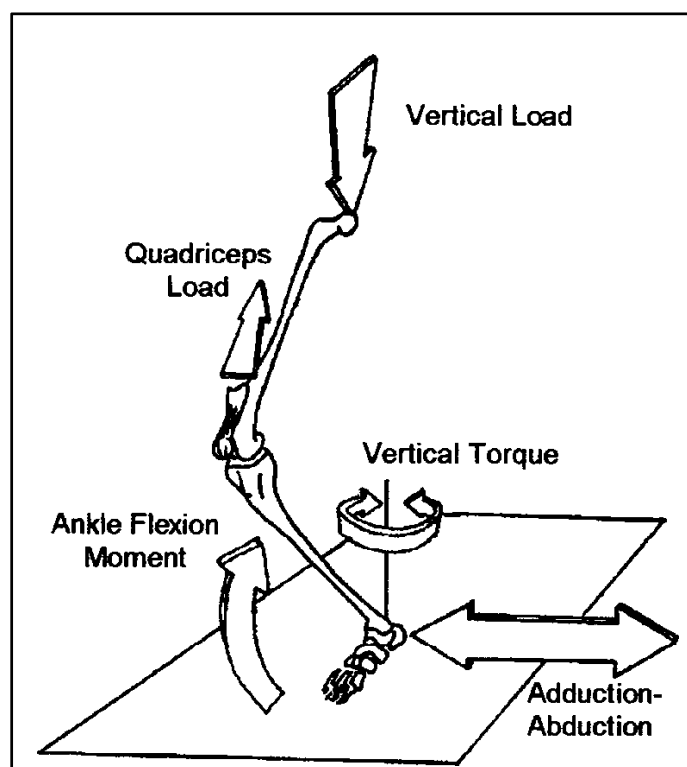


Figure 3.6 Schematic representation of the five axes loading of the knee simulator [9].

### 3.2 ROBOT-BASED KNEE TESTING SYSTEMS

Knee simulators allow the simulation of motion in a physiological way, since they simulate knee flexion by simulating the motion at the hip and ankle joints. They are used to measure the relative motion between bones when certain external loads are applied. Conversely, robot-based testing systems typically work in a way to completely block one bone of the joint and apply the motion (loads) to the other one, whilst measuring loads (motion). All the motion is so applied to one bone. In this sense, these rigs appear less physiological than the OKR-type ones.

Both serial and parallel architectures have been used to develop knee testing systems. Thus, in the following, they will be classified according to their serial or parallel architecture.

The most of these devices can be defined as quasi-static, in the sense that the knee can be positioned at the desired flexion angle and then loaded through the bones and muscles. Tests in which the flexion angle can be changed continuously, and the loads modified consequently, are very difficult to realise and sometimes are not necessary for the purpose of the analysis.

### *3.2.1 EARLIER MACHINES*

The first robot-type machines were born to measure the range of motion of the knee or for evaluating its behavior when it is subjected to anterior drawer, i.e. subjected to an antero-posterior load. In their simplicity, they allowed positioning of the knee at a certain flexion angle and applying a certain static load. They usually presented a serial architecture.

Xerogeanes et al.[28], for instance, created a rig able to apply only antero-posterior forces by using an Instron testing machine (Model n° 4502) equipped with custom clamps, designed to enable positioning and subsequent rigid fixation in five DOF; the sixth DOF, that is the AP is provided by the motion of the crosshead. As showed in Figure 3.7. The machine is equipped with a universal force sensor (UFS) that allows the measurement of the loads exchanged between bones. Once determined the unloaded pose (i.e. the pose a which non loads are measured by the UFS) at a certain flexion angle, the machine allows the application of an anterior load to the tibia and its consequent anterior motion with respect to the femur. The forces at the knee are recorded by the UFS and the AP displacement is measured. This adapted machine is really simple but allows the application of load in only one direction.

Similarly, a material testing machine has been used by Beynnon et al. in [29] to test anterior-posterior laxity of the knee. They designed a fixture which accommodate the positioning of the knee in 6 DOF. This rig has pins to align the rotational axes of the fixture with the anatomical based rotational axes of the knee. Load is applied to the femur through the testing machine at the desired flexion angle, whilst the tibia is held in horizontal position. The fixture allows imposing knee flexion angle and contemporary

leave the other DOF free to move in response to the applied loads. It constitutes an improvement with respect to the fixture designed by Xerogeanes et al.[28], since this fixture does not prevent coupled motion.

### 3.2.2 SERIAL RIGS

Rig based on serial manipulators are common in human knee testing. The spread of knee serial robot in manufacturing allows an easy access to the these robot, that have often been adapted to test human joints.

In 1993, Fujie et al. [10] presented a first version of serial robot equipped with a universal force-moment sensor test system (UFS), that allowed a load control of the robot.

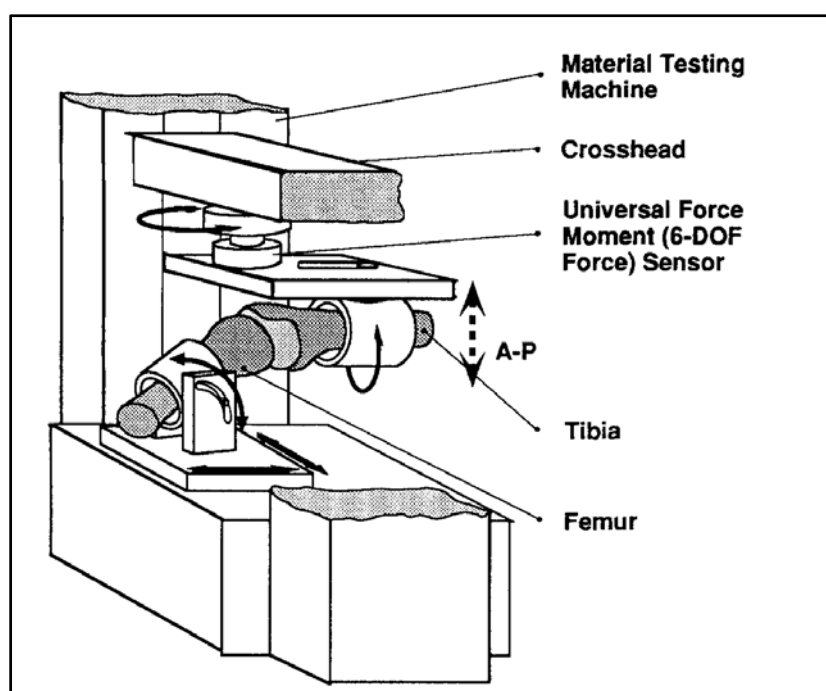


*Figure 3.7 The test set up used in [28]. Two DOF in positioning the joint are guaranteed by the upper part of the machine, three DOF are guaranteed by the femur fixation device. A-P displacement is applied during tests.*

Rudy et al. 1996 [30] and Li et al. in 1999 [31] took advantage of the idea, using a six-joint serial-articulated robot from Unimate (PUMA, model 762) to analyse the behavior of the intact and damaged knee joint. In its original version, the robot is position-controlled; for the application, it was modified to operate both in position and force control, by mounting a UFS at the end effector, as shown in Figure 3.8. The UFS provides a moment-force feedback.

During experiments performed by Rudy et al. [30], the 6 DOF passive (unloaded) motion of the intact knee is first measured and learnt by the robot and then applied to the modified (damaged) knee, controlling the variation in forces and moments. To determine the passive motion, the flexion range is divided in steps. At each value of flexion, the pose of the tibia with respect to the femur is found in a way that the load measured by the UFS is almost null (maximum values of 2 N and 0.2 Nm are admitted for forces and moments). In this phase, a force control is applied to the serial robot. When all the motion path has been identified and learnt by the robot, the knee is modified (cutting one or more ligaments) and the same path is imposed to the knee, thanks to the robot position control. Forces at the knee are measured and the effect of the cut ligament(s) is evaluated.

A system to simulate both quadriceps and hamstring muscles was mounted on the rig during experiments conducted by Li et al. [31]. The system permits the orientation of the simulated muscular loads thanks to some pulleys that can be oriented as shown in Figure 3.8. In addition to passive motion, this robot allowed the evaluation of the behavior when certain muscular actions were simulated, before and after the transaction of the anterior cruciate ligament. Generally, the muscular action were simulated by applying weight to the cables in the pulley, so muscular forces were considered as constant.

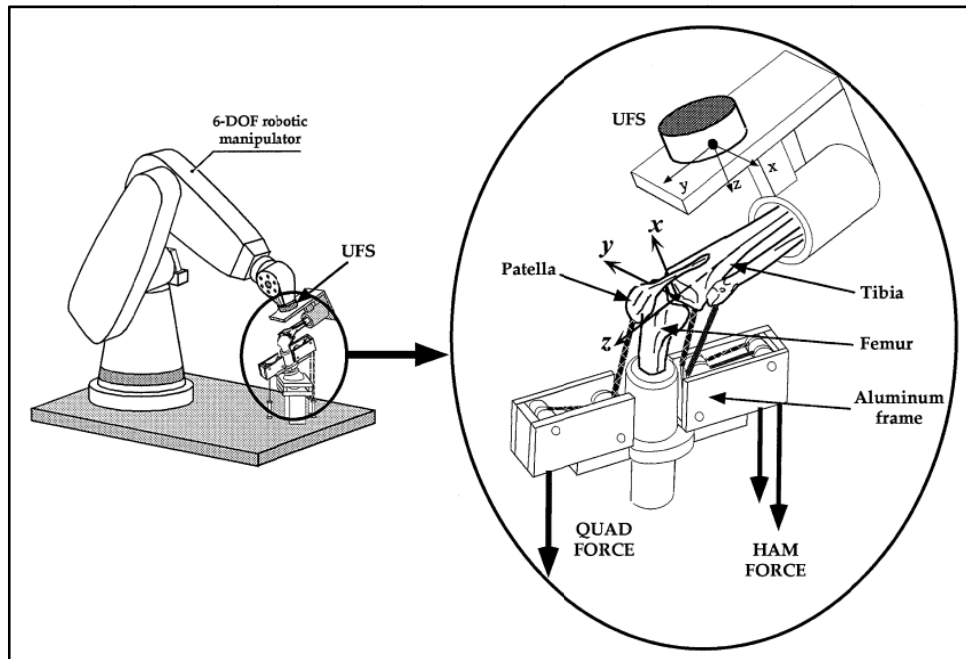


Figure 3.8: The experimental set up based on a serial manipulator; a system of pulleys is used to simulate muscles [31].

The same device was used also by Loh et al. [3] to compare the behavior of the knee after two ACL reconstruction procedures. In this case, besides the simulation of passive kinematics and the application of an anterior force, also a so-called combined rotary load, i.e. a combination of varu torque and internal tibia torque, was applied to the joint a certain flexion angles. In this tests, a combination of position and load control have been applied to the robot, since the object of the tests was to measure the natural movement of the bones in response to the applied loads.

In all the mentioned papers, no continuous flexion variation were performed and no general system of loads were applied. Quite wide flexion angles were reached during tests, up to  $120^\circ$  [31]. No mention of higher flexion angles was done in the paper. In [30] and [31], indeed, the force control was used only to allow the knee to reach the equilibrium pose. A more complex loading systems was applied in [3] but the limitation on the reachable load (450 N) do not permit to simulate daily activities.

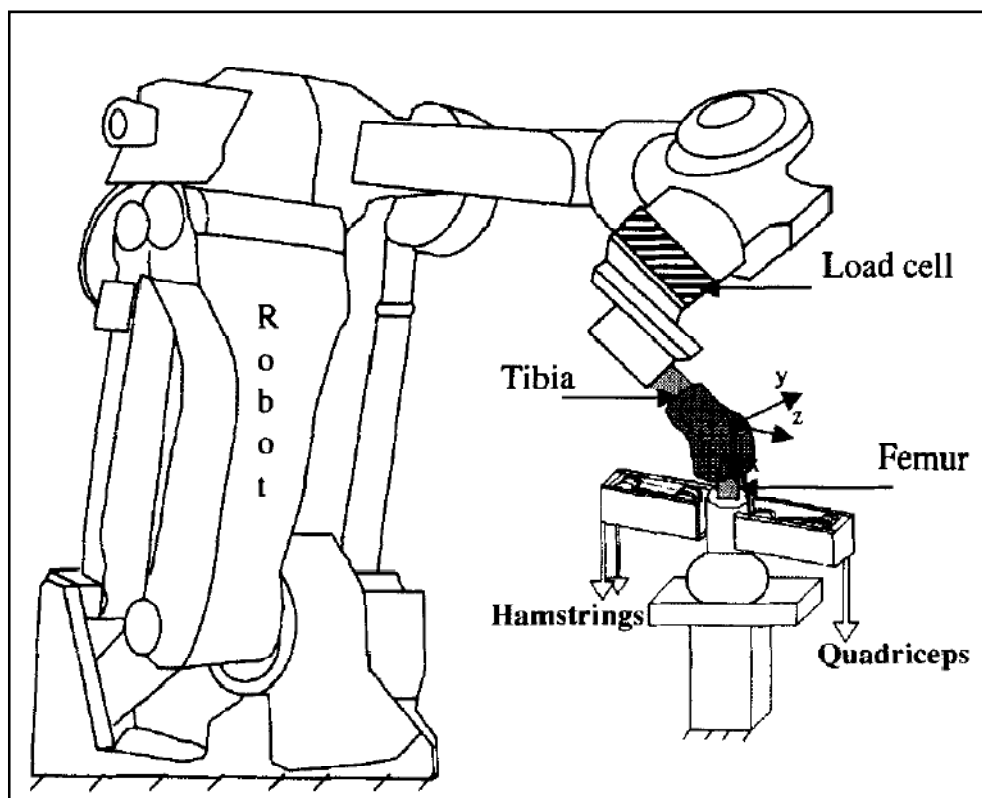


Figure 3.9: The knee testing system used by Li et al.[32] based on a serial robot equipped with pulleys to simulate muscular loads.

Higher loads can be applied by the industrial robot Kawasaki UZ150 (Kawasaki Heavy Industry, Japan) used by Li et al.[32]: payload reaches 150 kg. This robot was used similarly to the PUMA in [31], but with a wider range of flexion angle. Passive motion position were determined in a range of flexion angle going from  $0^\circ$  to  $150^\circ$ . Starting from the so determined unloaded positions, different combination of muscles loads were applied with the system of pulleys used in [31] and the joint movement was measured. The experimental set up is represented in Figure 3.9. This new system allows the application of higher loads on a wider range of flexion but still remains a quasi-static device that is used to apply loads only at fixed flexion angles.

A serial robot device system controlled in position was used also by Wunschel et al. [4] to evaluate the behavior of the joint after different techniques of arthroplasty have been applied. The robot (KUKA Robotics Corp., Augsburg, Germany) was used to replicate the kinematics previously measured by the knee simulator presented above, by moving

the femur, while the tibia is completely fixed with respect to the frame. Thanks to a UFS mounted at the end effector, forces and moments born from motion replication were measured and compared. Furthermore, the robot was used to apply loads in AP direction at fixed angles of flexion, and the forces are measured on the femur by the UFS. At this stage, though, the robot is position-controlled and the AP force is imposed by translating the femur until the desired value of AP force was reached. With this machine, indeed, tests in which the actuators are force controlled and the loads are varied with flexion have not been performed. Results are reported at flexion angles of  $110^\circ$ .

Furthermore the machine is not equipped with a system to simulate the muscular loads, which is not required by the purpose of this tests. The machine is presented in Figure 3.10.

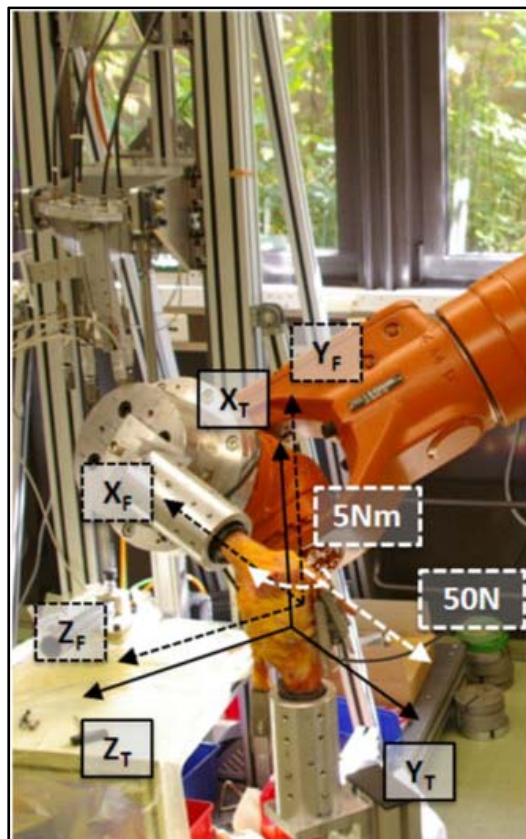


Figure 3.10 Experimental set up using the robotic UFS system[4].

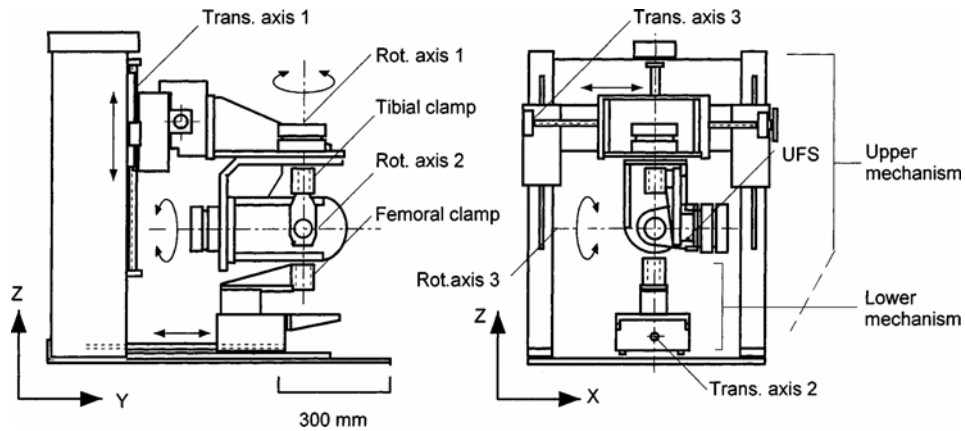


Figure 3.11 Diagram of the 6-DOF robotic system presented in [11]. The superior chain provides 5 DOF while the inferior chain provides 1 DOF.

All the serial robotic manipulators discussed above are obtained from adaptation of commercially available robots. Although commercially available manipulators have big workspaces, only the one used by Li et al.[32] permitted to reach high flexion angles, typical of deep flexion. Albeit an error evaluation was not performed on these systems, they are usually characterised by small precision and repeatability in positioning. The serial chain, indeed, causes a propagation on the end-effector final position of the effects of backlash and manufacturing error in each joint.

### 3.2.3 DECOUPLED RIG

To overcome the limitation due to the difficult repositioning, Fujie et al. [11] developed a robotic system whose architecture is designed in order to decouple forces and moments, simplifying the control. The manipulator has two different movable mechanisms. The upper mechanism consists of a serial chain with five DOF, i.e. two translational and three rotational axes, and is connected to the fixation clamp for the tibia. A UFS is mounted at the end of the serial chain, as shown in Figure 3.11. The lower mechanism has one translational axis and is connected to the fixation clamp for the femur. The manipulator is built in a fashion that the three translational axes are orthogonal to each other and the rotational axes always cross at a single point during

motion of the manipulator. The authors showed that a reasonably low clamp-to-clamp translational compliance (1-3  $\mu\text{m/N}$ ) was obtained with this orthogonal fashion; rotational compliance was not tested but good results were expected by the authors. A simple kinematic description is claimed by the authors, compared to that of other manipulators, since this particular fashion permits the decoupling of the forces and moments. The control of the manipulator is so simplified.

The robot test system designed by Fujie et al. [11] presents a hybrid control system: both position and load control are used to realise tests. Unloaded motion can thus be measured at the joint by controlling the system with a null force at the actuators (null force at the load cell) and can be replicated by putting all the DOF under position control. Furthermore, general loads can easily be applied. The hybrid control, indeed, is possible only when the difference between the prescribed load and the actual load is bigger than some specified values; otherwise, only the load control is present. Another drawback claimed by the authors is the low speed reachable by the actuator in position control, thus hindering the simulation of daily activities at the real speed.

### *3.2.4 PARALLEL RIGS*

In the last years, the application of parallel robot to the study of human joint behavior has raised the interest worldwide. Parallel architectures, indeed, guarantee a larger stiffness, reducing weights, thus offering a more precise positioning and a higher repeatability, if compared with serial ones. Furthermore, they offer a higher load capacity with comparable actuator size and they are more compact [12]. Nevertheless their spread in human joint testing [12][33], not many models have been developed especially focused on the knee.

Howard et al. [33] first used a commercial parallel robot (Rotopod series, R-1000 and R-2000, PRSCo, Hampton, NH) to reproduce in vivo motion of animal knees as shown in Figure 3.12. The commercial robot is a 6-6 parallel manipulator, where the six legs connected to the base and to the platform via spherical joints. The legs have a fixed length and are actuated about a circular track on the base. The changes in the relative

pose of the joints between leg and base causes the motion of the knee in six DOF. This configuration allows a wide rotation of the end effector ( $\pm 720^\circ$ ) about the central axis of the rig, and a smaller one ( $\pm 14^\circ$ ) about axes perpendicular to the central one. To take advantage of the wide range of rotation guaranteed about the central axis (that is vertical), during experiments the knee was mounted with its sagittal plane parallel to the movable platform. The approximate knee flexion axis was fixed coincident with the central axis of the rig. The femur was mounted on the testing rig, while the tibia was fixed to the frame after adjusting its position thanks to the fixation system.

In its first application [33], the rig was positioned and the repeatability of in vivo measured kinematics was tested. More recently [34], the device was used to apply forces and measure displacements. Loads are applied both in position and force control. When the robot is operated in force control, the movement of the joint was permitted in only one DOF, for robot mechanical limitation. Loads are applied at fixed flexion angles: continuous variation of the angle was not performed. The experimented range of flexion is  $30\text{-}90^\circ$ , since the robot geometry allows the complete analysis of the motion only in this range.

The same parallel robot (Rotopod R2000, Parallel Robotic System, Hampton, NH) was used by Barsoum et al. [35] to test human knees. Also for this application, the tibia was kept fixed and it is connected to a six axes force-moment sensor. The femur was cut very close to the joint line and was mounted on the rig via custom clamps. The fixation system is not accurately described and a few information are furnished about the relative pose of specimen and test rig at the beginning of the test. Some specific loading conditions were applied at the joint at different flexion angles:  $0^\circ$ ,  $30^\circ$  and  $60^\circ$ . The knee was used to compare different TKA techniques for which the analysis at static loads can be sufficient. No deep flexion was considered and only static tests were performed. No muscular forces are simulated in tests performed with the Rotopod rig.

If a particular version of the 6-6 Stewart platform has been adopted in the above mentioned studies, also a traditional version of the hexapod have been developed and used by Ding et al. [12] [36] to test human joints. In this version, represented in Figure 3.13, the platform is moved by six linear ballscrew actuators that are connected to both

platform and base via spherical joints. The actuators have adjustable limit switch positions and anti-rotational pistons. Each actuator is capable of generating 4kN of thrust and has a maximum linear velocity of 0.2 m/s. Six linear encoder are used to measure and control the length of the actuators. The robot top assembly includes a specimen fixation plate to which the specimen and the encoder are mounted. The fixation plate is so connected via a six axes load cell to the platform standing above it. Actuators are connected to the platform. So the fixation plate and the platform are decoupled. The specimen is mounted with one end connected to the fixation plate and the other end fixed to the frame. The load cell measures forces and moments on the sample in six DOF. Displacements are measured by encoders, and the measurements are decoupled from the load cell compliance thanks to the mounting system equipped with two platforms. This complex mounting assembly makes the control system definitely complex, but allows a very accurate control of the test rig.

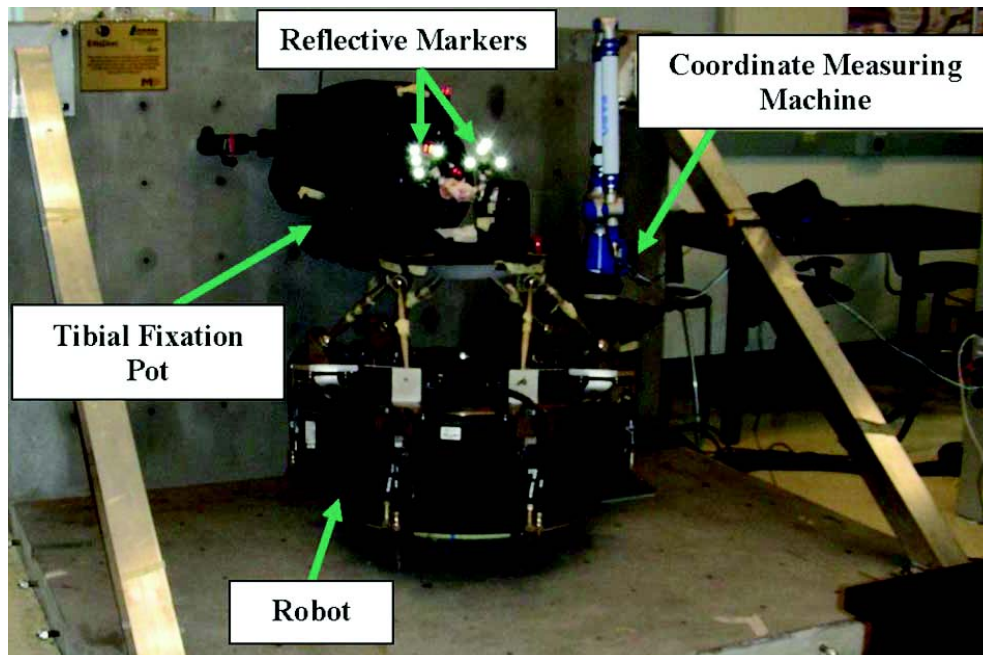


*Figure 3.12 Experimental set up with the use of Rotopod 2000 [33].*

In addition to the most common position control, also a velocity based load control has been developed for the rig [36], that is able to apply a real-time load waveform at physiological rates in one DOF while maintaining a constant force target in the other five DOF. This control embeds an adaptive stiffness matrix of the specimen. At the moment, only tests on the spine have been performed on this rig: since it guarantees a more constant stiffness, smaller problems should be encountered in the definition and adaptation of the stiffness matrix parameters. No tests on knees have been reported in the literature. The biggest hindrance to the application of this machine for knee testing is related to the small achievable rotation angles:  $\pm 25^\circ$ .

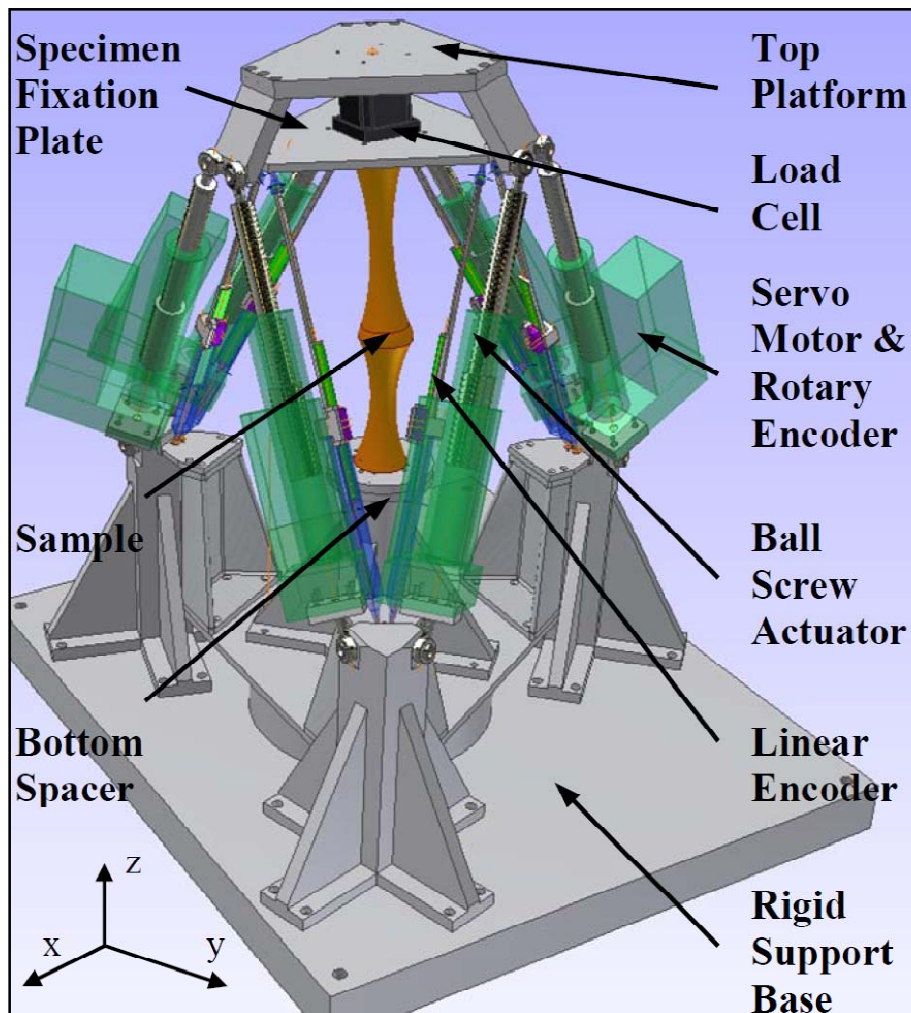


Figure 3.13 Schematic of the hexapod robot assembly recently presented in [12].

As the reader can observe from the overview, the test rig available in the literature are definitely different from one another and a great variety is available. This great variability permits the satisfaction of the several needs that arise from different studies.

In general, the main limitation of the RBTS are related to the impossibility to reach high flexion angles. The replication of the flexion-dependent loading history, typical of the principal daily activities, is an issue that can be faced by realizing a force control that do not further constrain the joint response in terms of motion. The replication of muscular loads appears particularly difficult, especially for the geometry of the rig that do not offer much space to fit the systems dedicated to muscle simulation.

Conversely, knee simulators more easily reach high flexion angles of the knee, trying to replicate hip and ankle joint conditions. The principal advantage of the knee simulators is that they are simple and allow the measurement of the knee motion in certain conditions. Given to their structures, they can host devices for muscle simulation. The simulation of loads that varies with the angles, though, is definitely complex: a complex system of actuated joints is required and the real-time measurement of the knee angle results very complex.

### 3.3 TEST RIG BASED ON CABLE-DRIVEN LOADING SYSTEM

Aside from this classification, a knee test rig has been developed by the author's research group [38] in order to replicate general loading conditions, such as common daily activities, in a wide range of flexion angles, and to measure the joint natural response in terms of movement. Its structure can be considered as a mix of the presented ones, so it is hard to classify it according to the proposed method. The loading system is realized by means of a cable-driven fully parallel manipulator with pneumatic actuation, as represented in Figure 3.14. The structure of the rig is constituted by a portal (1) connected to the base (5) via a revolute joint (O is the trace of the axis of the joint is projected in a plane orthogonal to the axis itself). The femur (3)

is connected to the portal (1) and rotates about the revolute axis. The loading system is connected to the tibia (10). The choice of controlling the flexion angle of the knee with a dedicated device (the portal (1)), different from the loading system arises from the consideration that the flexion/extension has the widest range (150-160°) of variation among motion parameters; its range is considerably larger than the others. Furthermore, flexion is the reference parameter for describing the loading history, as described in 2.2.4. In particular, the knee is mounted in a way that the transepicondylar axis is coincident with the rotation axis of the test rig, so that the knee flexion axis and the portal rotation axis are coincident. The knee flexion angle is set by rotating the portal and changing the angular position of the femur while keeping the axis of the tibia vertical. A flexion angle of 135° can be reached.

In this previous version, the tibia (10) is held (6) by a ring, which directly represents the movable platform of the loading manipulator. As shown in Figure 3.15, the tibial ring is driven by a system of 12 cables two by two,  $(a_1, a'_1), (a_2, a'_2), \dots, (a_6, a'_6)$ , acting in the same direction. Each pair of cables  $(a_i, a'_i)$ ,  $i=1, 2, \dots, 6$ , belongs to a closed loop (realized by means of pulleys) which includes a double-stroke pneumatic actuator ((8) in Figure 3.14) with double-ended piston rod. Each cable is slightly slack, as shown in the same figure, in a way that while the tensioned side of the loop provides a force to the tibial ring, the natural motion of the tibia is not resisted by the untensioned side. At any angular position of the portal (femur), i.e. at any knee flexion angle, only one branch of each of the six pairs will be in tension according to the wrench to be applied to the platform (tibia), the other corresponding branch being slack. In particular, the cylinders work in pairs. Each pair generates a force and a moment component respectively along and about one of the three axes of a reference system. The arrangement of the cables and their connections to the tibial ring are such that, in a relatively large workspace of the tibial ring, the wrench provided to the platform can be practically fully decoupled. When moving apart from the reference position, though, coupling of the forces and moments is present.

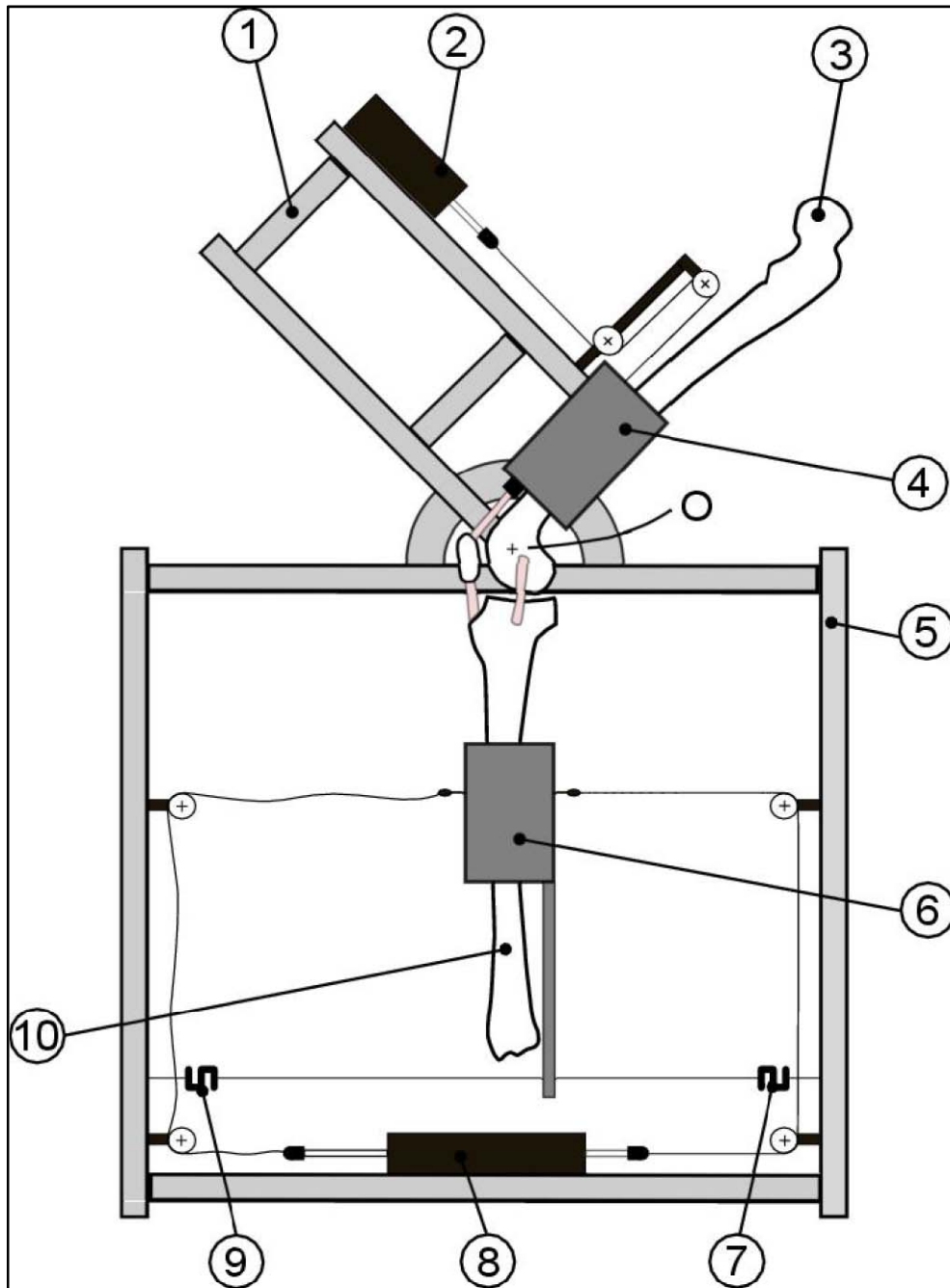


Figure 3.14 Structure of the previous version of the test rig: portal (1); single-acting pneumatic actuator (2); femur (3); femur fixation system(4); base (5); tibial ring (6); load cells (7) and (9); double-acting pneumatic actuator (8); tibia (10) [38].

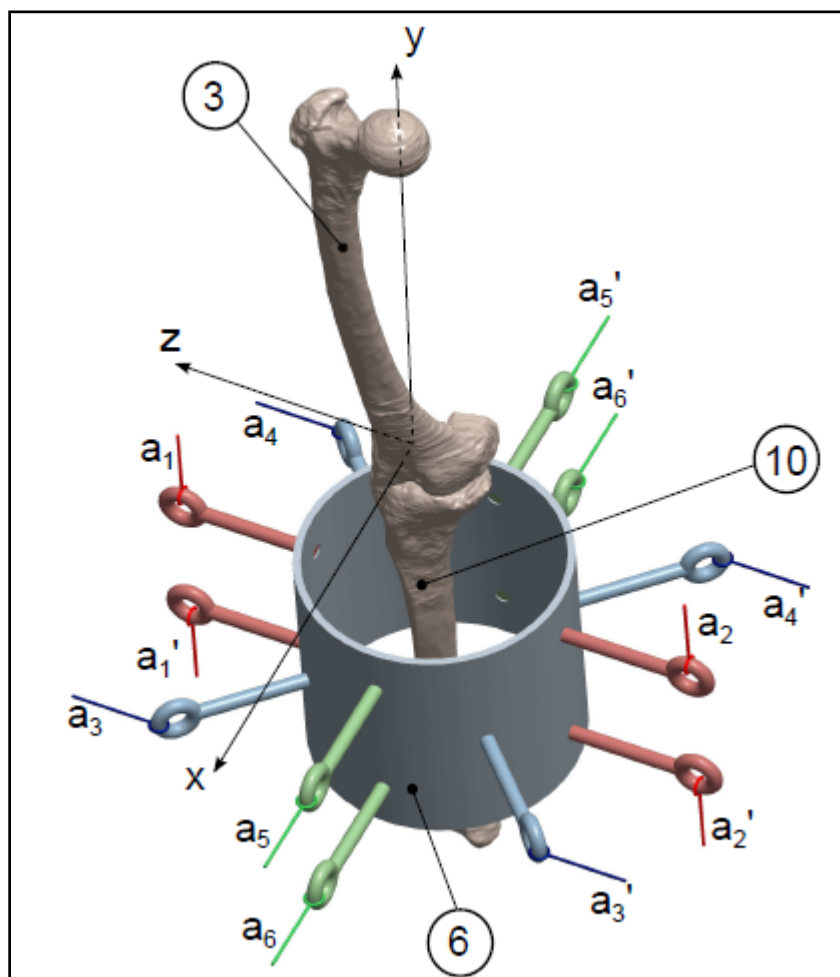


Figure 3.15 Cable arrangement and connections for the tibia loading system [38].

Beside the application of external loads, muscle force are applied on the system. In particular, extensor force are applied by means of a cable connected to a piston (2). Flexor muscles are simulated via the load applying system. Values of muscle forces are not imposed but computed in order to guarantee the equilibrium of the moment about the rotation axis with trace O. This effect is guaranteed thanks to a control system that acts in order to null the difference of tension in two load cells (7 and 9) connected to the tibia.

The pneumatic actuation is an important feature that provides an inherently force control system, thus allowing the loaded tibia to freely move in space with respect to the

femur. Six DOF are left to the tibia by the load application system. Actually, five DOF of the tibia are definitely free, since the flexion is controlled via the muscle simulation system: the projection of the tibia longitudinal axis on a plane perpendicular to the portal revolute axis is constrained to remain vertical in order to control the flexion angle. So five DOF are left to the tibia with respect to the frame: the tibia is free to move in order to reach the equilibrium pose, due to the effect of the loads and of the knee structures (articular surfaces, ligaments and muscles when activated).

The pneumatic actuation guarantees a simple open-chain force-control to the tibia, since pneumatic actuators can be controlled in force through their pressure control, after a first calibration, on the one hand. On the other hand, effects of the static friction at the beginning and at the inversion of the motion at the actuators must be considered. Alteration of the applied forces and the stick-slip effect have been observed during tests, and they cannot be considered by the control code. In addition, the pneumatic system creates some problems in the realization of tests at a speed close to that of the real movements, since quite long time is required to the actuators to reach the desired pressure.

Furthermore, the simple force control does not allow considering in real time the movement of the tibial ring (6 in Figure 3.14), which brings the system out of the decoupled configuration. This results in a variation of the applied load dependent on the position of the ring, which can be estimated only after tests when the motion is analysed.

Finally, the large sizes of the fixation systems and of the tibial connection for the cables of the manipulator limit the range of motion of the rig.  $135^\circ$  are guaranteed to the knee. For common daily activities, the flexion angle is satisfactory, but deeper flexion angles can be reached by the knee.

## CHAPTER 4.

# TECHNICAL SPECIFICATIONS OF THE NEW TEST RIG

### 4.1 RANGES OF MOTION AND LOADS

The purpose of the rig is the in-vitro evaluation of the behavior of the knee joint in loaded and unloaded conditions. As explained in Section 2.2, the evaluation of the behavior in unloaded conditions consists in the measurement of the relative pose of the tibia and the femur at each knee flexion angle, when virtually no loads are applied to the joint. The evaluation of the behavior in loaded conditions consists in the measurement of the relative poses when loads related to several given tasks, such as clinical tests and daily life activities, are applied to the joint. To permit these tests, the rig is required to let the tibia move freely with respect to the femur at each imposed flexion angle according to the applied loads, i.e. when either virtually no loads or known given loads are applied. Therefore, the rig must not introduce unwanted additional constraints to the motion components. Without introducing constraints, the test rig must be able to apply general loading conditions typical of the most common tests. Indeed, the load history during flexion strongly depends on the task: when executing clinical tests (such as the anterior drawer), in fact, loads are applied along one anatomical axis (e.g., the anterior-posterior axis); on the contrary, more general loads are applied to the joint when replicating daily activities (such as walking, sit-to-stand and squat).

Requirements on the range of the applied loads, arise from the tests reported in 2.2.4. The combinations of loads and angles are important in order to define the forces and moments component that need to be replicated at the knee according to a chosen reference system.

From the description of the movement presented in Chapter 2, it is possible to deduce the range of motion required to test normal knees. If injuries occur at the joint, indeed, the ranges of motion increase considerably [39]. Since the rig can be used to test injured knees and prostheses too, the specification in terms of motion require wider range than those determined in section 2.1.4.

Ranges of motion considered for the machine design assume the following values:

- i) Flexion/extension: total  $[-10^{\circ}; 150^{\circ}]$
- ii) Internal/external rotation:  $[-30^{\circ}; +30^{\circ}]$
- iii) Ab/adduction:  $[-30^{\circ}; +30^{\circ}]$
- iv) Medial/lateral displacement:  $[-50 \text{ mm}; +50 \text{ mm}]$
- v) Compression/distraction displacement:  $[-50 \text{ mm}; +10 \text{ mm}]$
- vi) Anterior/posterior displacement:  $[-50 \text{ mm}; +50 \text{ mm}]$

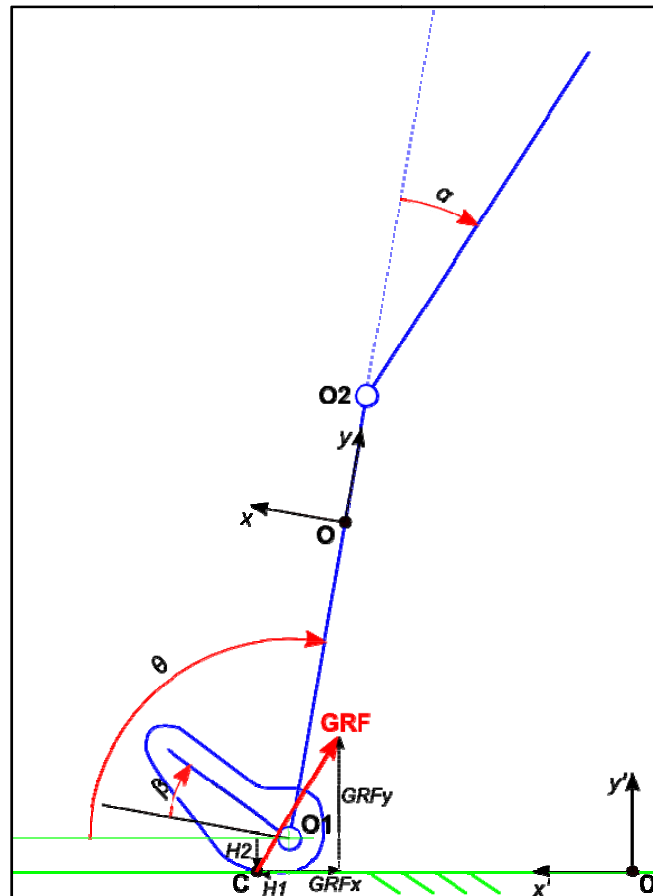
The motion requirements, indeed, have been defined in terms of 3 rotations of the tibia according to the Grood and Suntay joint coordinate system [22] and 3 translation of the center of the tibia reference system with respect to the femur reference system. The forces requirements have been defined in terms of 3 components of the ground reaction forces (GRF) with respect to a fixed reference system defined in Section 2.2.4, together with the segment angles with respect to the ground and the foot. The requirements in terms of movement and forces of the actuators strongly depend on the geometry chosen for the loading system.

A simple planar model has been used to transform the system of forces measured at the ground in the system of forces and moments that needs to be applied at knee and consequently in the system of forces and moments that needs to be applied at the reference point of the loading system. The simple model is represented in Figure 4.1 and is based on the geometrical characteristics of the specimen and on the values of the angles measured during motion.

With reference to the single model, forces are applied at the centre of pressure C on the foot. Considering the angle  $\beta$  between the longitudinal axis of the foot and the ground and the angle  $\theta$  between the tibia and the ground and the lengths of the bone segments, the

effect of the GRF at the knee can be calculated. An equivalent system of forces and moments (wrench) is so provided. At the same time, the equivalent wrench can be defined for each chosen reference point. In order to apply loads, in the new test rig a loading system will be connected to the tibia and the wrench at the loading system reference point can be calculated and explained above. Furthermore, since the relative orientation of the tibia and floor varies during motion, the wrench must be projected along the axes of a reference system fixed to the tibia, i.e. fixed to the loading system.

With this operation, the wrench of forces that the loading system has to generate on the tibia, variable with the flexion angle, can be computed, for each of the four considered tasks. The specifications in terms of the overall wrench are so defined.



4.1 Schematic representation of the planar model used to transform the system of GRF in the system of forces and moments applied by the loading system.

The adopted model is planar and thus causes some inaccuracies in the definition of the loads at the knee. Ankle and knee are modeled as revolute joints, the other associated movements are neglected. The centre of pressure is considered as aligned with the center of the knee on the sagittal plane. Medial-lateral displacement can also be considered, if necessary in this model. A more detailed model can be developed, but the one presented here is satisfactory for the scope of this work.

## 4.2 OTHER REQUIREMENTS

Furthermore, the rig must simulate the most important muscle forces and evaluate their contribution in motion: when simulating daily activities, muscles play an important role in providing the joint equilibrium and applying significant forces.

The test rig must allow easiness of specimen unmounting and remounting, together with the possibility of a precise positioning and repositioning of the specimen itself within different tests. Indeed, several experimental procedures and protocols require that some tests are repeated on the same specimen but at a different time, as, for example, before and after the implantation of a prosthetic device, thus making it necessary to unmount and remount the specimen from and to the test rig. Similarly, the specimen should be precisely aligned with the rig according to some anatomical landmarks, so that the applied loads have exactly the desired directions with respect to the joint.

Loading conditions should also show a good repeatability. These characteristics are important to guarantee the consistency among the measurements from several tests on the same or different specimens.

Since tests are performed on specimens with a wide range of sizes, the test rig is required to be versatile and easily adjustable for any leg size. The device has to be cheap and easy-to-clean. Finally, its usage in contact with human specimens determines some limitations on the materials chosen for its construction.

## CHAPTER 5.

# DESIGN OF THE NEW TEST RIG

From the technical specifications with respect to the motion and the loads presented in Section 4.1, the new rig is required to overcome both the limitation on the range of flexion noticed in the robotic-based knee testing systems (RKTS) and the limitation in the load application without altering motion encountered for the knee simulators (KS). Furthermore, it is required to overcome the critical aspects noticed in the previously realised test rig based on a cable-driven parallel manipulator. The test rig, indeed, presented also many interesting characteristics and strengths that have been exploited in the new test rig design. The functional analysis and adopted design solutions are presented in this chapter.

### 5.1 OVERALL DESCRIPTION OF THE MACHINE STRUCTURE

The frame of the new test rig is made up of three main parts, as shown in Figure 5.1: a base (4), a portal (9) and a the loading system. The frame is constituted by aluminium profiles (Bosh Rexroth 60x60) fixed together by means of standard angle connections and bolts. Similarly to the previous version of the rig, flexion is imposed to the knee, by rotating the femur (7) about an axis fixed to the frame and approximately coincident with the transepicondylar knee axis. The femur (7) is connected to the portal (9) via a six DOF femur fixation system (6) explained in detail in Section 5.3.1 The movable portal is connected to the base by a revolute kinematic pair (revolute joint), whose trace in the plane orthogonal to the joint axis is point O. Differently from the previous version, in the new one the portal is actuated. The femur, so, can only rotate about axis O fixed to the frame. The remaining coupled knee motion is permitted to the tibia (5), thus making this bone movement approximately free from the flexion component. Motion of the tibia is so

smaller. The tibia (5) is connected to the loading system (3) via a six DOF tibia fixation system (4) described in Section 5.3.2. The loading system is a 6-6 Gough-Stewart platform with electromechanical actuators (2 and 11) equipped with force sensors. Imposing flexion by means of a separated device, allows the author to develop a rig of the robot-based kind, able to reach high flexion angles. At the same time, the application of loads and the evaluation of movement can be performed quite easily. As it will be explained in the following, the control of the angular position of the portal can be approximately assimilated to the control of the flexion angle of the knee, at least for the application of the load history.

Furthermore, a system to simulate extensor muscle load is present: the muscle force is applied by means of a cable connected to the patellar tendon on one end and to an electromechanical actuator (12) on the other end. A system of pulleys (8) guides the cable that simulates extensor muscles. Finally, a control system similar to that of the previous test rig is used to control muscle forces: a load cell (1) is connected to the tibia distally and measures the movements in terms of applied forces in both traction and compression. This system permits to simulate flexor or extensor muscle loads to guarantee the equilibrium of the joint, as it will be further explained in Section 5.5.

## 5.2 TIBIA LOADING SYSTEM

The core of the test rig is the device for the simulation of external loads. As explained in the previous sections, this device must be able to apply to the tibia a wrench able to replicate at the knee joint the effect of the ground reaction forces. The wrench is a function of the flexion angle and of the replicated activity (like squat and walking). The measure of the response to applied loads in terms of relative motion between tibia and femur is the scope of the test. Thus it is important that no further constraints, except for those due to internal structures (i.e. articular surfaces and ligaments) and to muscular actions, are introduced by the loading system.

The definition of the mechanisms starts from the idea of exploiting the accuracy and repeatability of the parallel mechanisms, by realising the loading system as a parallel

---



### *5.2.1 DEFINITION OF THE ACTUATION SYSTEM*

To overcome the limitations highlighted for the previous version of the rig, the new test rig loading system is based on linear ballscrew actuators. Electromechanical actuation, indeed, seems to be the solution that offers the best benefits among the analysed ones. The characteristics of the different kind of actuations have been evaluated. In particular, pneumatic and hydraulic actuators, linear motors and rotary motors connected to ballscrews have been considered. Their properties and their dynamic characteristics have been analysed. A 6-6 Gough-Stewart platform has been taken as a reference in order to estimate the required loads and to evaluate the dynamic behavior.

Pneumatic actuation presents the advantages of being cheap and requiring a simple control system: a close-loop system control system is not necessary to impose the required force. As a drawback, friction in the seals causes resistance to motion and stick-slip phenomena can be observed. Furthermore, the air compressibility causes uncertainties and vibrations in the system; it could partially be controlled by increasing the complexity of the control system. The high forces that the system has to exert with the considered 6-6 Gough-Stewart arrangement require high pressures or big sizes of the actuators.

Hydraulic actuators present the advantage of being controlled in force through pressure, thus requiring a quite simple control system as the pneumatic ones. The regulation of the forces results a bit more complex since at high pressure a moderate percentage variation of pressure generates a big variation in terms of generate force. An accurate force control, thus, requires good quality valves and an accurate control system, which increase the total costs of the implant. In addition, the problem of friction at the inversion of motion and of stick-slip phenomenon is not solved with hydraulic actuation, since hydraulic pistons still have seals mounted on them. Particular constructive solutions can reduce the phenomenon but they require a special design. Finally, the pump, the tank and the other devices for producing high-pressure oil are heavy and difficult to transport.

Last, electric actuation has been evaluated. In particular, two kinds of solution have been considered: linear stepper motors, and linear ballscrews equipped with rotary stepper motors. As a common point, these two kind of actuators require a closed-loop control system, since a direct force control is difficult to realise. In detail, linear stepper motors guarantee precise positioning and low vibrations. On the counterpart, they are very expensive and the longer the stroke is, the heavier and the more expensive they are. Their cost is about five to ten times the cost of the other commercial actuators. As linear stepper motors, also rotary stepper motors connected to ballscrews guarantee precise positioning and low vibrations. The connection between the motor and the mechanical actuator introduces some backlash that must be reduced or considered in the control system. If compared with the linear stepper motors, they are cheaper.

From the general considerations reported above, pneumatic actuation has been discarded because of the several drawbacks difficult to overcome without increasing the system complexity, thus losing its advantages. The costs, too high for this kind of testing rig, has lead the author to discard the linear stepper motor too. Hydraulic actuators and ballscrews with rotary motors both offer advantages and disadvantages. The dynamic performances of hydraulic actuators seem to be a bit better of those of the ballscrews with a comparable size. In particular, the piston of hydraulic actuators can reach high velocities, since the oil acts directly on it. Conversely, in the electromechanical actuators there is a transmission system and a reduction ratio between the motor and the ballscrew, in order to exert the high forces. Thus, the electromechanical actuator results less quick than the hydraulic one, but it still satisfies the specifications.

Given that the hydraulic solution seemed to be the better one, some hydraulic actuators producers have been contacted in order to understand the possible solution to overcome, or at least reduce, the problem of friction and stick-slip. Albeit some solutions exist, they need to be studied for the precise applications and prototypes need to be realized in order to understand if the problem can be solved or not. This way, the costs of the pneumatic system increases. Mainly for this reason and for the high weights of the hydraulic solutions, the electromechanical one has been preferred.

### 5.2.1.1 CHOICE OF THE ACTUATORS

Once the electromechanical actuation has been chosen, the opportunity to buy the actuators by using some funds came out. The evaluation of the loads and the velocity, i.e. the power, required to the actuators has been done on the base of two reference architectures: a classical 6-6 Gough-Stewart platform and a decoupled architecture (see Subsection 5.2.2.1). The two architectures are not described in details here, for the sake of brevity and because an extensive discussion on the optimal architecture is reported in the next section. Two mounting positions for the platform with respect to the knee have been tested.

Forces required to the leg in order to replicate the most demanding wrench representative of the motion tasks have been calculated by means of the software Matlab®. The loading conditions were replicated at different poses of the platform. Furthermore, with the same architectures, some experimentally measured trajectories have been simulated in order to understand the required velocities. The most demanding combination of forces and velocities are reported in Table 5.1 for each architecture. Required power is reported in the same table. Based on the geometry of the tibial fixation of the previous rig [38], the maximum required stroke of the actuators was calculated to be 180 mm.

*Table 5.1: Maximum loads and velocities at the actuators and derived power, calculated for classical 6-6 (CL) and decoupled (DEC) architectures mounted in positions 1 and 2.*

	F_max [N]	V_max [m/s]	P_max [W]
CL_1	2843	0.1526	433.9640
CL_2	3672	0.1526	560.4854
DEC_1	0935	0.2778	259.8275
DEC_2	1146	0.2778	318.3992

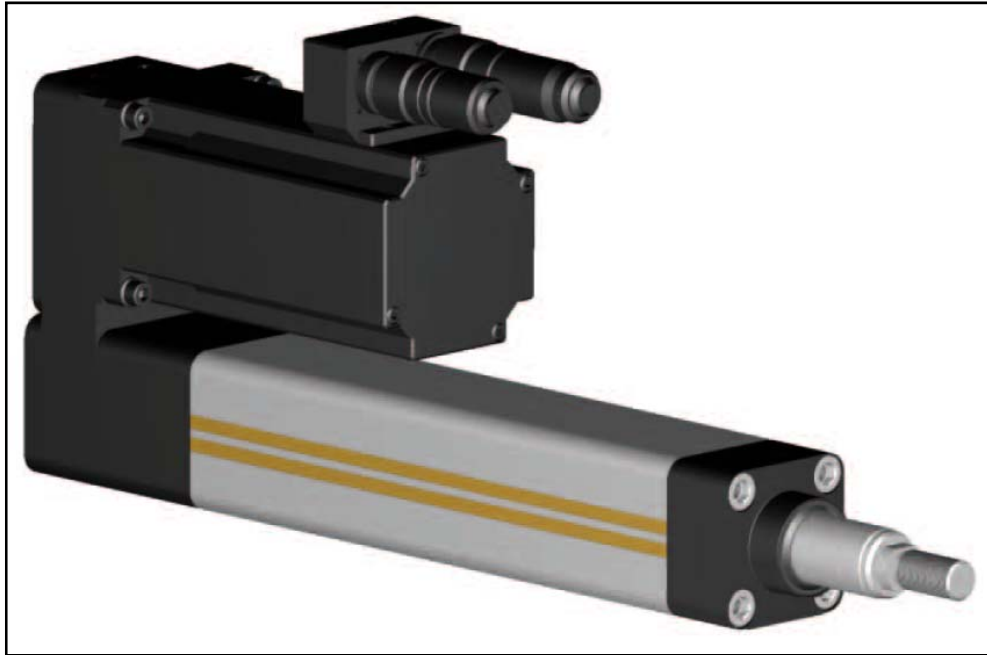


*Figure 5.2 Ballscrew with motor mounted in parallel.*

Then, by evaluation of this specifications and other technical aspects as sensibility and resistance to lateral loads, linear ballscrew Parker actuators, Model ETH05M05C1K1CCSN0300B (Figure 5.2) have been chosen. In Attachment A1, the principal characteristics of the selected actuator are reported.

To face the high lateral loads due to the action of their own weight in certain mounting condition, the actuators have been chosen higher than 200 mm so that the actuator could bear a higher lateral force.

Rotary stepper motor SMEA8230038142I65D52 1 has been chosen for linear ballscrew. This motor is equipped with resolver and brake. The resolver is useful to constantly measure the position of the actuator, while the brake allows blocking the actuators in any desired position.

### 5.2.1.2 LOAD CELLS FOR ACTUATORS

Since a closed loop force control is required, the actuators have been equipped with force sensors, in order to continuously control the force they apply. The nominal force of the load cells is high, since 4 kN can be exerted by the actuators, so must be measured. The accuracy of measurement is an important aspect for the correct loading system control and load replication. The load cell accuracy, indeed, influences the calculation of the wrench applied by the loading system on the specimen.

Furthermore, the actuators working condition foresees their mounting between two universal and/or spherical joints: not only axial load is present on the load cell, but also bending due to actuators weight. Thus, loads cells have been chosen in order to have small bending influence.

Force transducers U10M have been chosen. Their mounting configuration on the actuators is represented in Figure 5.3. These load cells guarantee high accuracy (accuracy class 0.03) and reduce bending moment influence (<0.01%). As a drawback, they have big dimensions, as shown in Attachment A2.

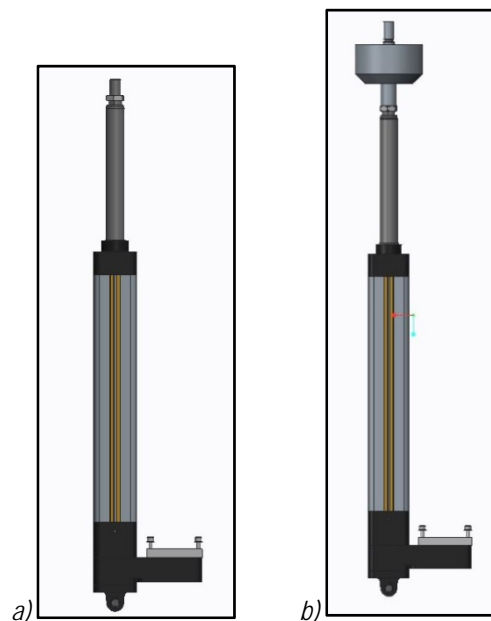


Figure 5.3 Actuator without ( a ) and with ( b ) load cell mounted on it.

## 5.2.2 IDENTIFICATION OF THE BEST CONFIGURATION

Once chosen the 6 actuators, a deep analysis has been performed in order to compare different assembly architectures for the manipulator due to load application. All of them are fully parallel, in order to guarantee stiffness, precise positioning and high load capacity. Dexterous workspaces, singularities and maximum required forces have been evaluated and compared. The most suitable architecture has been chosen.

### 5.2.2.1 ANALISED ARCHITECTURES

The following architectures were analysed and compared at first:

- i. the common 6-6 Gough-Stewart platform architecture;
- ii. the common 6-3 Gough-Stewart platform architecture;
- iii. the *in-line* leg architecture;
- iv. the *decoupled* architecture;
- v. the *lying-leg* architecture.

For each architecture, different assembly configurations were evaluated, taking as a reference for the geometry the dimension of the mobile platform and the leg length. The leg length, indeed, depends on the dimension of the actuators. The reference dimension of the platform has been chosen as the smallest dimension that allows to contain and fix the tibia. In the following, the tested geometries are described. Descriptions will be enriched with figures representing the geometrical characteristics of the various architectures when the platform is in its rest (or reference) position. The rest pose is the pose in which:

- the platform has zero rotation about all the three axes, i.e. the platform is parallel to the base;
- the actuators have all the same length  $L_0$ , which is coincident with the mean possible length of the actuators (exception is made for the *in-line leg* architecture, as it will be clarified below).

i. the common 6-6 Gough-Stewart platform

The centers of the twelve couples that provide connections between legs and base (six) and between legs and platform (six) lie on the concentric circumferences and the geometric parameters are defined as follows, with reference to Figure 5.4:

- vii) diameter of the platform (fixed):  $d_{plat} = 130 \text{ mm}$ ;
- viii) diameter of the base:  $d_{base} = [600 \ 700 \ 800 \ 900 \ 1000 \ 1100] \text{ mm}$ ;
- ix) semiangle of the platform:  $\alpha_{plat} = 15^\circ$
- x) semiangle of the base:  $\alpha_{base} = 5^\circ$

Varying the dimension of the base, the final configuration changes, and thus the workspace and the forces.

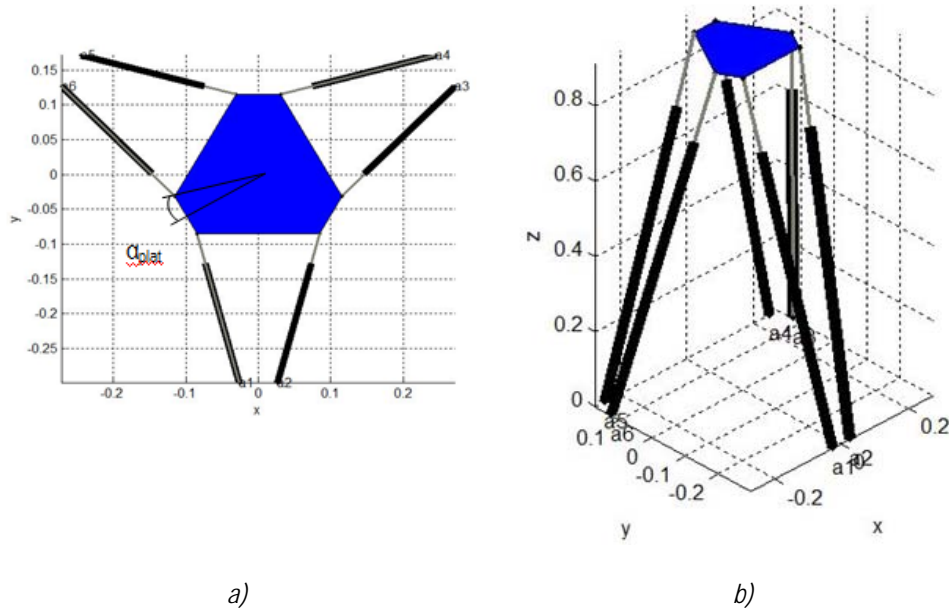


Figure 5.4 Configuration of the common 6-6 Gough Stewart platform; a) top view; b) 3D representation.

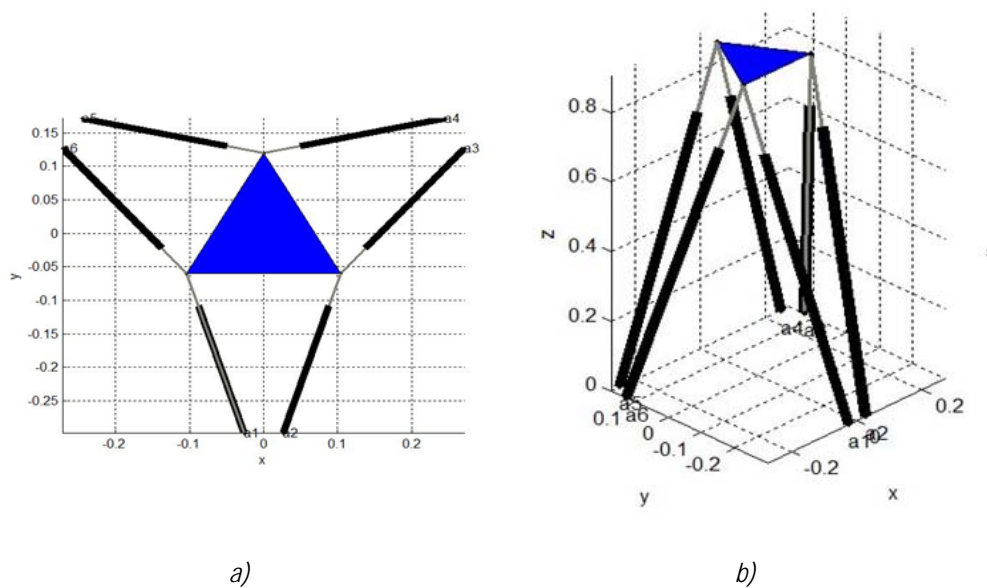


Figure 5.5 Configuration of the common 6-3 Gough Stewart platform: a) top view; b) 3D representation.

## ii. the common 6-3 Gough-Stewart platform architecture

The centers of the six couples that provide connections between legs and base are disposed as described for the 6-6 Gough-Stewart platform. On the platform, the legs are connected in pairs to the same point, thus only three connection points are defined on the platform ( $\alpha_{plat} = 0^\circ$ ). The same dimensions as for the 6-6 architecture have been tested for base and platform. A schematic representation is reported in Figure 5.5.

## iii. the *in-line* leg architecture

This architecture is similar to a traditional 6-6 Gough-Stewart platform but presents a different disposition of the attaching points of the actuators. Indeed, the attaching points on the base are aligned on two parallel lines, disposed on the two sides of the specimen, in order to obtain visibility from the front and the rear parts of the machine, i.e. to facilitate the motion recording with the stereophotogrammetric system. The architecture is represented in Figure 5.6. The attaching points on the platform are defined consequently on a circumference with  $d_{plat} = 130 \text{ mm}$ .

During the analysis, parameters  $d$  and  $b$  are modified together in a way that  $d = b = [200\ 250\ 300\ 350\ 400]\text{ mm}$ .

With this configuration, actuators 2, 3, 5 and 6 are consistently longer than actuators 1 and 4 at the rest position of the platform. Both the solution of increasing the lengths by adding a cylindrical piece to the actuator and by lifting the attaching points of the actuators of 100 mm have been considered in order to not limit the range of motion for assembly necessities.

### iii. the *decoupled* architecture

This configuration is born from the idea of decoupling forces and moments in order to minimize the forces on the actuators, similarly to what was done with the cable-driven manipulator described in Section 3.3. Actually, the decoupling is realized just at the reference pose of the platform, while coupling among forces and moments appears when a movement is realized. This architecture, indeed, is the one that guarantees the lowest forces at the actuators.

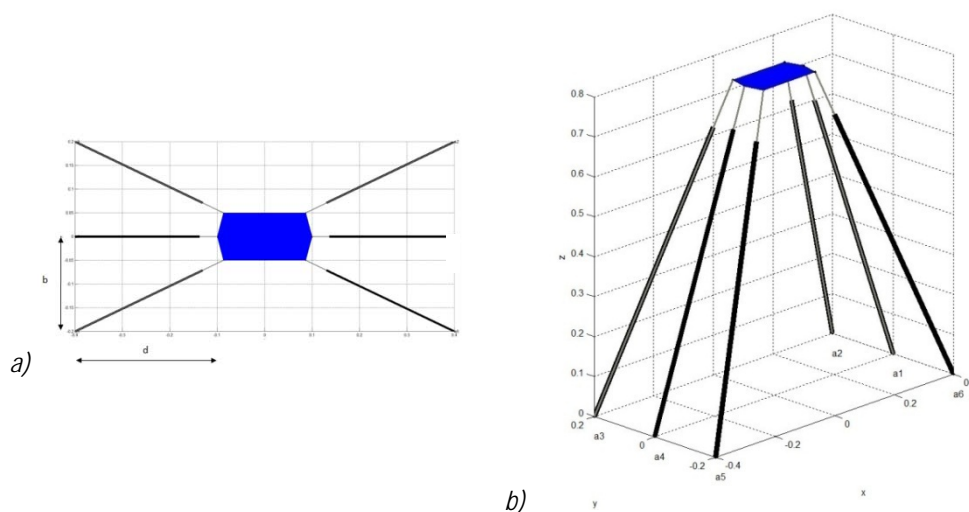


Figure 5.6 Characteristic parameters of the in-line leg configuration.

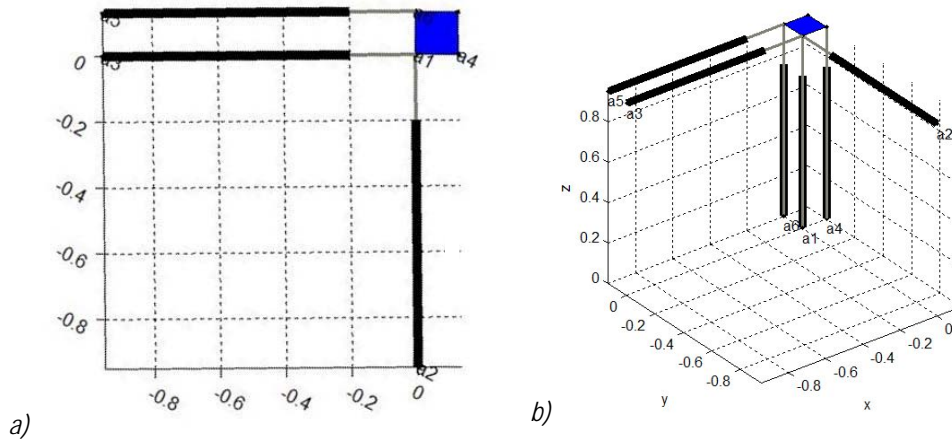


Figure 5.7 Decoupled architecture: a) top view; b) 3D view.

To obtain this configuration, it is necessary to have 3 actuators disposed perpendicular to one another, i.e. along the three axis of an orthogonal reference system, and converging to the same point (actuators 1, 2 and 3 in Figure 5.7). These three actuators control the pose. The three other actuators can be disposed in the space in order to generate moments about the three axes. In particular, with reference to Figure 5.7, actuator 2 applies a force along  $x$  axis, actuators 3 and 5 apply a force along  $y$  axis, actuators 1, 4 and 6 apply a force along  $z$  axis; furthermore, actuators 1 and 6 generate a moment about  $x$  axis, actuators 1 and 4 generate a moment about axis  $y$  and actuators 3 and 5 generate a moment about  $z$  axis. In this sense, not all the actuators are involved in generating all the forces and all the moments, but their role is limited to some components of moment and forces.

The described is only one of the possible solutions that can be adopted to obtain a complete or partial decoupling. This solution requires a difficult-to-realise triple spherical couple at the connections among platform and actuators 1, 2 and 3. In the first phase, different architectures have been developed in order to obtain partial or complete decoupling, on the one hand, and to simplify the assembly on the other hand. They are analysed in the following and are reported in Figure 5.7. The common

characteristic of the actuator is that the length of the edge of the platform (in  $x - y$  plane) is 130 mm.

- a. Configuration similar to the one described above, with the translation of the attachment points of three actuators converging at the triple spherical couple. The leg are moved of a small quantity (25 mm) along the axis of the actuators, in order to separate the attachment points and realize 3 different spherical couples. Both configurations in which actuators 2 and 3 (Figure 5.8a) are moved and actuators 1, 2 and 3 are moved with respect to the reference point have been analysed. This geometry permits to solve the constructive problem without altering the functional characteristics described above.

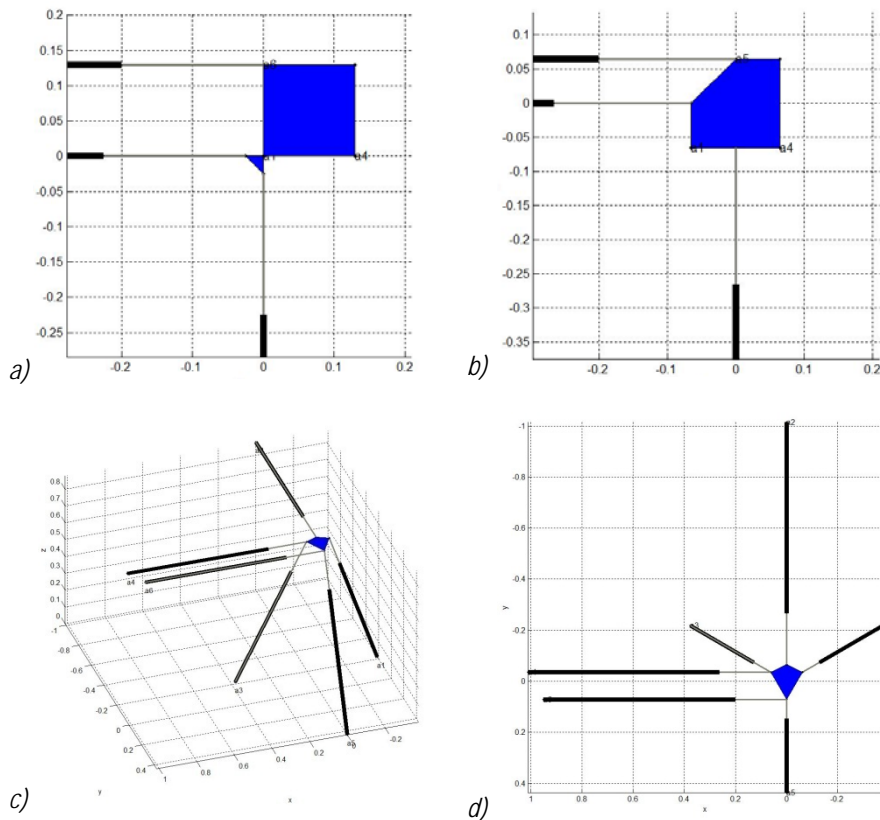


Figure 5.8 Variations of the decoupled architecture: a) configuration a, with two actuators of the spherical couple translated in space; b) configuration b, with three actuators converging in the center of the platform; c) 3D view and d) top view of the tetrahedral architecture.

- b. Actuators mounted in a way that the converging point of the actuators 2 and 3 is in the center of the platform (Figure 5.8b). This way, advantages on decoupling are obtained but a wider range of motion of the center of the platform is obtained, thus profiting the most of this architecture.
- c. Actuators 1, 3 and 5 are disposed perpendicular to one another and along three edges of a tetrahedron converging to the same vertex and the other three are disposed in a way to obtain the decoupling (Figure 5.8c and d). This way, the decoupling is not obtained along the three principal direction of the joint, but along the directions of the actuators. So coupling would be necessary to generate forces along x, y and z axis. At the same time, the actuators could be mounted in a way that the vertex is close to the centre of knee joint. To obtain this configuration, larger spaces are necessary.

When analysing the different architecture, the distance between the attachment points of actuators 4, 5 and 6 has been modified, maintaining constant the platform size. Distance from the spherical couples were varied from 130 to 80 with step of 10 mm. This way, the relative position between actuators and the centre of the platform has been varied.

iv.      the *lying-leg* architecture

Differently from the other configurations, the actuators of the system lie on the floor and their sliding causes the motion of the platform via 6 fixed-length legs. Actuators and fixed-length legs are connected via spherical couples. This configuration allows to minimize the forces applied to the actuators and to significantly reduce the weight of the moving part. The realization of a sliding couple between the floor and the end effector of the actuators is required in correspondence or close to the spherical couple with the fixed-length legs, to bear the lateral loads on the end effector and to allow a correct functioning of the actuators. This sliding couple introduces friction, whose effects imply higher complexity in the control system. In Figure 5.9 the mounting condition of the platform at its reference pose is shown.

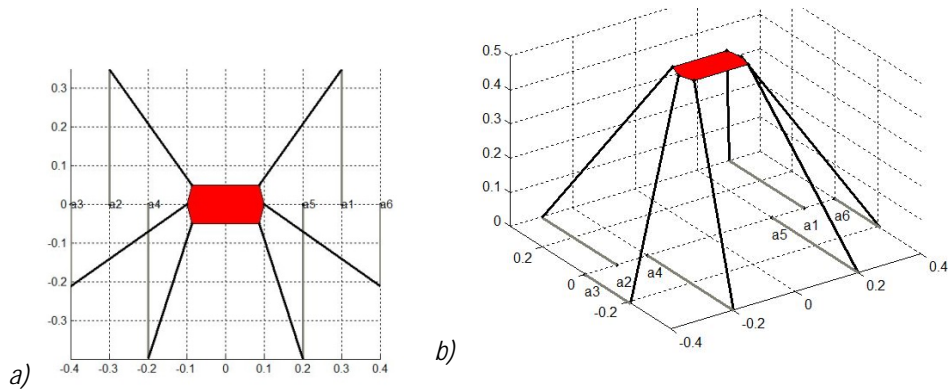


Figure 5.9 Geometry of the lying leg architecture: a) top view; b) 3D view.

### 5.2.2.2 COMPARATIVE ANALYSIS 1.0

In order to define which of the previously described configurations is the most suitable for the considered application, analysis have been performed in terms of dexterous workspace, singularities and forces. The methods adopted to perform these analyses and the obtained results are described in the following.

It is worth noting that the specifications in terms of loads have been defined in Section 4.1 as the GRF, i.e. the forces exchanged between foot and ground. The displacements have been defined at the knee joint. Both these specifications, indeed, have been transformed in the specifications at the parallel manipulator, by considering that the tibia was mounted with its long axis perpendicular to the plane of the platform. Furthermore, the centre of the platform has been posed in correspondence of the centre of the knee in medial-lateral and anterior-posterior direction, but moved distally toward the foot of 100 mm. The simple planar model presented in Section 4.1 has been used to define the wrench to be applied at the reference point.

## DEXTEROUS WORKSPACE

### METHOD

The dexterous workspace of a manipulator is the manifold of the point reachable by a reference point on the platform while the platform has a certain orientation.

The dexterous workspaces has been analysed by founding the volume that the centre of the platform could reach with the platform allow orienting according to all the combinations of the following extreme rotations (defined according the Grood and Suntay joint coordinate reference system [22]):

- i) Flexion:  $[-10^\circ; 0^\circ; +10^\circ]$ ;
- ii) Adduction:  $[-30^\circ; 0^\circ; +30^\circ]$ ;
- iii) Internal rotation:  $[-30^\circ; 0^\circ; +30^\circ]$ .

The dexterous workspace has been calculated for all the architectures varying the size parameters. It has been compared with the required dexterous workspace, i.e. the manifold of point included inside the range of translations reported in 4.1.

The calculation method is based on the so-called geometrical approach. It is based on the determination of the geometrical limits of the manipulator workspace, by considering the geometrical limits imposed by each leg on a reference point. In particular, taken the center of the platform as the reference point, all the reachable positions with a certain orientation  $j$  of the platform are calculated as the results of the constraint imposed by the single leg  $i$ . The space  $W_i^j$  is so obtained. The reachable workspace  $W^j$  at the configuration  $j$  is computed as the intersection of the 6 workspaces  $W_i^j$  allowed by the 6 legs of the manipulator. Finally the dexterous workspace is the intersection of the workspaces computed for all the 27 combinations of rotations. In particular, let the reader analyse a 6-SPU Gough-Stewart platform. If considering each single leg  $i$ , the only constraint is due to the length of the leg, which can vary between  $r_{min}$  and  $r_{max}$ . The connecting point between the leg and the platform  $B_i$  is constrained to remain inside the space included between the surfaces of two spheres of radii  $r_{min}$  and  $r_{max}$ , both centered in the connecting point between the leg and the base  $A_i$ , as show in

---

Figure 5.10. If considering the point  $C$  taken as the reference point on the end effector, since a certain orientation has been imposed, it is constrained to remain in a similar workspace, with the center translated of the vector  $B_i C$ .

## RESULTS

The results in terms of dexterous workspaces are represented as scatter plots in the following for the different architectures, with different colors for different dimensional parameters. The required workspace is also represented as blue parallelepiped in order to understand if the platform meets the specifications or not.

In Figure 5.11 the three dimensional and the projected dexterous workspace is represented for the 6-3 and 6-6 architectures for different values of the radius of the circumference on which the actuators are connected on the base (as reported in Section 5.2.2.179). As expected, the dexterous workspace is larger for small values of the base diameter (red color) than for big values (blue color). Furthermore, the 6-3 platform (first line in Figure 5.11) guarantees wider motion than the 6-6 architecture (second line in the same figure). All the dexterous workspaces determined with the different architectures and dimensions are sufficient to satisfy the specifications in terms of motion.

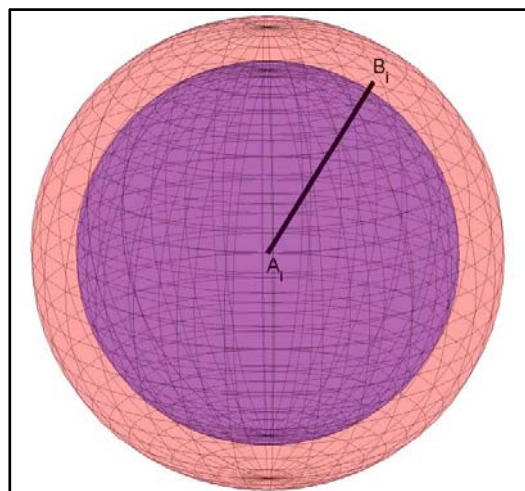


Figure 5.10 The space that point  $B_i$  can reach is contained between the surfaces of the purple and pink spheres, both centered in  $A_i$ .

In Figure 5.12 the three dimensional and the projected dexterous workspace is represented for the 6-6 architecture with the actuators disposed in line at different values of the  $b$  and  $d$  parameters. In the first line from the bottom of Figure 5.12b, the attaching points of the actuators on the base are all on the same plane, while in the second line results are reported for the assembly with the attaching points of the external actuators lifted from the base of 100 mm. As in the previous case, the dexterous workspace is larger for small values of the base dimensional parameters (red color) than for big values (violet color), but presents a different geometry. The computed dexterous workspaces are sufficient to satisfy the specifications in terms of motion, since the required workspaces are included in them. The only case that does not satisfy the specifications the one with the wider dimensions, with the external actuators lifted with respect to the central ones (violet, first line).

In Figure 5.13. the three dimensional and the projected workspace is represented for the decoupled architecture in its classical and its variation a) assemblies, varying the distance between the actuators, without varying the dimension of the platform. With reference to Figure 5.13b, in the last line, the standard version of the decoupled platform is represented. In the second and in the third lines, the dexterous workspaces are represented for the two variation a): attachment points of the actuators 2 and 3 and of the actuators 1, 2 and 3 moved for the second and third lines respectively. The reader can note that the reference point, i.e. the centre of the square platform, presents a dexterous workspace shifted with respect to the required workspace. Actually, if the centroid of the computed workspace was shifted in correspondence of the centroid of the required workspace, the required workspace would be included in the computed workspace. This would correspond to a different reference position for the platform, i.e. it would correspond to a rest point at which no decoupling is present. In Figure 5.14 the three dimensional and the projected dexterous workspace is represented for the decoupled architecture type b. As it can be noted, the required workspace is contained in the computed dexterous workspace. For the decoupled architecture, only this type of assembly can satisfy the specification in terms of dexterous workspace, whilst conserving the advantages in terms of decoupling of force and moments.

---

Finally, in Figure 5.15 the dexterous workspace computed for the lying-leg configuration is represented. As the reader can easily notice, the computed dexterous workspace has a shape that does not contain the required workspace.

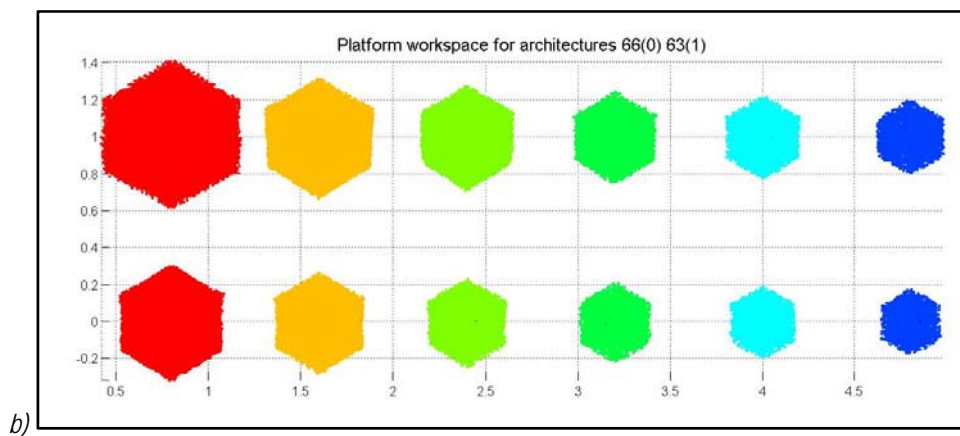
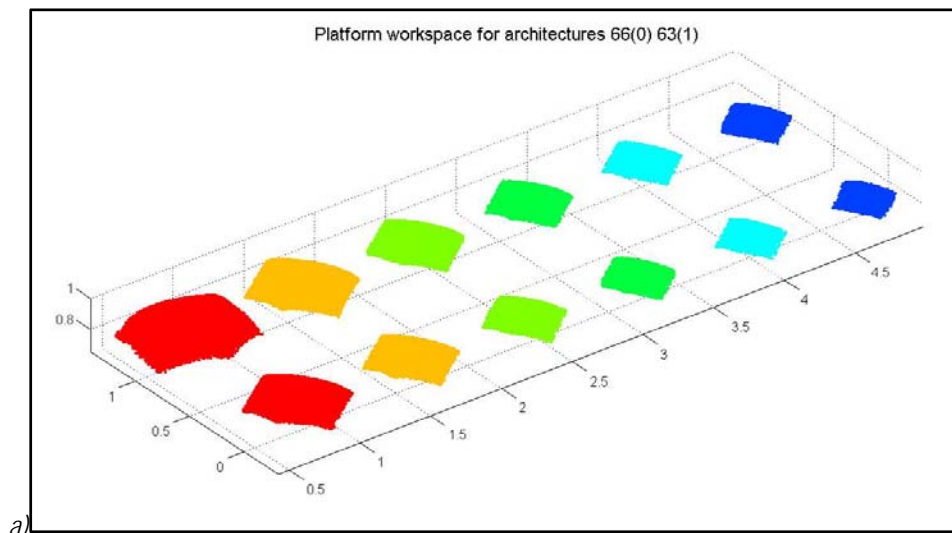


Figure 5.11 Dexterous workspaces for the 6-3 (first line) and 6-6 (second line) classical Gough-Stewart platform with different bases diameters. Base diameters increase from left to right side. a) 3D-workspace; b) workspace from the top.

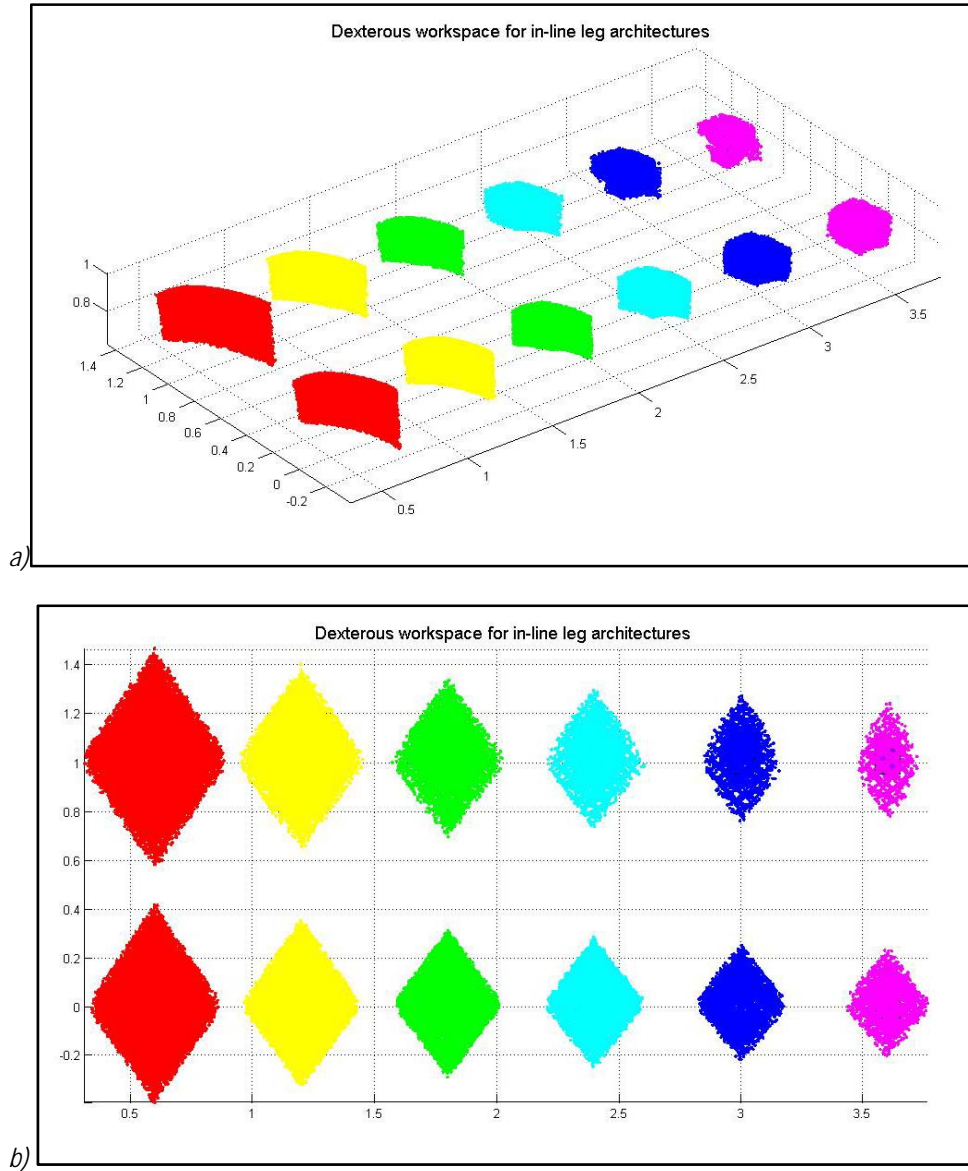


Figure 5.12 Dexterous workspaces for the in-line leg architecture with different base parameters, with joints attached on the same plane or at different heights with respect to the base. Base parameters increase from left to right side. a) 3D-workspace; b) workspace from the top.

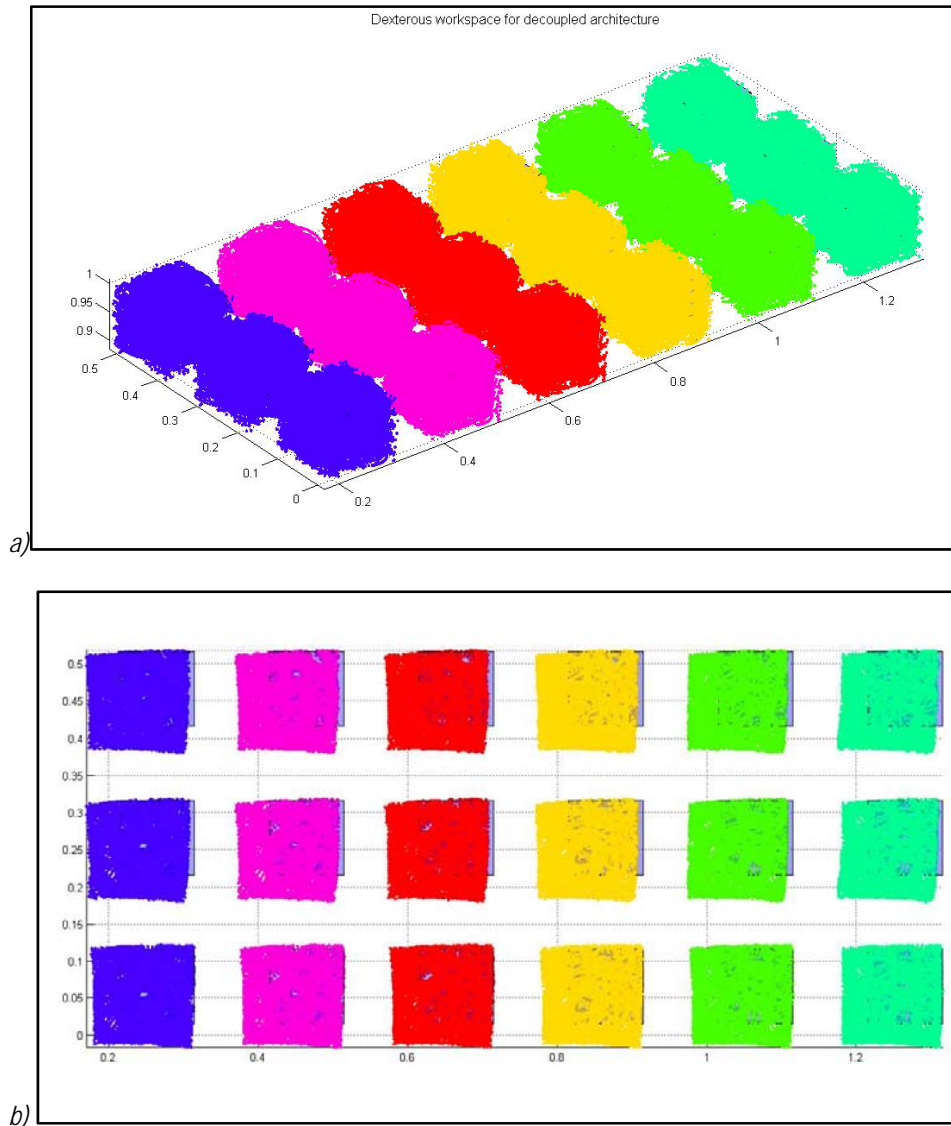


Figure 5.13 Dexterous workspaces for the decoupled architecture in its standard version and two variation type a) with different attachment point on the platform. Distance between actuators decreases from left to right side. a) 3D-workspace; b) workspace from the top.

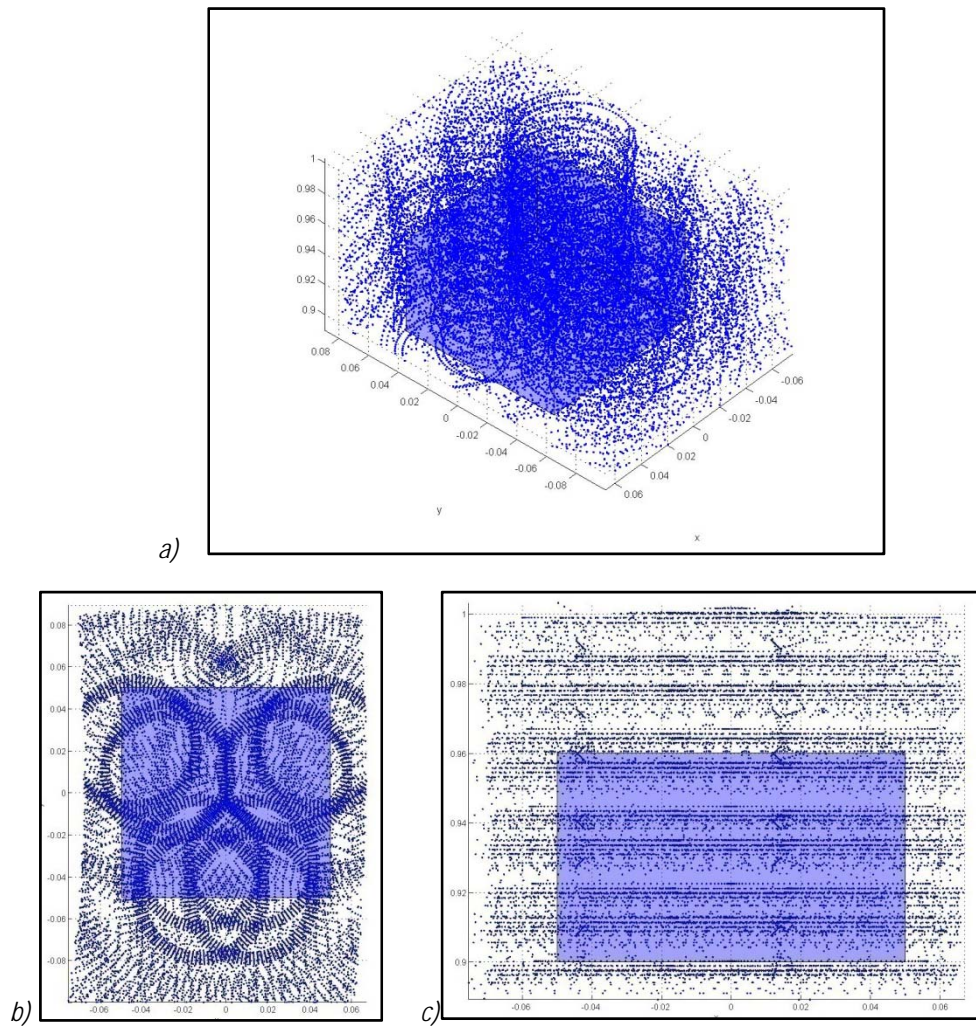


Figure 5.14 Dexterous workspace for the decoupled architecture, type b: a) 3D-workspace; b) workspace from the top; c) workspace from the side.

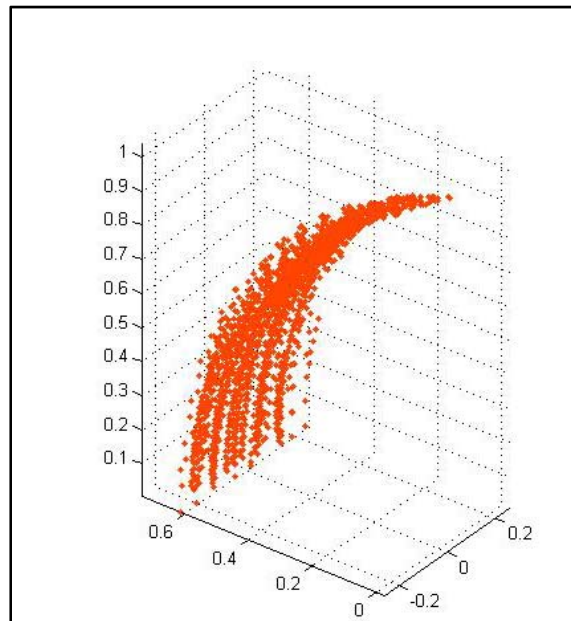


Figure 5.15 3D dexterous workspace for the lying-leg architecture.

#### FINAL CONSIDERATIONS ON THE WORKSPACE

From the analysis of the dexterous workspace, it has been noted that with the considered dimensions, the 6-6 and the 6-3 traditional Gough-Stewart architectures offer the possibility to reach all the pose required by the specifications. Also the *in-line leg* architecture offers this possibility for almost all the dimensions. The *decoupled* architecture presents problems, which let the author discard some of the proposed solutions, in particular the basic decoupled architecture and its variations a. Only the variation b satisfies the specifications. The *lying-leg* architecture does not satisfy the specifications in terms of workspace.

## SINGULARITY ANALYSIS

### METHOD

Let the reader consider a non redundant parallel robot with 6 gdl. The pose of the end-effector is described by a vector  $\boldsymbol{x}$  with six components. The kinematic relationship relates the pose of the end-effector  $\boldsymbol{x}$  to the vector of joint coordinated  $\boldsymbol{q}$ , and can be written as:

$$\boldsymbol{f}(\boldsymbol{q}, \boldsymbol{x}) = \mathbf{0} \quad (5.1)$$

The system presents 6 equation with 6 unknowns.

By deriving the expression, it is possible to write the relationship between the velocity of the end-effector  $\dot{\boldsymbol{x}}$  and the velocity of the joints  $\dot{\boldsymbol{q}}$ :

$$\boldsymbol{J}_x \dot{\boldsymbol{x}} = \boldsymbol{J}_q \dot{\boldsymbol{q}} \quad (5.2)$$

where  $\boldsymbol{J}_x = \frac{\partial \boldsymbol{f}}{\partial \boldsymbol{x}}$  and  $\boldsymbol{J}_q = \frac{\partial \boldsymbol{f}}{\partial \boldsymbol{q}}$ .

And by inverting matrix  $\boldsymbol{J}_x$ , it is possible to write:

$$\boldsymbol{J} \dot{\boldsymbol{x}} = \dot{\boldsymbol{q}} \quad (5.3)$$

Where  $\boldsymbol{J} = \boldsymbol{J}_q^{-1} \boldsymbol{J}_x$  is called Jacobian matrix of the system.

A similar relationship can be written between the wrench applied at the end-effector and the forces/moment at the joints

$$\boldsymbol{J}^{-1} \boldsymbol{F} = \boldsymbol{\tau} \quad (5.4)$$

For an assigned wrench  $\boldsymbol{F}$  at the end-effector, this system has a unique vector of joint forces  $\boldsymbol{\tau}$ , except in case of singularity. Singularity occurs when the Jacobian matrix is not invertible, so the parallel robot acquires uncontrollable DOF. In this situation, forces at the actuators can become incredibly high without generating forces at the end-

effector. In singularity configurations, the pose of the end-effector cannot be controlled. It is so necessary to verify that singularities do not occur during motion. This kind of singularities are called kinematic singularities.

Furthermore, a robot can present singularities caused by its particular architecture. In this case, singularity is present at every configuration of the robot and is called architectural singularity. This kind of singularity occurs when the base and the platform are shaped as two equal or similar regular polygons. Once verified that the architecture of the robot does not cause an architectural singularity, it is necessary to verify the absence of kinematic singularities during the motion of the robot, at any interesting configuration.

To verify that no configuration presents singularities, the determinant of the Jacobian matrix  $\mathbf{J}$  must be calculated at each pose according to the used numerical method. Indeed, the Jacobian matrix is obtained from the product of two matrixes:  $\mathbf{J}_q$  and  $\mathbf{J}_x$ , so singularities can occur when the determinant of matrix  $\mathbf{J}_q$  is null and/or when the determinant of matrix  $\mathbf{J}_x$  is null.

When  $\det(\mathbf{J}_q) = 0$ , it is possible to move joints with vector  $\dot{\mathbf{q}}$  and no motion will be registered at the end-effector. The manipulator loses one or more DOF. At the same time, forces can be applied at the end-effector without applying forces at the actuators. This kind of singularity generally appears at the limits of the workspace and is called inverse-kinematic singularity.

When  $\det(\mathbf{J}_x) = 0$ , it is possible to move the end-effector with certain vectors  $\dot{\mathbf{x}}$  without inducing motion at the actuators. This means that infinitesimal displacements at the end-effector can occur when the joints are blocked.

For the evaluation of the singularities of the machine, the two matrixes can be analysed. For the specific case, matrix  $\mathbf{J}_q = \mathbf{I}$ , so it is never singular. The analysis is focused on the matrix  $\mathbf{J}_x$ . It has been performed numerically, by investigating the values of the matrix determinant on a high number of points inside and outside the required

workspace. In particular, a grid of point has been investigated around the reference position of the end-effector, with the parameters reported in Table 5.2.

Furthermore, the evaluation of the determinant along the points of some curves crossing the workspace have been analysed.

*Table 5.2 Parameters of the workspace grid in which the determinant has been investigated*

Direction	Minimum value [mm]	Maximum value [mm]	Step [mm]
Anterior/Posterior	-100	+100	5
Lateral/Medial	-100	+100	5
Compression/Distraction	-60	+20	3

## RESULTS

For each of the architectures and the possible dimensions, the minimum value of the determinant has been registered. In particular, the minimum determinant registered for 6-6 and 6-3 architectures is reported in Figure 5.16.

No singularities have been registered for all the analysed architectures, both the traditional and the less common ones.

The value of the minimum determinant for the 6-3 architecture is about 1,5 times the value determined for the 6-6 architecture ( $2.490 * 10^{-4}$  for the 6-3 and  $1.616 * 10^{-4}$  for the 6-6). The value of the determinant grows with the base, as shown in Figure 5.16. The last result could be expected, since a more uniform distribution of the legs in the three directions is obtained by enlarging the base.

In general, the *in-line leg* architecture presents lower value of the determinant if compared with all the analysed geometry. The lowest value ( $5,353 * 10^{-5}$ ) has been registered for the in-line leg architecture, smallest base, with lateral actuators lifted from the base. Furthermore, as expected, the decoupled architecture is the one that presents

the highest values of the determinant ( $1.431 * 10^{-3}$ ). As a reference for this study, the value of the 6-6 in an architectural singularity is about  $1 * 10^{-56}$ .

## CONSIDERATIONS

No singularities have been identified for the considered architectures in the considered points. The comparison of the values of the determinant highlights the advantages guaranteed by the decoupled architecture in terms of forces distribution. Conversely, the smallest determinant of the Jacobian has been shown by the *in-line leg* architecture. If considering Equation 5.4, it reveals that high forces at the actuators are required to obtain certain forces at the end-effector. For this reason, the *in-line leg* architecture has been discarded.

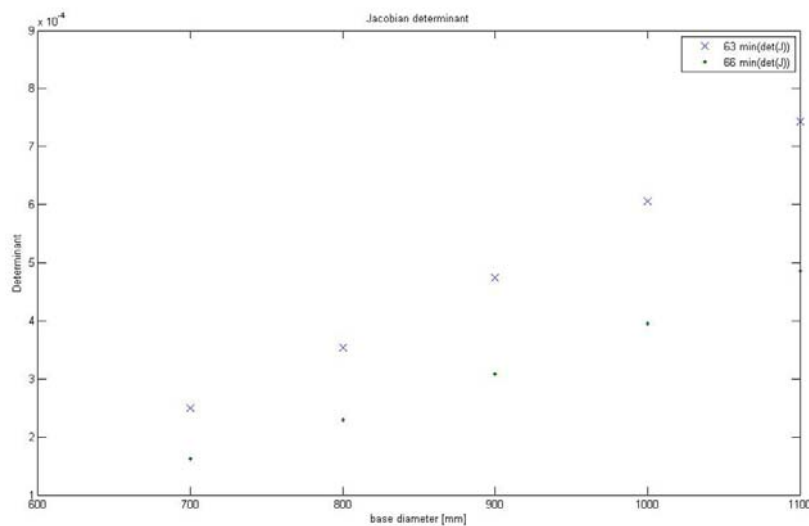


Figure 5.16 Values of the minimum determinant computed for the 6-3 and 6-6 Gough-Stewart architectures.

## STATIC ANALYSIS

### METHOD

The static analysis of the manipulator has been executed by simulating the three common tasks widely explained in Section 2.2.4. The wrench  $\mathbf{F}$  that the parallel manipulator has to apply at the tibia has been calculated via the planar model, as already discussed. The wrench is function of the task  $t$  and the flexion angle  $\alpha$  of the knee.

The vector  $\boldsymbol{\tau}(t, \alpha)$  of the forces necessary at the actuators to apply the desired wrench  $\mathbf{F}(t, \alpha)$  has been calculated via the  $\boldsymbol{\tau}(t, \alpha) = \mathbf{J}^{-1}\mathbf{F}(t, \alpha)$  already discussed above. Forces have been estimated as if the variable wrench was applied at the centre of the platform kept at the reference pose, i.e. applying the forces at a fix point. After that, some measured paths of motion have been simulated while the corresponding wrench were applied, in order to consider the possible displacements and rotations of the platform due to the knee reaction to loads. The maximum forces at the actuators have been evaluated.

### RESULTS

In Figure 5.17 the calculated forces at the actuators of the 6-6 Gough-Stewart platform for the sit-to-stand are reported as a function of the flexion angle for the various dimensions of the base. The complete results for all the tasks and architectures are reported in Attachment A3.

From the static analysis, the highest required forces have been calculated. The highest values for the 6-6 architecture are required during sit-to-stand task. The highest load is required at the actuator 3 (directed in anterior and lateral direction); its value is between 650 and 700 N, depending on the diameter of the base. In general, for the 6-6 configuration, it can be said that the wider is the base, the smaller are the highest loads.

The highest load for the 6-3 architecture is also required during sit-to-stand and also at the actuator 3 (directed similarly to 3 in architecture 6-6); its value is between 550 and 600 N, depending on the diameter of the base. In general, loads required at the 6-3 are lower than loads required at the 6-6.

Conversely, loads required at the decoupled architecture, variation b, are comparable with those of the 6-6 and 6-3 architectures. The highest load is required during squat at the actuator 6; its value is about 570 N.

Loads required at the *in-line leg* architecture have also been analysed. As expected from results on the evaluation of the determinant of the Jacobian matrix, loads are higher than those required at all the other configurations. The highest load for the in-line leg architecture is required during walking A at the actuator 1 and its value is between 3000 and 4500 N, depending on the dimension of the base.

#### RELATIVE POSITION BETWEEN TIBIA AND PLATFORM

Finally, the relative orientation between the tibia and the loading system was analysed. The tibia indeed could be mounted on the platform in two extreme positions:

- i. with its longitudinal axis quasi-perpendicular to the plane of the platform at the resting pose, called "horizontal platform"
- ii. with its longitudinal axis contained in a plane parallel to the plane of the platform at the resting pose, called "vertical platform".

Both for the horizontal and vertical configurations, the desired workspace is contained into the computed dexterous workspace for almost all the configurations. Forces required at the actuators are generally higher for the vertical platform than for the horizontal one, but still definitely under the maximum value that can be provided. The mounting condition, though, is different. In the horizontal platform configuration, the actuators are oriented almost vertically, thus only a small component of their weight generates flexion and acts as a lateral load at the joint actuator extremity. In the vertical configuration, instead, the actuators are almost horizontal, so their weight introduces

big lateral components and flexion. This working condition is not suitable for ballscrews. The horizontal configuration has been chosen.

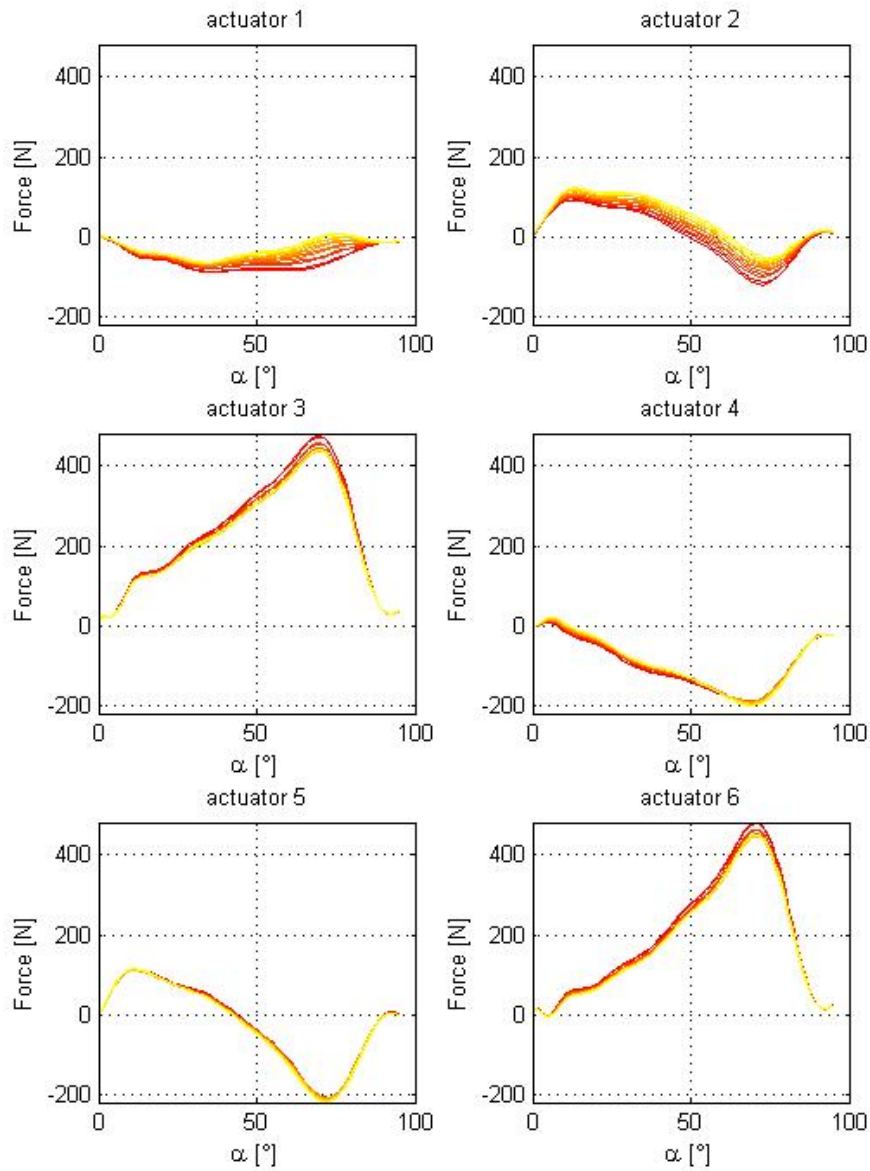


Figure 5.17 Trend of the forces required during sit-to-stand at the actuators of the 6-6 Gough-Stewart architecture as a function of the flexion angle  $\alpha$  at various diameter of the base: smallest diameters in red color, larger diameters in yellow.

Considerations and results reported in the previous parts of this section are referred to the horizontal platform, since it has been chosen for the final design.

### FINAL OVERALL CONSIDERATIONS

Different architectures of the Gough-Stewart platform have been analysed in this paragraph, by comparing the behavior in terms of dexterous workspace, singularities and Jacobian matrix stability, and forces distribution. For each architecture, different geometries have been tested, by varying some dimensional parameters. In particular, the length of the legs and the dimension of the platform have been fixed, while the characteristics of the base have been varied for the 6-6, 6-3 and *in-line* leg architectures and the disposition of the attachment points has been varied for the *decoupled* architecture.

From the comparison of the required dexterous workspace with the reachable ones, it is possible to conclude that the *lying-leg* architecture and some of the solution analysed for the *decoupled* architecture do not satisfy specifications, unless renouncing at the decoupling; only *decoupled* version b) satisfies the requirements. Conversely, all the 6-6, 6-3 and *in-line leg* architectures guarantee all the necessary workspace.

Among the satisfying architectures, the *in-line leg* presents a determinant of the Jacobian matrix of an order of magnitude smaller than the determinants of the other architectures. It requires higher forces to replicate the loading conditions. These forces reach the limit value that an actuator can apply, so it has been discarded.

From the analysis of the forces, the one that requires lower forces is the 6-3 configuration; however, the force required by 6-6 and decoupled architectures are slightly higher but still comparable with those required by 6-3. They all are widely under the limit presented by the actuators.

### 5.2.2.3 DESIGN RESTRICTIONS

In Section 5.2.2.2 an evaluation of the behavior of different architectures for realising the loading platform has been performed. In this part, indeed, the design requirements (volume of the components, interference during motion, joint connections) has not been taken into account.

If analyzing the geometry and the volume of the actuators, the volume occupied by the load cell immediately comes to the eyes. As explained in Section 5.2.1.2 the big volume is necessary in order to guarantee stiffness and small signal alteration due to flexion and torsion on the actuator. Furthermore, the closer the load cell is to the platform, the lower the bending moment it undergoes is, so the more precise the signal is.

When assembling the components, the space occupied by the joints has to be taken into account and, unless complex geometries are identified for the platform, they reduce the distance between the platform and the rotation axis of the knee. In addition, a tibial fixation system has to be mounted on the platform in order to allow tibia fixation, positioning and repositioning on the rig. Finally, the interference between the legs and between legs and tibia during motion has to be taken into account when designing the loading system.

These assembly aspects and volume constraints have been considered in order to assemble the actuators according to the different architectures. PTC Creo® has been used to create assemblies.

At first stage, the architectures were assembled with UPS legs. The interference both in assembly and at all the combination of extreme orientation at the extreme pose of the platform has been evaluated.

For both the classical 6-6 and the 6-3 Gough-Stewart platform, assembly is a problem, since none of the dimensional parameters allows mounting the actuators on a platform with a diameter of 130 mm without interference at the load cells. The problem is bigger for the 6-3 platform, since the attaching points are two by two coincident, i.e. the

extremities near the load cells are closer than in the 6-6 architecture. The bigger the base is, the smaller the interference is, but it is still present also with a base with diameter of 1100 mm, as showed in Figure 5.18. In order to avoid interference a bigger platform is required.

For the decoupled architecture, this kind of problem do not occur if particular attention is posed to the determination of the optimal geometry of the platform. The problem in this case is that considering the volumes of the joints and of the load cells, the space for inserting the tibia becomes very small. The fixation of the tibia becomes so very difficult in a reduced space, as shown in Figure 5.19. Furthermore, during motion interference between the tibia and the actuators are expected.



*Figure 5.18 Classical 6-6 Gough-Stewart architecture with base diameter of 1100 mm and platform diameter of 130 mm. Interference can be noted at the load cells.*

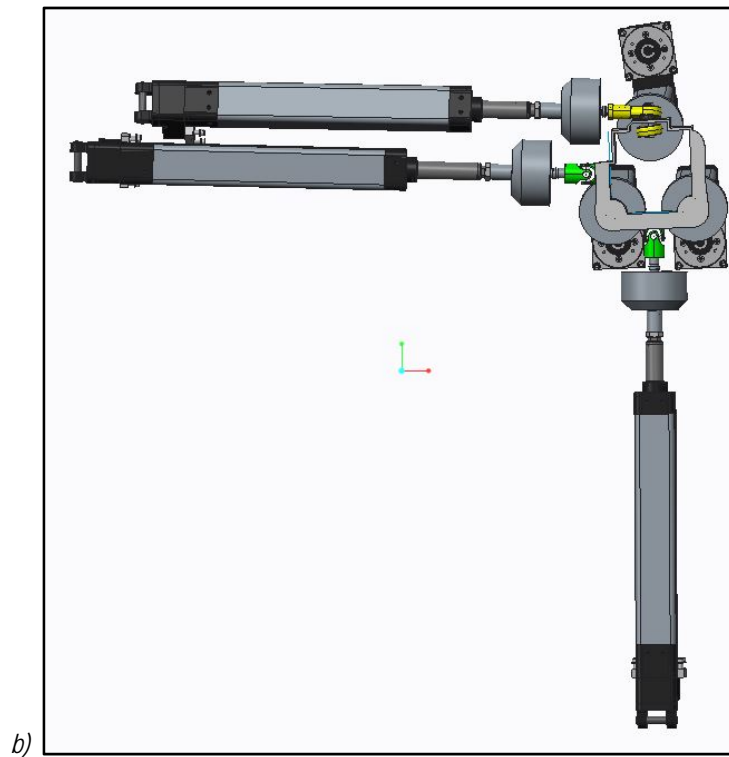
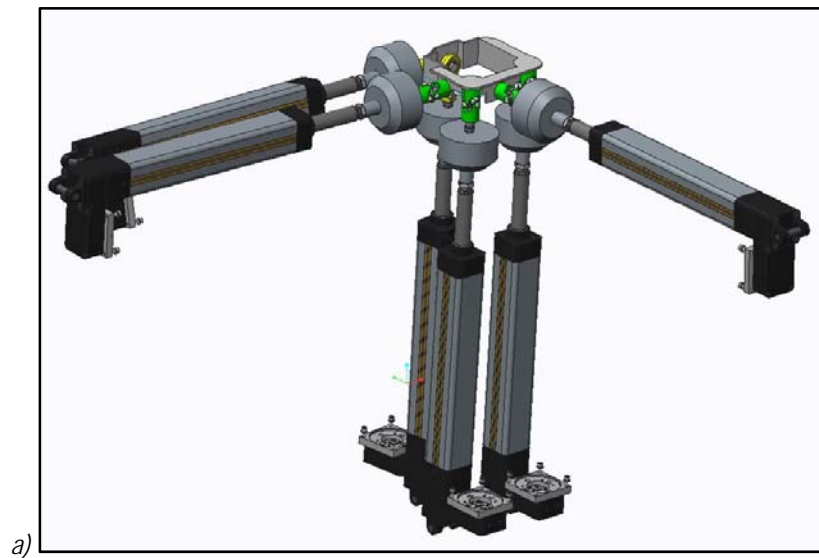


Figure 5.19 Decoupled configuration, type b. No interference can be noted at the load cells, but no space is left for the tibia. a) 3D view; b) view from the top.

The parameters utilized for the comparative analysis of the different architectures do not allow the functional design of the loading system. It is evident that to allow mounting the components, a bigger platform is necessary. Furthermore, to enlarge the space for fixing the tibia, the platform can be moved distally along the axis of the tibia, thus increasing its distance from the centre of the knee.

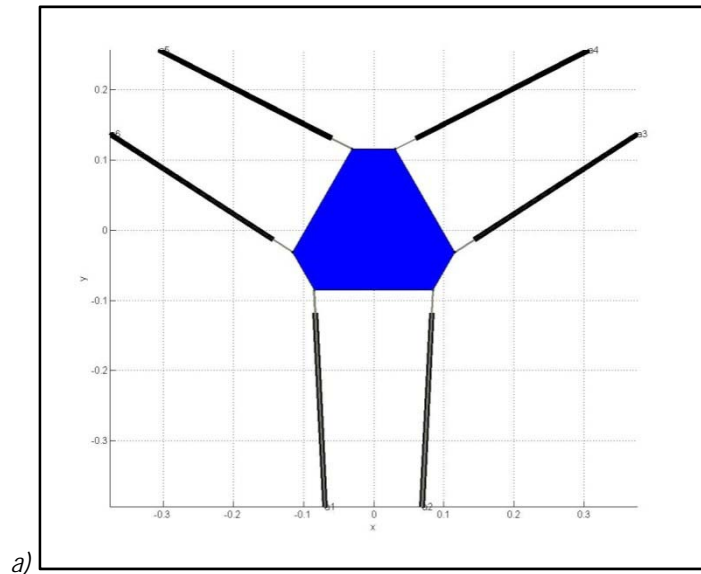
A trial and error optimization of the geometry has been performed for the 6-6 platform, in order to obtain a mounting configuration with a platform having proper dimensions and avoiding interferences among legs and between each leg and the tibia. The platform have been shifted distally of 150 mm (i.e. posed at 250 mm from the axis of flexion/extension of the knee) and the dimensional characteristics are:

- platform diameter:  $d_{plat} = 240 \text{ mm}$
- base diameter:  $d_{base} = 800 \text{ mm}$
- semiangle at the platform:  $\alpha_{plat} = 15^\circ$
- semiangle at the base:  $\alpha_{base} = 10^\circ$

The designed solution is reported in Figure 5.20.

The same optimization has been performed for the 6-3 architecture too. In order to avoid collision between load cells, a cylindrical piece has been added at the end of each actuator and the leg thus has become 100 mm longer, as shown in Figure 5.21a. Actually in order to reduce the length of the actuators, the load cells in two close actuators have been put on different distance from the spherical joints, as shown in Figure 5.21b. It is worth noting that putting the load cells at two different level permits to shorten the leg of 30 mm, with respect to the case of load cells at the same distance, not introducing any significant difference on the rig. As for the 6-6 architecture, the platform have been shifted distally of 150 mm and its dimensional characteristics are:

- iv) platform diameter:  $d_{plat} = 240 \text{ mm}$
- v) basediameter:  $d_{base} = 800 \text{ mm}$
- vi) semiangle at the base:  $\alpha_{base} = 10^\circ$



a)



b)

Figure 5.20 Classical 6-6 Gough-Stewart architecture with base diameter of 800 mm and platform diameter of 240 mm. Interference is not present. a) attachment points representation; b) 3D view of the assembly.



Figure 5.21 Classical 6-3 Gough-Stewart architecture with base diameter of 800 mm and platform diameter of 240 mm. Interference is not present. a) solution with load cells in the same position for all the actuators ; b) solution with load cells at different height.

As shown in Figure 5.14 in Section 865.2.2.2 the computed dexterous workspace for the decoupled architecture has the same dimensions of the required one. Increasing the distance between the attaching points in order to enlarge the space for the tibia would reduce the workspace. The required workspace thus would not be contained in the computed workspace, since leg length and stroke are fixed. So enlarging the platform would not be a possible solution for the decoupled architecture. By mounting the platform in a more distal position, the required workspace could be reached by the reference point at a distance of 100 mm from the axis of the knee (which would not be coincident with the centre of the platform anymore) even if the platform was bigger. This displacement would increase the height of the machine, whose minimum value depends on the length of the actuators and on their mounting conditions. Furthermore, the decoupled architecture has the limitation of foreseeing actuators mounted in horizontal position, between a spherical and a universal joints. This forces the actuator to work under the later load generated by its own weight. As explained in Section 5.2.1.1, actuators have been chosen longer than the necessary to increase the lateral load. Anyway, the presence of this lateral load generate problems at the loading system, not for actuator resistance, but mainly for friction condition that would not be easy to control.

#### 5.2.2.4 COMPARATIVE ANALYSIS 2.0

A comparative analysis have been performed again for the two optimized architectures. Dexterous workspaces and forces have been calculated at first. Angles between the platform and the legs and between the base and the legs have been identified then.

##### DEXTEROUS WORKSPACE

###### METHOD

The method for dexterous workspace calculation has been explained in Section 5.2.2.2 Even though the platform has been moved distally, dexterous workspace has been calculated with respect to a reference point posed in the same pose as the previous

one, i.e. coincident with the centre of the platform and moved 150 mm proximally. Furthermore, considering that no actuator is mounted in horizontal, i.e. no actuator is subjected to the whole component of its weight as a lateral force, a longer stroke has been allowed to actuators with respect to the value considered in Section 5.2.2.2.: a maximum stroke of 250 mm has been permitted.

## RESULTS

The results in terms of workspaces are reported in Figure 5.22 and in Figure 5.23 for the 6-6 and 6-3 architectures respectively. Both the 6-6 and the 6-3 optimised architectures allow reaching all the required workspace.

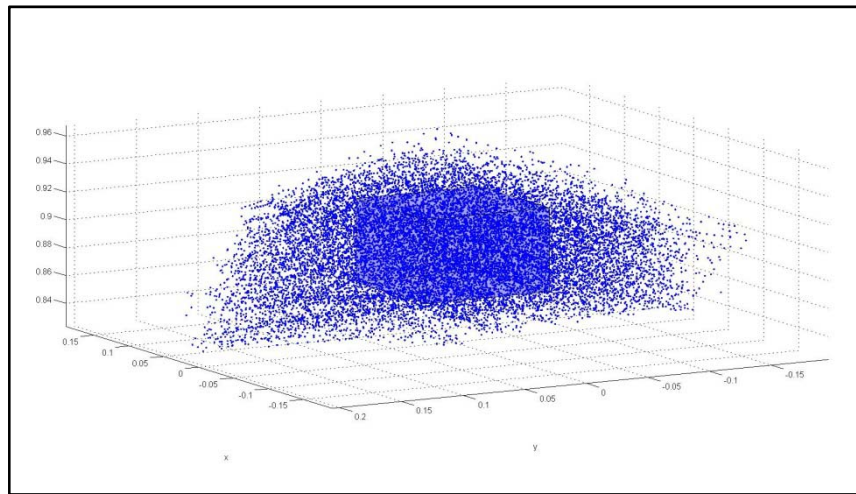
## STATIC ANALYSIS

### METHOD

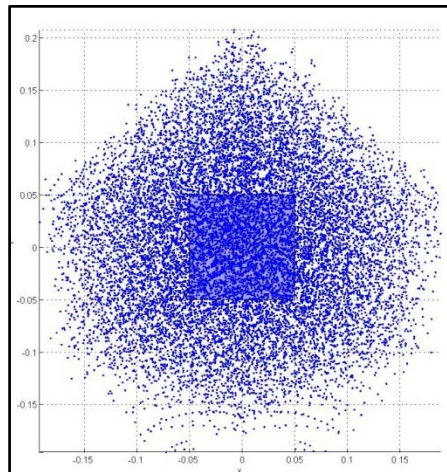
The method used to perform static analysis has been explained in Section 5.2.2.2. As for the workspaces, even though the platform was moved distally, forces were calculate with respect to a reference point posed in the same pose as the previous one, i.e. coincident with the centre of the platform and moved 150 mm proximally.

### RESULTS

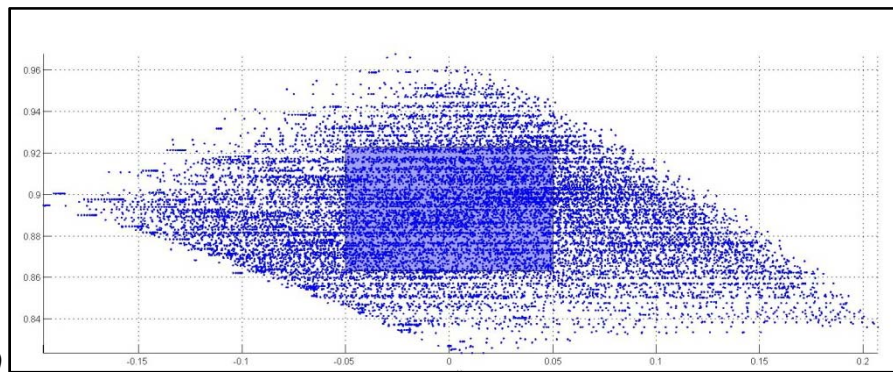
The results in terms of forces are reported in Figure 5.24 and in Figure 5.25 for the 6-6 and 6-3 architectures respectively. Both the 6-6 and the 6-3 optimised architectures require lower loads at the actuators then those calculated at the first analysis. The required forces are comparable for the two architectures and reach peaks of 400 N.



a)



b)



c)

Figure 5.22 Dexterous workspace for the optimized 6-6 architecture: a) 3D-workspace; b) workspace seen from the top; c) workspace seen from the side.

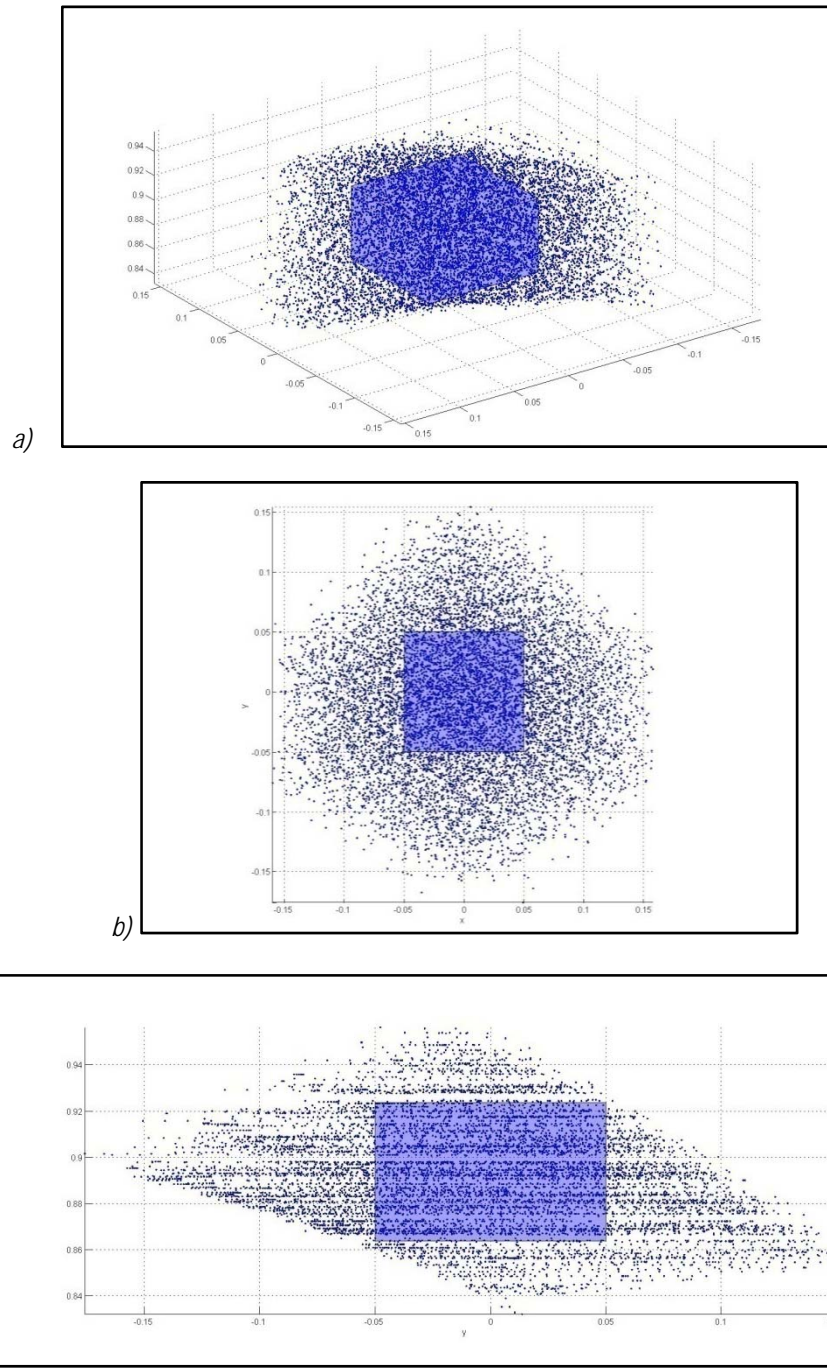


Figure 5.23 Dexterous workspace for the optimized 6-3 architecture: a) 3D-workspace; b) workspace seen from the top; c) workspace seen from the side.

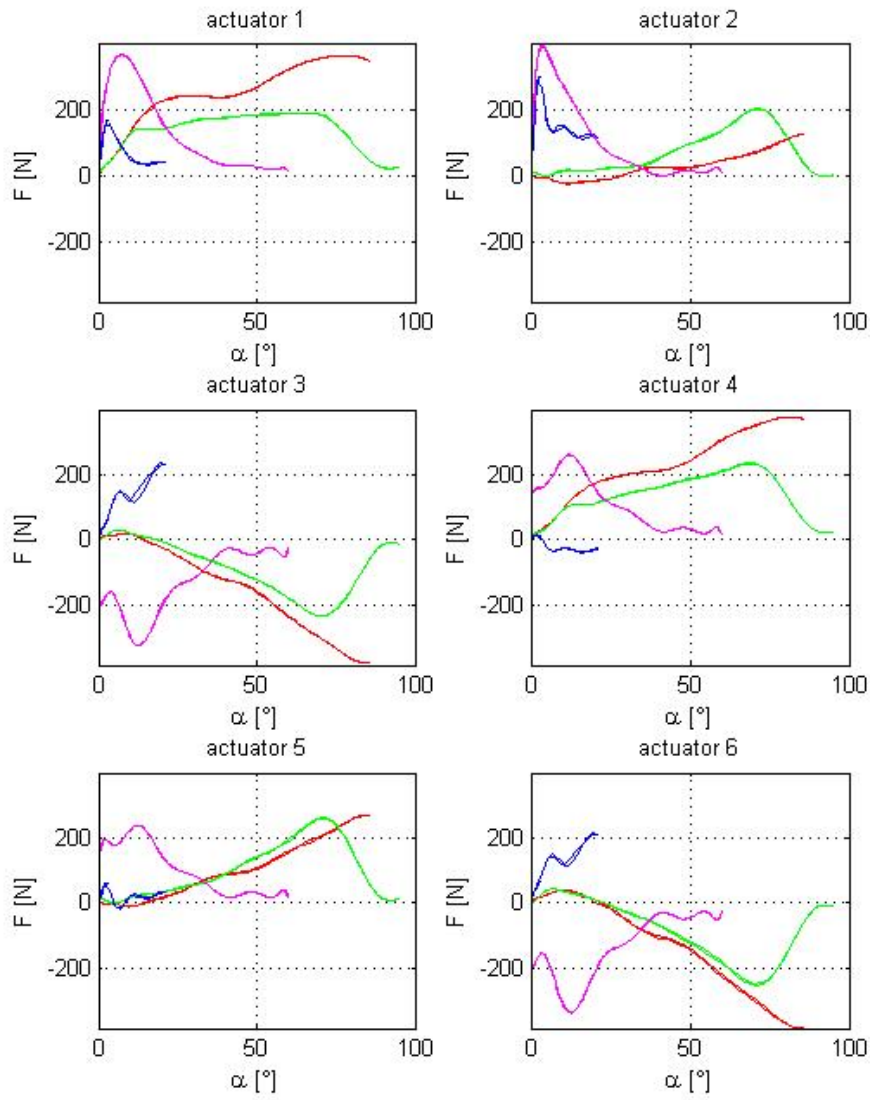


Figure 5.24 Forces at each actuators to perform the 3 motion tasks (sit-to-stand, squat, walking phase A and walking phase B) for the optimized 6-6 Gough\_Stewart architecture.

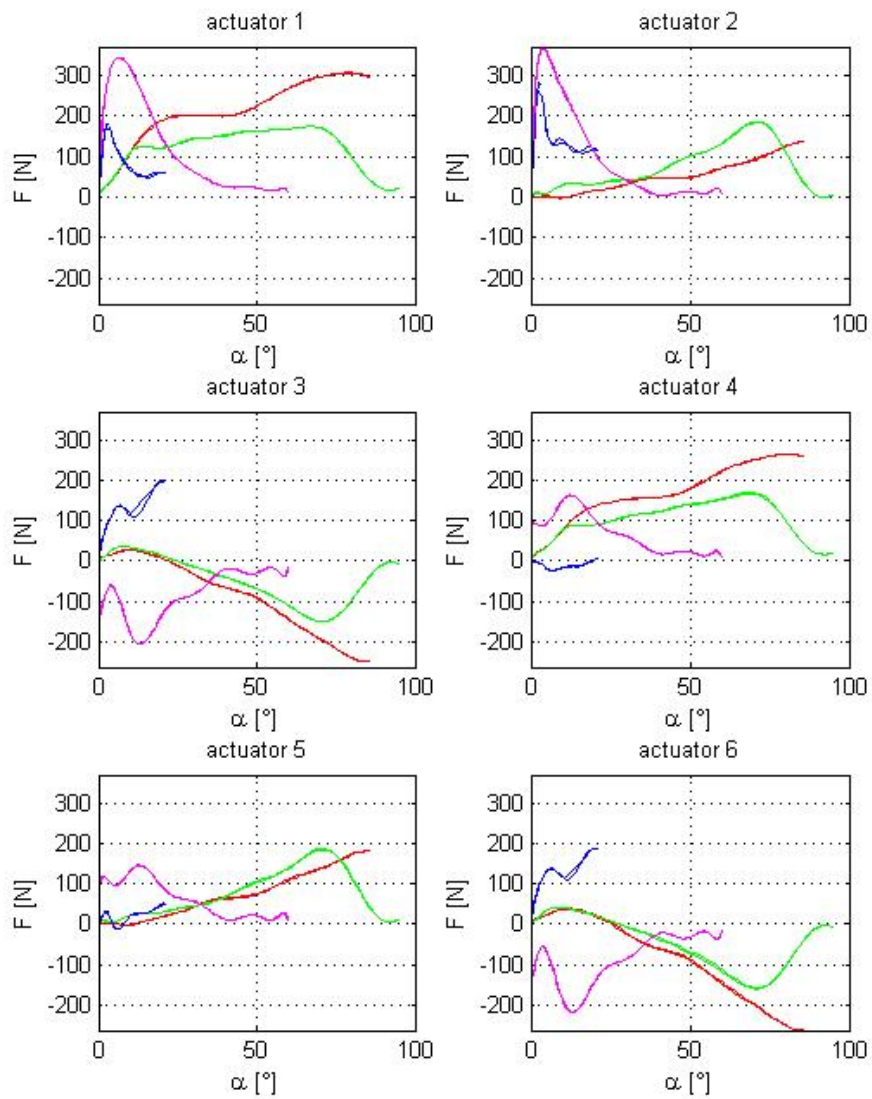


Figure 5.25 Forces at each actuators to perform the 3 motion tasks (sit-to-stand, squat, walking phase A and walking phase B) for the optimised 6-3 Gough\_Stewart architecture.

### ANALYSIS OF THE ANGLES

A further topic of investigation is the range of rotations between the legs and the platform and the legs and the base. When building the machine, the range of these rotation is limited by the constructive characteristics of the joints. For constructive constraints, spherical joints usually allow a complete rotation about an axis  $i$  and an oscillation inside a cone of semiangle  $15-18^\circ$  with the axis perpendicular to the direction of  $i$ ; universal joints works at a maximum angle of  $45^\circ$  but also permit to reach higher angles if they do not have to transmit torque.

An analysis in order to define the required angles have been performed for both the architectures. The angles between the platform and the axis of each leg and between the base and the axis of the each leg have been identified according to the following considerations.

If named  $\bar{s}_i$  the direction on the axis of the  $i$ -th leg, i.e. the direction of translation of the prismatic couple on the  $i$ -th actuator, and named  $\bar{v}_i$  the direction of the axis of the rotation couple of the ball and socket or of one of the rotation couple at the universal joint between the  $i$ -th leg and the platform, the angle  $\vartheta_i$  between the two axes can be computed as:

$$\vartheta_i = \arccos\left(\frac{\bar{s}_i \cdot \bar{v}_i}{\|\bar{s}_i \cdot \bar{v}_i\|}\right) \quad (5.5)$$

Similarly, if called  $\bar{u}_i$  the direction of the axis of the rotation couple of the ball and socket or of one of the rotation couple at the universal joint between the  $i$ -th leg and the base, the angle  $\varphi_i$  between the two axes can be calculated as:

$$\varphi_i = \arccos\left(\frac{\bar{s}_i \cdot \bar{u}_i}{\|\bar{s}_i \cdot \bar{u}_i\|}\right) \quad (5.6)$$

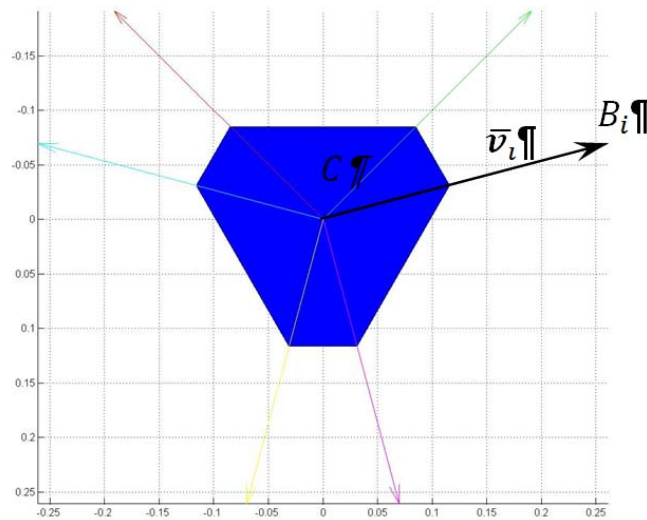


Figure 5.26 Schematic of the platform for the identification of vector  $\bar{v}_i$

## RESULTS

Results in terms of angles  $\vartheta_i$  are reported in Figure 5.27a and in Figure 5.28a for the 6-6 and 6-3 architectures respectively. Results are reported as variation with respect to the angle  $\vartheta_0$  at the reference pose of the loading system.  $\vartheta_0$  is defined as the angle between vectors  $\bar{s}_i$  and  $\bar{v}_i$  when the platform is at its reference pose. It is possible to see that the highest angles are required at the 6-3 and they reach  $46.67^\circ$ . For the 6-6 architecture, angles are a bit smaller and reach peaks of  $43.48^\circ$ .

Results in terms of angles  $\varphi_i$  are reported in Figure 5.27b and in Figure 5.28b for the 6-6 and 6-3 architectures respectively. Results are reported as variation with respect to the angle  $\varphi_0$  at the reference pose of the loading system.  $\varphi_0$  is defined as the angle between vectors  $\bar{s}_i$  and  $\bar{u}_i$  when the platform is at its reference pose. It is possible to see that the highest angles required for both the architectures reach  $14^\circ$ .

From this first analysis, universal joints can be used to connect the platform with the legs, while spherical joints can be used to connect the base and the legs. These two

joints, together with the actuated prismatic joint guarantees 6 DOF to each leg, thus 6 DOF to the platform.

Realization of a double connection of the legs with the platform in the same point with a universal joint, as required for the 6-3 architecture, could be very tricky. Special universal joints should be built for the application, with the risk of introducing excessive backlash and misalignments. Furthermore, high angles are required, so wide ranges of motion should be permitted by these joints. Since the 6-6 and the 6-3 architectures both satisfy the requirements in terms of dexterous workspace and offer comparable performances in terms of force, the 6-6 architecture has been chosen.

#### 5.2.2.5 FINAL CONSIDERATIONS ON THE LOADING SYSTEM

From the considerations reported in this Section, the classical 6-6 final architecture was chosen among the five proposed, i.e. classical 6-6, classical 6-3, *in-line leg*, *decoupled* and *lying leg* architectures.

The *lying leg* architecture presented constructive complexity and limited dexterous workspaces, even if the forces distribution on actuators could be advantageous. Conversely, maximum forces required by the *in-line leg* architecture are an order of magnitude larger than those required by the other architectures, even if it offered high visibility, which is important during tests. The *decoupled* architecture has limited ranges of motion, at fixed actuator lengths and strokes; to guarantee the necessary dexterous workspace, the dimensions do not allow the mounting and the motion of the tibia. Finally among the two classic 6-6 and 6-3 configurations, the 6-3 reveals to be trickier to design in terms of joints. The 6-6 architecture is the one that offers the best compromise if workspaces, loads and constructive aspects are considered.

The optimal compromise between volume and performances were determined, so the final geometry of the loading system is the one proposed in Figure 5.20.

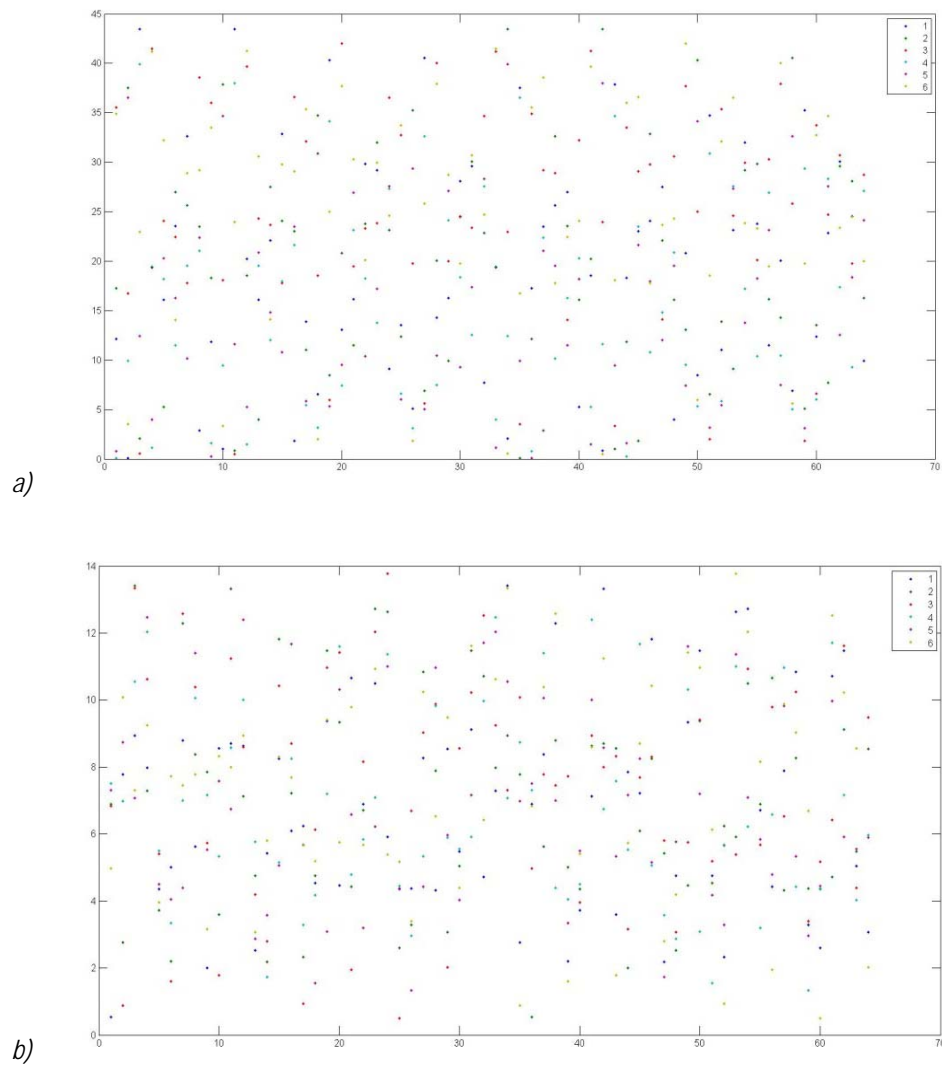


Figure 5.27 Angles of inclination of the actuators during motion in the whole workspace for the 6-6 architecture. a)  $\theta_i$  between legs and platform, with respect to the reference mounting value; b)  $\varphi_i$  between legs and base, with respect to the reference mounting value.

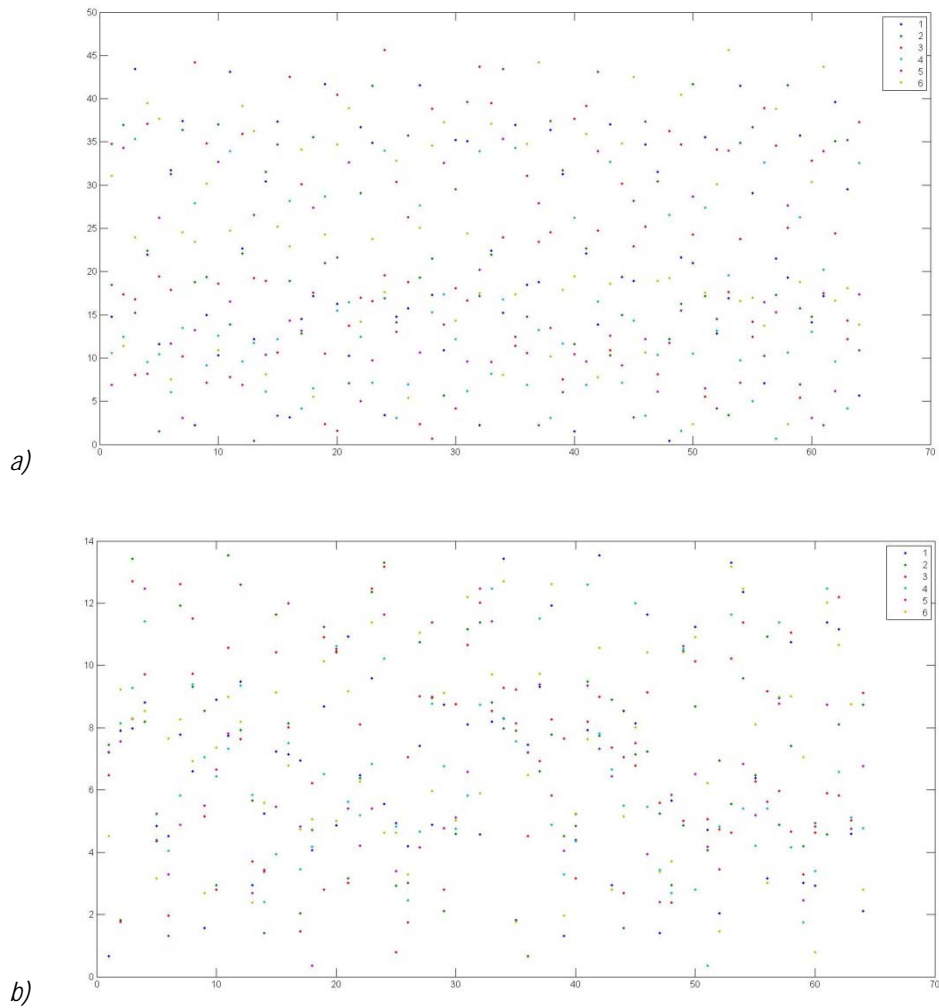


Figure 5.28 Angles of inclination of the actuators during motion in the whole workspace for the 6-3 architecture. a)  $\theta_i$  between legs and platform, with respect to the reference mounting value; b)  $\phi_i$  between legs and base, with respect to the reference mounting value.

### 5.2.3 CONTROL OF THE LOADING SYSTEM

Another important aspect of the loading system is its control. As widely explained in previous sections, the system is required to apply to the tibia a load history that depends on the flexion angle and on the desired motion task. Its control system, thus,

needs to command the application of a different wrench at the reference point of the platform at each flexion value.

If the position of the reference point with respect to the centre of the knee and the anatomical parameters of the specimen are known, and the kind of task is chosen, the wrench  $\mathbf{F}(\alpha)$  to be applied as a function of the flexion angle  $\alpha$  can be computed from the GRF and the angles reported in Section 2.2.4, by means of the simple model reported in Section 4.1 or a more complex one. The loads at the actuator  $\boldsymbol{\tau}$  can be obtained with static analysis, i.e. by using Eq. 5.4, from wrench  $\mathbf{F}(\alpha)$ . Since the Jacobian matrix of the system depends on the pose of the platform, the vector of loads at the actuators  $\boldsymbol{\tau}$  is a function of both the pose of the platform  $\boldsymbol{x}$  and the flexion angle  $\alpha$ :  $\boldsymbol{\tau} = \boldsymbol{\tau}(\alpha, \boldsymbol{x})$ . Pose of the platform  $\boldsymbol{x}$  can be computed from the actuator pose  $\boldsymbol{q}$ , measures via the resolver mounted on the rotary motors.

The evaluation of the load to apply at the actuators  $\boldsymbol{\tau}$  is thus defined based on the motor angular poses and the flexion angles. Some inaccuracies are introduced in the definition of the platform geometries from the angular position of stepper motors measured via resolvers, due to backlash in kinematic chains and manufacturing errors. An accurate process of calibration needs to be executed in order to evaluate the magnitude of these inaccuracies and to consider their correction in the control code.

Once the loads at the actuators are defined and applied, the motors are controlled in closed loop by means of the load cells mounted at the extremities of each actuators. The loads at each actuator is adjusted in order to obtain the desired value based on the load cell signal. It is worth noting that the accuracy of the load cells is important for the correct definition of the wrench applied to the tibia. Errors in the measurement of the forces, indeed, affect the overall evaluation of the wrench on the tibia, at different extents depending on the architecture of the loading system and on its pose.

## 5.3 FIXATION SYSTEMS

For the correct functioning of the machine, the positioning of the specimen is a key operation. The transepicondylar axis of the femur identified by a surgeon must be placed in coincidence with the rotation axis of the portal, thus guaranteeing the approximate separation of flexion from the other motion parameters. Thus, the femur has to be accurately positioned and mounted on the rig at first. Once the femur has been positioned, the tibia has to be connected to the loading system without introducing relative displacements between the tibia and the femur. In order to guarantee the correct positioning, both tibia and femur fixation systems need to have 6 DOF and to regulate them according to the anatomy and the pose of the leg. Furthermore, as explained in Section 4.2, the possibility to unmount and remount the specimen in the same position is required to accurately repeat tests on the same specimen after surgery.

Both the tibia and femur fixation systems play an important role for the correct positioning and repositioning and will be described in the following. Two different devices have been designed in order to satisfy the different requirements, in terms of available spaces and required ranges of motion. A common characteristic of the two systems is that they grasp the bone without damaging it. So the systems are thought in order to apply loads through friction between bones and mechanical elements. Screws across bones or bone cutting and potting are avoided.

### *5.3.1 FEMUR FIXATION SYSTEM*

The femur fixation system is required to grasp the femur and connect it to the movable portal. As briefly mentioned above, the specimen must be positioned in a way that the transepicondylar axis is coincident with the rotation axis of the portal. This allows putting the femur in charge of almost all the flexion/extension motion of the knee. The transepicondylar axis, indeed, is the closest to the natural flexion/extension axis of the knee, which has a spatial motion with a movable axis. The more precise the positioning

is, the smaller flexion component is left to the tibia in order to follow its natural path of motion, i.e. the path of motion imposed by anatomical and physiological constraints. The femur fixation system, thus, is required to adapt to different geometries, both in terms of bone shape and in terms of whole-leg anatomical differences and problems (for example: genu varum, genu valgus).

If considering the normal femur geometry, the shaft is the part that shows the most regular surface. Femur grasping is so realized on this part of the bone. As explained in Section 262.1.3, a variable orientation of the femur shaft axis with respect to the femur longitudinal axis (i.e. the axis that connects the centre of the epicondyles with the centre of the femoral head) has a medium inclination of 6-7°. In addition, an inclination of 3° can be observed between the femur longitudinal axis and the vertical direction. So a mean inclination of the shaft of the femur (i.e. the grasped part of the femur) of 9-10° is physiological. This means that passing from right to left side, there is a change of the inclination of the shaft of about 18-20°, if considering healthy knees. If diseased knees are considered, the variation of the inclination can be larger. In addition, in order to allow the transepicondylar axis to coincide with the portal rotation axis, translation of some centimeters must be allowed.

The femur fixation system has thus been thought with a wide range of motion, in order to guarantee the six DOF in positioning. The femur grasping is guaranteed by a femur grasping platform (2) represented in Figure 5.29. Fixation fingers are free to translate in different directions in order to secure the femur, as shown in Figure 5.30. The femur grasping platform is univocally referred to the movable platform (1) of a passive parallel manipulator and fixed to it. Two reference elements guarantee a univocal reference between the movable and the fixation platform.

Ideally, the femur could be mounted on its grasping platform in any position, also far from the machine. Then the femur is positioned inside the machine and its optimal pose is defined. The movable platform of the passive parallel manipulator (Figure 5.31: Femur mounted on the 6 GdL manipulator for its positioning and fixation. Figure 5.31) is brought proximal to the femur grasping platform on the femur. Finally the fixation platform is secured to the movable platform. The six legs of the parallel manipulator are

then blocked. Once the femur fixation parallel manipulator is blocked, the femur together with its fixation platform can be unmounted and remounted in the same pose, thanks to the reference elements between the two platforms.

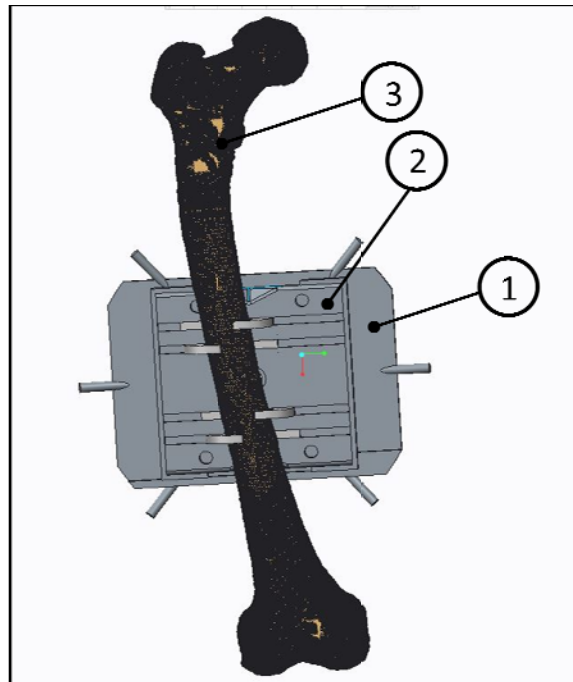


Figure 5.29 Femur grasping platform mounted on the femur fixation system: (1) femur grasping movable platform; (2) femur fixation platform; (3) femur.

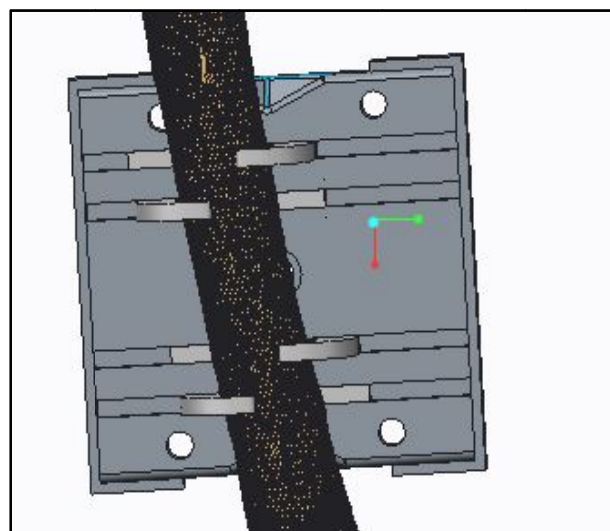
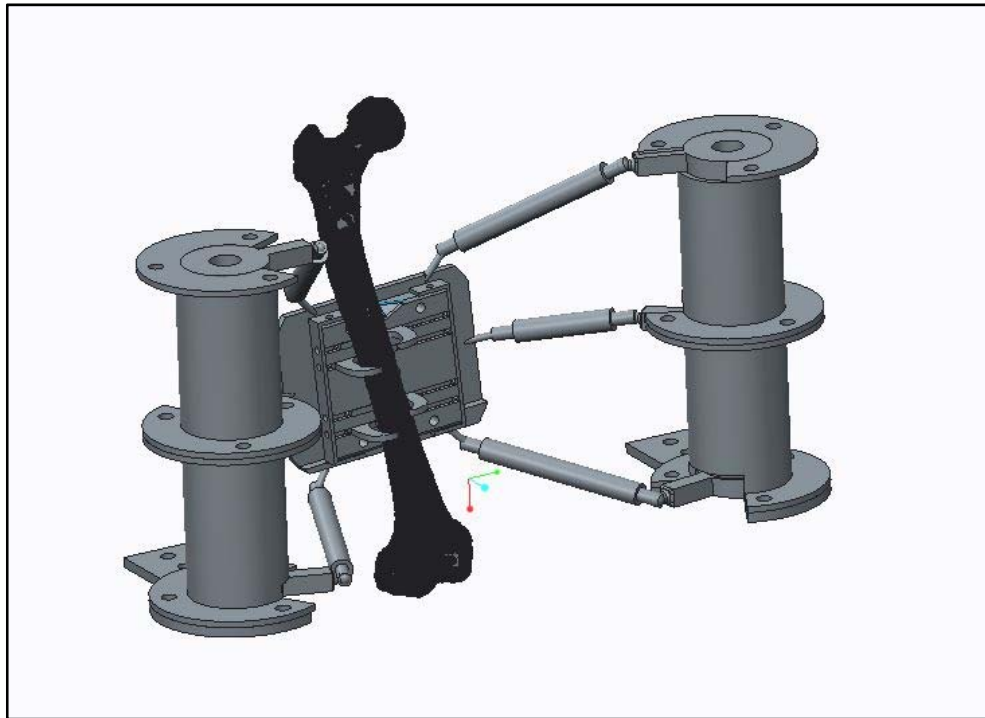
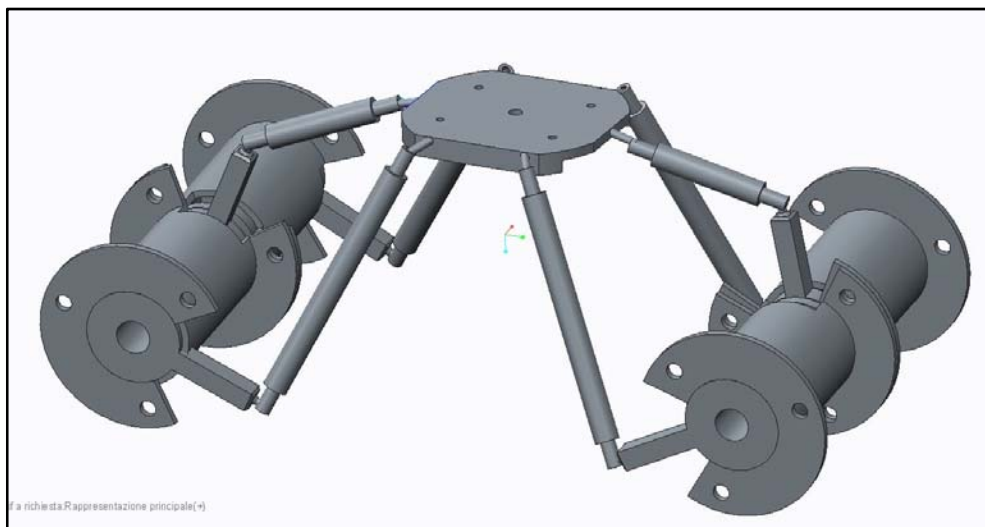


Figure 5.30 Detail of femur grasping platform.



*Figure 5.31: Femur mounted on the 6 GdL manipulator for its positioning and fixation.*



*Figure 5.32 6 GdL manipulator for femur fixation and positioning.*

The manipulator is represented in Figure 5.32. It is composed by the movable platform which is connected to six fixed-length legs via universal joints. Each leg is connected via a spherical joint to a link which can rotate with respect to the mechanism frame via a rotation couple. The axis of the link revolute couples are three by three coincident. So the legs are disposed in a way that three legs have common rotation axis on the right side of the femur and three legs have common rotation axis on the left side of the same bone, as showed in Figure 5.32. The mechanism allows six DOF to the movable platform and can be blocked by fixing the six revolute couples (three by three aligned).

The device devoted to block the legs has been studied in order to minimize the time of specimen positioning. It consists of two groups of elements. Each of them blocks contemporary the three legs on the same axis, by screwing a bolt which connects the three legs to the frame passing through a hole in the movable elements. The fixation system is realized via two conical couplings between two leg-links (1 and 3) and the frame (2) and a friction coupling between two rotating link (3 and 4), as show in Figure 5.33. Once the bolt is screwed, friction in all the couples blocks the six DOF of the mechanism.

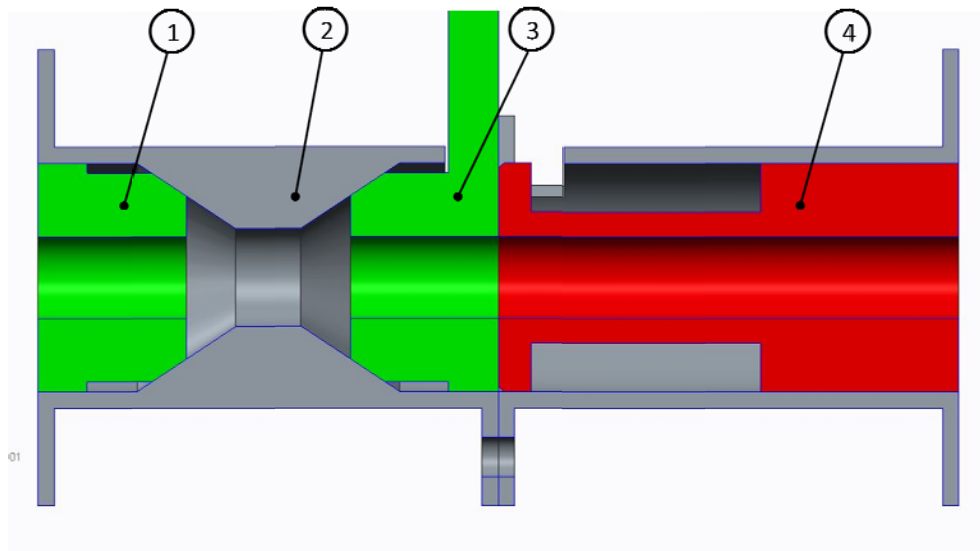


Figure 5.33 Fixation system for the 3 revolute couples of the mechanism. 1 and 3. movable elements of conical couplings, each connected to one leg, 2. frame, and 4. cylindrical movable element connected to one leg.

In addition to the six legs of the manipulator, two more elements have been added in order to guarantee a preload and eliminate the backlash in the kinematic couples. The preload is realized via two stretchers connected via hooks and rings and are tensioned after blocking the six principal legs of the parallel manipulator.

### *5.3.2 TIBIA FIXATION SYSTEM*

The tibia fixation system is required to grasp the tibia and connect it to the movable platform of the loading system. The positioning of the tibia occurs as a consequence of the femur positioning and the knee anatomical characteristics. Generally, the tibia presents an axis more vertical than the femur and smaller variations in terms of rotations. It is worth noting that the tibia is not the only bone in the shank: also the fibula is present. However, fibula is not involved in the grasping problem, but its volume must be considered in order to develop a suitable grasping system for both the leg bones. If lower rotations and displacements are necessary, smaller spaces are available for the grasping mechanism. The only graspable part of the tibia is the segment between the tibial tuberosity and the level of the platform, i.e. a segment of about 150-180 mm. Above the tibial tuberosity, indeed, ligaments and patellar tendon are inserted.

At the first stage, two approaches were considered for the mechanism:

- i) Using the DOF of the loading system both to accommodate the tibia and to allow motion during loading application;
- ii) Using a system to connect the tibia separated for the loading system.

In the first case, part of the loading platform workspace would be employed to reach and grasp the tibia. Thus, a range of motion wider than that considered in specifications would be required. Conversely, this solution would decrease the backlash in the whole loading system but the replication of the position during unmounting and remounting could be very difficult. Thus, the second approach has been chosen and a dedicated system has been designed.

Two different solutions have been explored. A simpler and more common one foresees to regulate the six DOF by regulating three translations (thanks to sled) and three rotations (thanks to a blocked spherical extremity) in a serial way. On the other side, a more complex solution foresees the realization of another parallel manipulator to guarantee femoral grasping. For the small available spaces, the first solution has been preferred, even if less innovative.

The tibia (2) grasping is guaranteed by a grasping device represented in Figure 5.29 composed by two coupled pieces (one anterior (4) and one posterior (5)) connected by screws. Tibia fixation screws (3) with V-shaped terminal elements are used to secure the tibia to the system. Several access points for the fixation screws are created on the grasping device in order to permit grasping of the tibia, without involving the fibula (1). Since both the extremities of tibia-fibula complex are large if compared with the tibial shaft, the device is realized in two pieces in order to allow the insertion of the tibia (2) together with the fibula (3) and contemporary reduce the device size. Furthermore, one the posterior pieces (5) has a simple rectangular shape, so that it can be used as a fixation reference on a vice when the specimen is unmounted.

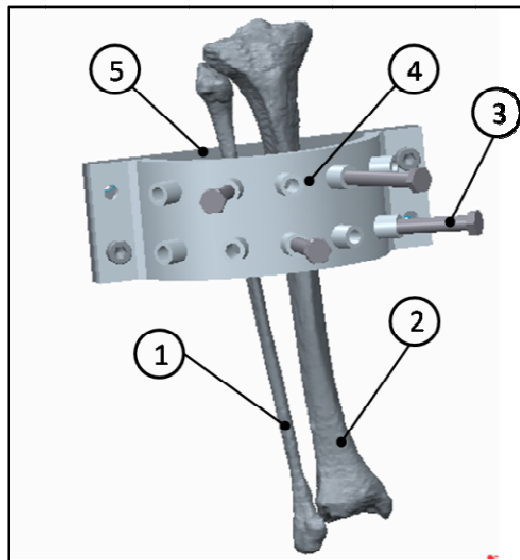
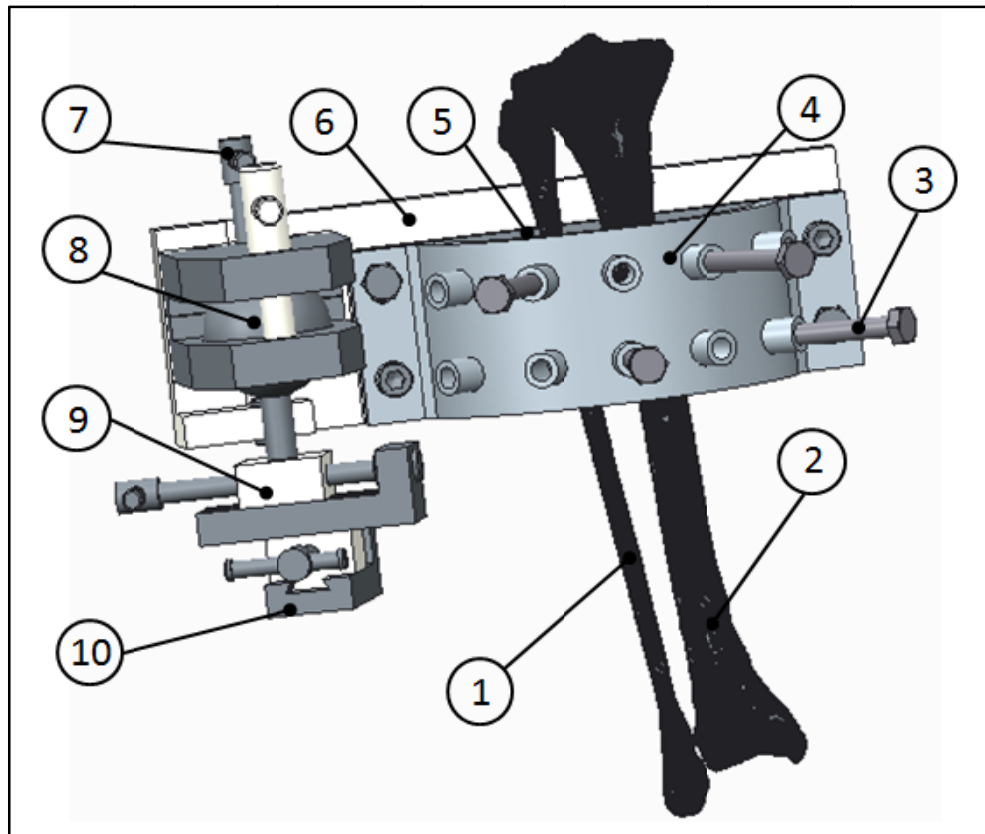


Figure 5.34 Tibia grasping device: (1) fibula; (2) tibia; (3) fixation screw; (4) grasping devices front part; (5) grasping device back part.

As shown Figure 5.35, the grasping system is univocally referred to the movable end effector (6) of a serial manipulator via two dowel pins and it is fixed to it by screws. The serial manipulator is composed of a three prismatic (7), (9) and (10) and one spherical joints (8). In order to match the reduced space, the manipulator is of kind PPSP. The serial manipulator permits the grasping of the tibia in its natural position once the femur has been fixed to the test rig.

Furthermore, once the serial manipulator is positioned, the specimen can be unmounted and remounted in the same pose thanks to the two reference elements between the grasping device and the end effector of the manipulator. In Figure 5.36, the specimen unmounted from the rig is reported together with its two grasping systems.



*Figure 5.35 Tibia fixation and positioning system: (1) fibula; (2) tibia; (3) fixation screw; (4) grasping devices front part; (5) grasping device back part; (6) end effector; (7), (9) and (10) prismatic couples; (8) spherical couple.*

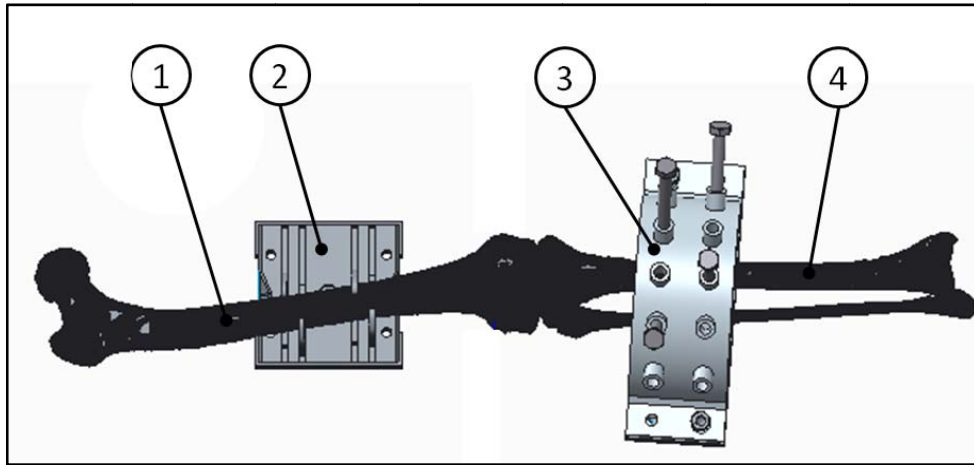


*Figure 5.36 Specimen with the grasping devices: (1) femur; (2) femur grasping platform; (3) tibia grasping device; (4) tibia.*

## 5.4 FLEXION ROTATION SYSTEM

One of the most innovative and relevant characteristics of the test rig proposed by the research group and described in [38] is the fact that the principal movement of flexion is mainly executed by the femur, whilst the other movements are left to the tibia. To guarantee femur rotation, the machine is equipped with a portal which rotates about a fixed axis. As explained in Section 5.3.1, the femur is mounted on this element via the femur fixation system. If on the one side the described femur fixation system allows a precise positioning and repositioning of the femur, on the other side this mechanism has been designed in order to participate in the realisation of the portal. The two cylindrical elements that host the three revolute couples and guarantee the block of the femur fixation mechanism (1) and (5), indeed, are connected to the portal rotation axis via two aluminium profiles (2) and (4), as shown in Figure 5.37, by obtaining two L-shaped elements. A crossbeam is placed between the two cylindrical elements and connects them, thus generating the closed portal. It is worth noting that the crossbeam (6) can be unmounted and remounted very easily. When it is unmounted, operations can be performed on the specimen fixed between the two L-shaped elements having a wide accessibility to the knee.

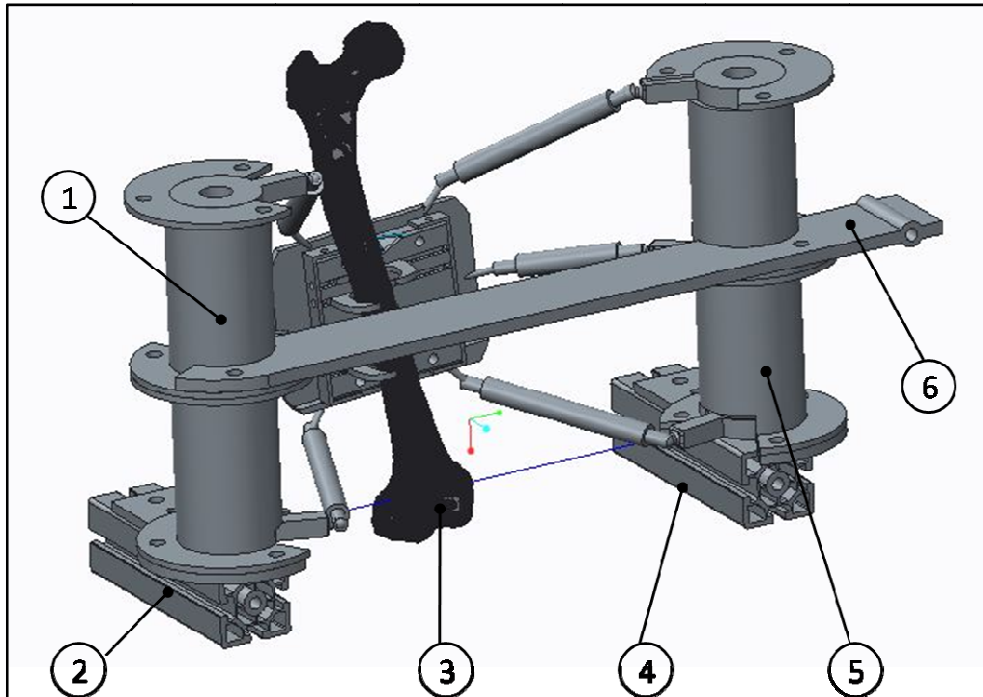


Figure 5.37 Femur fixation system integrated in the portal: (1) and (5) fixation element of the femur fixation system; (2) and (4) Bosch aluminium profiles; (3) femur; (6) crossbeam.

#### 5.4.1 ACTUATION OF THE PORTAL

A system have been designed for rotating the portal about the axis of the rotational couple that connects it to the frame. An analysis of the rotation resistant torque composed by the resistant component applied to the portal via the femur connections and the inertial contribution of the whole portal has been estimated. The small contribution of the muscle simulation has been considered too. A maximum torque of 200 Nm has been calculated. Low speeds of rotations are required for replicating tests, of the order of 15 rpm.

A stepper motor combined with a bevel gear reducer is used to move the portal. High velocity reduction is required, since the rotation is performed at low speed. A motor of the same kind of those used for the ballscrew actuation has been chosen. In the proposed solution, the axis of conducted shaft of the reducer is aligned with the rotation axis of the portal and connected to it via a Oldham joint, as represented in Figure 5.38.

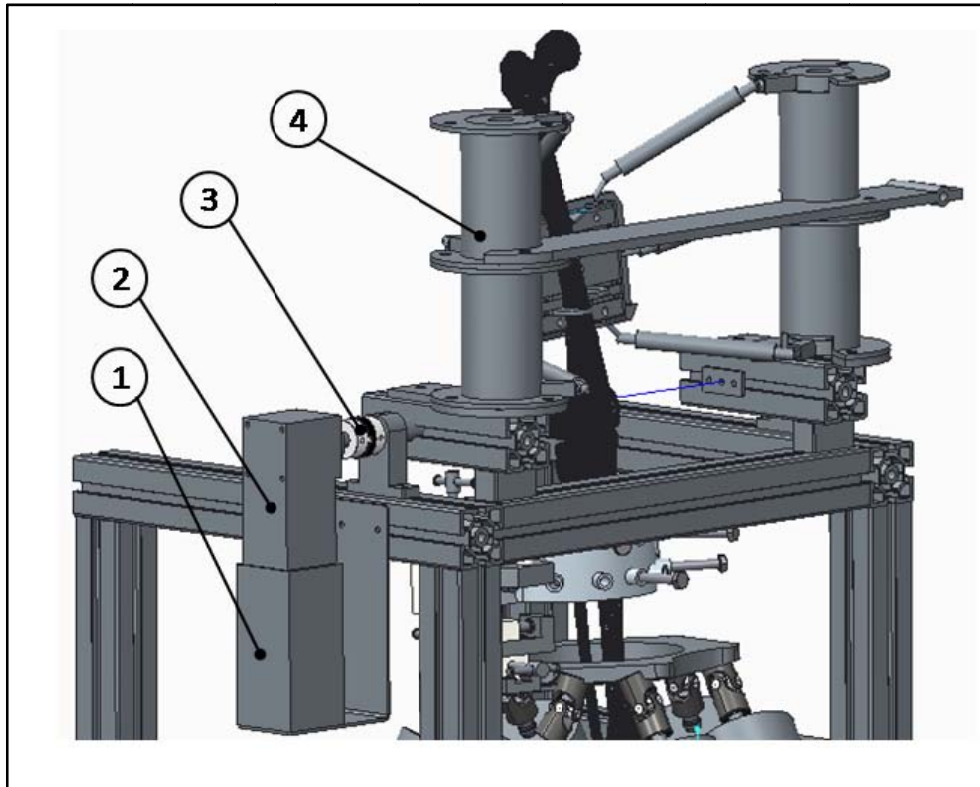


Figure 5.38 Portal actuation (1) motor; (2) bevel gear reducer; (3) connection joint; (4) portal.

Different solutions have been explored. In particular a slider-crack mechanism and a mechanism with pulleys and belt have been designed and studied. These mechanisms could be actuated by pneumatic pistons or electric motors (linear for the first option, linear or rotary for the second one). Electric solution has been preferred by the author, for similarity with the actuation of the loading system. The integration of the control can be performed easily and the compressed air is thus not necessary. In addition, the velocity control of the rotating portal is easier if electric motors are used instead of pneumatic ones. Finally, the solution with the motor aligned with the portal has been chosen because of its compactness and the lower costs of a rotary motor with respect to the linear one.

## 5.5 MUSCLE SIMULATION

The application of muscular loads during simulation of daily activities is essential for the replication of real conditions. When active tasks like walking and squat are performed, the muscular actions are fundamental to guarantee the knee stability and motion. Flexor and extensor muscles are simulated in two different ways which will be described in the following sub-sections.

### *5.5.1 EXTENSOR MUSCLE SIMULATION*

As described in Section 2.1.2.3, the extensor muscles are grouped in the quadriceps, whose tendon embraces the patella and inserts just above the tibia tuberosity. Since the evaluation of the motion of patella is of interest for the purpose of the tests, this bone must be included in the specimen and the simulation of the quadriceps must be done by grasping the quadriceps tendon above the patella. A mean direction of the force exerted by quadriceps can be defined as follows: if projected on the frontal plane, it is parallel to the long axis of the femur, i.e. from the patella it is directed to the head of the femur; if project in the sagittal plane, it is directed parallel to the axis of the femur, but moved forward of the thickness of the patella.

A system for simulating this load has been designed as shown in Figure 5.39, composed of: i) a patellar tendon grasping device (5), ii) a steel cable, iii) four pulleys (1, 2, 3 and 4), and iv) a ballscrew actuator. The grasping device connects the patellar tendon on the one side to the steel cable on the other side. The steel cable is positioned in order to replicate the direction of the quadriceps by means of the first pulley. To simulate the fact that the quadriceps inserts into the femur, maintaining a constant direction with respect to the femur itself, the pulley must move together with the femur during knee flexion. The first pulley is so mounted on the crossbar of the portal that connects the two cylindrical blocks, as show in Figure 5.39. The other pulleys are disposed in order to drive the cable to the ballscrew actuator which is mounted on the frame. One pulley is mounted on the portal and the other two are

mounted on the frame. The latter are adjoining one another and have parallel axis. According to the angular position of the portal, just one of the pulley is embraced by the cable. This way the circuit is constituted by 3 pulleys, the minimum number necessary for realising the switch from the moving system and the fixed one. The number of pulleys has been reduced to the minimum possible in order to reduce friction losses in the circuit.

The position and orientation of the first pulley need to be defined once the specimen has been mounted, in order to try to replicated the mean line of action of the quadriceps force. The pulley support has been designed in order to allow changing in both position and orientation. The position of the second pulley is fixed but it can rotate about its axis in order to match the direction of the wire coming from the first one. The third and fourth pulleys are mounted on the same support, which can orient about an axis perpendicular to the pulleys' axes and approximately coincident with the exit direction of the cable.

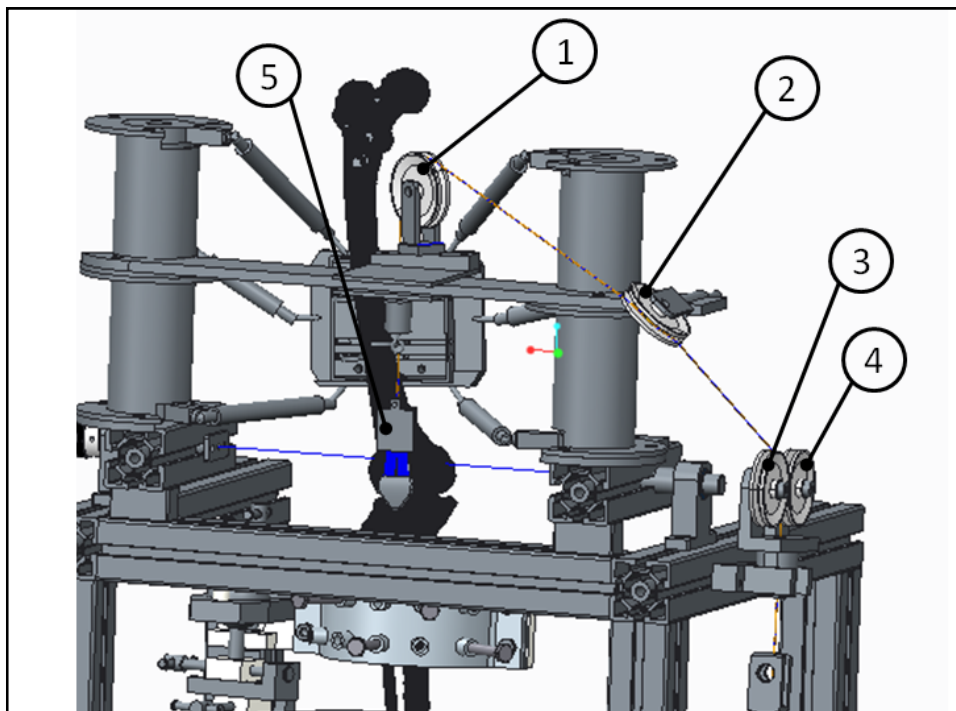


*Figure 5.39 Pulleys for femur simulation mounted on the portal: (1) and (2) pulleys mounted on the portal; (3) and (4) pulleys mounted on the frame; (5) patellar tendon grasping device.*

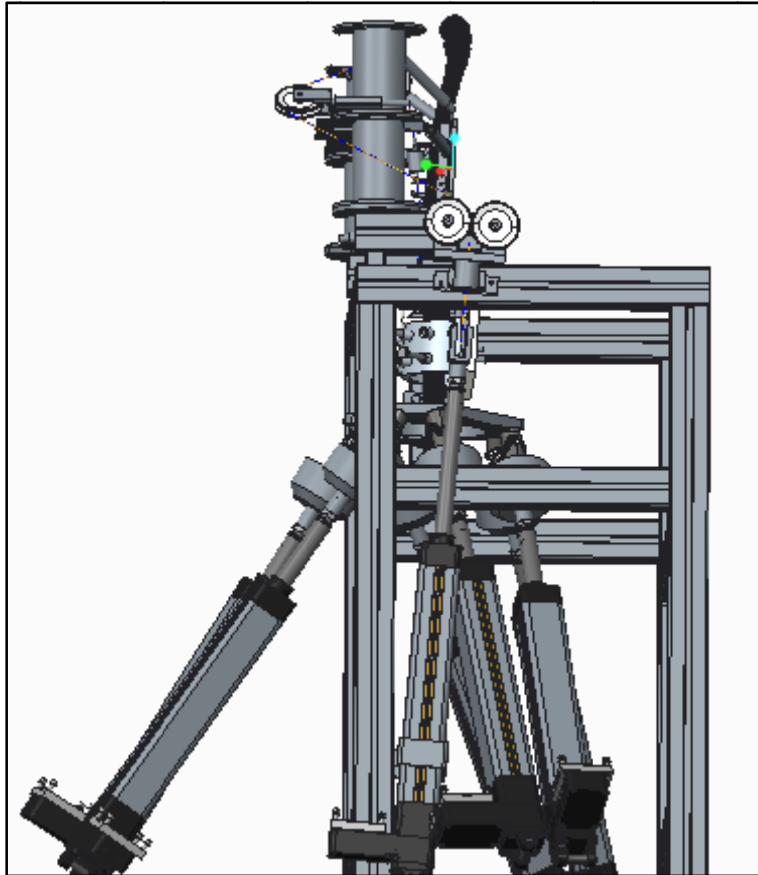


*Figure 5.40 Side view of the test rig with the system for extensor muscles simulation.*

A study has been performed on the optimal exit position of the cable. Both the moments on the portal and the knee lengthening and shortening at the variation of the angle have been considered. Looking at the rig on the sagittal plane, indeed, in the first part of flexion the cable unwinds from the pulley 3, while it wraps around pulley 4 in the second part. This wrapping and unwrapping must be compensated by the stroke of the actuator, which is force controlled. At the same time, thus, when flexing the femur, the patella acts as a pulley at the knee, so longer cable is required when the flexion angle increases. If choosing a correct positioning of the pulleys, the two phenomena of lengthening/shortening can partially compensate each other. As evidenced in figure, if the axis of the pulley 3 is posed in coincidence with the axis of rotation, the most compensation is obtained. At the same time, the effect of the forces exerted at the two extremities of the cable (i.e. force on the quadriceps tendon and force at the actuator)

are compensated since their levers (i.e. approximate distance between the anterior surface of the patella to the axis of rotation of the portal and distance between the cable and the axis of rotation of the portal, respectively) have approximately the same length and are at the opposite sides of the revolute axis. Thus, only a small contribution of the moment due to femur simulation needs to be balanced by the motor that rotates the portal.

The actuator is mounted in a quasi vertical position, so that it does not interfere with the other actuators, as shown in Figure 5.40. Its axis is coincident with the direction of the exiting cable. It is connected to the base via a spherical joint which can compensate the small misalignments of the cable that arise due to constructive and mounting tolerances. A reference elements prevents it from falling when no load is applied.

### *5.5.2 FLEXOR MUSCLE SIMULATION*

The extensor muscles are simulated thanks to a system that is connected to the real tendon and tries to replicate, even though simplifying, the anatomy of the simulated muscles. This is not possible for the flexor muscles, since the posterior space in the posterior side is limited, especially when the leg is deep flexed. As explained in Section 2.1.2.3, indeed, many muscles contribute to knee flexion, with different insertions on the tibia and different lines of action.

Since the reduced space is not enough to create systems similar to that designed for the extensor muscles, a different way of simulating posterior muscles has been introduced. It is based on the calculation of the wrench generated on the tibia by all the flexor muscles and the application of an equivalent wrench via the loading platform. This approach takes advantage of the superimposition principle, by applying to the tibia both the effect of the GRF and the effect of the flexor muscles.

The more the definition of the flexor muscle lines of action and efforts is detailed and precise, the more accurate the simulation of posterior muscles is.

### *5.5.3 MUSCLE CONTROL SYSTEM*

The new rig presented here is based on the concept of not imposing muscular loads, differently from what most of the rig described in Chapter 3 do. The muscular loads are evaluated, instead, by imposing the equilibrium to tibia rotation about the flexion axis. The flexion angle is imposed by rotating the femur about the transepicondylar axis that is coincident with the knee flexion axis, and maintaining the longitudinal axis of the tibia quasi vertical, if projected in the sagittal plane. Since during motion the equilibrium at the knee is guaranteed by the muscular and passive structures forces that counterbalance the external forces, it is possible to say that the flexion angle, i.e. the vertical position of the tibia, must be guaranteed by the action of muscles and passive structures. The muscle control system, thus, has been studied in order to guarantee that the tibia maintains its vertical position in the sagittal plane.

The control of the tibia position is realized in force. A load cell is mounted posteriorly at the distal end of the tibia as represented in Figure 5.1. It is connected to the tibial platform on one side and to the frame on the other side, via rigid connections. The rotation of the tibia about the medio-lateral axis generates a compression/tension in the load cell. The tension measured at the load cell is used to control the system for the simulation of the extensor or flexor muscles. The control system works in order to minimize the tension/compression at the load cell, so that flexion/extension moment due to external loads is equilibrated only by the simulated quadriceps or posterior muscles and by the other knee internal structures (ligament and contact surfaces) at the given flexion angle.

If, as a consequence of the external loads, the knee tends to flex (i.e., the distal part of the tibia rotates backwards), the load cell is compressed and the actuator simulating the quadriceps is activated to eliminate the load cell compression, thus maintaining the tibia in a vertical position. Conversely, if the knee tends to extend (i.e., the distal part of the tibia rotates forward), the load cell is tensioned and posterior muscles are activated: based on the superposition principle, as described in Section 5.5.2 additional loads,

equivalent to the resultant force of the flexor muscles, are applied to the tibia via the loading platform.

Thus, the load cell has two parallel roles: to reveal a flexion-extension rotation of the tibia, on the one hand, and on the other hand to maintain the tibia vertical in the during transient state. The control is thus realized in force, but, during transient state, the presence of the load cell obstruct the tibia flexion/extension.

This system makes it possible to simulate the real effect of the muscles on the tested leg. Indeed, it applies a load that balances the knee flexion/extension moment and allows the evaluation of the muscle contribution during daily activities. However, only the difference of the action of the antagonist muscles can be evaluated, since the present control system does not consider contemporary contraction of anterior and posterior muscles. The possibility to evaluate the net joint moment represents a very important feature of the test rig: also the characteristics in terms of forces required to muscles during motion can be evaluated during tests and compared in specimen before and after surgery.

## CHAPTER 6.

# DISCUSSIONS AND CONCLUSIONS

The purpose of this work was to develop a new test rig, able to investigate the behavior of the human knee under loaded and virtually unloaded conditions in a wide range of motion. In particular, the rig is required to apply a system of loads that simulates typical daily actions, without constraining the knee motion. The knee response in terms of displacements and rotations, indeed, must be guided solely by the action of the knee anatomical structures, i.e. articular surfaces, ligaments, tendons and muscles. The new rig presented in this work represents an innovative solution to satisfy the specifications. It conserves some key concepts introduced in a previous test rig based on a cable driven parallel system [38], but overcomes its main limitations. Indeed, thanks to its key features described in detail in Chapter 5, it allows overcoming most of the limitations of other rigs realized in the past by this and others research groups [6]- [13].

The first key feature that stands out when the overall structure is analysed is that the knee flexion angle is controlled and imposed separately from the other motion parameters. The regulation of the flexion position is executed by rotating the portal connected to the femur while maintaining the tibia vertical, and allows reaching high flexion angles. During flexion, variable load histories can be applied to the tibia by means of an parallel manipulator. The devices for flexion-angle variation and for load application are independent from one another.

The use of a 6-6 Gough-Stewart parallel manipulator for load application guarantees precise positioning and high repeatability, thanks to the higher stiffness of the parallel configuration, if compared to a serial one. The architecture and size of the loading system have been optimized in order to satisfy the motion and loads specification and to match the design and functional needs. This loading system requires the development of a closed-loop force control which increases the level of complexity if compared with the control of the previous version. However, its adoption is necessary

since it guarantees the possibility of applying a system of forces to the tibia without introducing further constraints to its motion. The evaluation of the tibia natural response, i.e. the evaluation of the knee natural motion, can thus be performed. The changes in the loading system configuration due to tibia motion, are taken into account by the control system. The latter, indeed, is based on the measurement of the position thanks to the resolver mounted on the stepper motors of the ballscrew actuators. Some errors in the evaluation of the pose of the platform could arise from backlash in the kinematic chain. To limit this effect, joints and actuators have been chosen with attention to backlash parameters. The closed-loop force control system is also based on the forces measured by the load cells mounted on the actuators. The wrench on the platform, i.e. the wrench applied to the tibia, results from the real applied forces. A difference between the real and the desired wrench on the tibia arises from the errors introduced by load cell accuracy and of friction in joints and by the manufacturing and mounting errors on the platform. Also for this reason, attention has been devoted to an accurate design and choice of the components, in order to limit backlash. Load cells have also been chosen in order to achieve the best possible accuracy, thus accepting their quite big sizes. However, it is worth noting that the magnitude of the estimated inaccuracies introduced by these factors is small if compared with the uncertainties on the loads, which are obtained from the adaptation of in-vivo measurements on different subjects. Even if further evaluation on the assembled machine is needed, the accuracy of the loading system is expected to be sufficient for the purpose of the test rig. If loads on the specimen need to be measured with higher level of accuracy, a six axis load cell can be mounted between the specimen and the platform. A modification of the tibia fixation system would be necessary. Since the fixation system is composed of a device fixed to the tibia univocally referred to the position regulation system, the load cell could be easily mounted at the interface of this two functional blocks.

The separate control of the flexion position of the femur together with the system for simulating the muscle actions makes it possible to evaluate the net joint moment about the flexion axis at the knee. The most of the available machines, indeed, impose muscle forces based on literature data, while the control of this new test rig varies muscle forces until they guarantee the equilibrium to rotation about the axis of the portal, thus

evaluating the net joint moment. At the knee, the net joint moment is the result of the difference between the moment generated by extensor muscles and the moment generated by flexor ones, since contemporary contraction (co-contraction) of anterior and posterior muscles is often present during motion. While the net joint moment (i.e. the difference between the flexor and extensor muscle contributions) can be evaluated by the rig, the contribution of each single muscle cannot be identified, since infinite combination of forces would guarantee the equilibrium to the considered rotation. If some muscular forces or a proportion between flexor and extensor muscle forces were imposed, co-contraction could be taken into account. In this case, further hypotheses would be introduced, thus bringing in some not well known variables. For the scope of the rig, thus, the choice of not introducing additional variables has been done, and the activation of either anterior or posterior muscles is performed by the control system.

The tibia and femur fixation systems are two other key elements of the rig. They guarantee the possibility of a precise specimen positioning, by adjusting all the six DOF between the rig and the specimen. They also guarantee the possibility of unmount and accurately remount the specimen in the same pose, thanks to two coupled and univocally referred elements. This feature allows repeating the same tests on specimens whose functional characteristics have been modified, for example after ligament cutting and/or reconstruction or after prosthesis implant. The elements fixed to the bones guarantee bone grasping and their regular geometries permit an easy fixation on a vice or on other systems while surgical operations are performed on the specimen. With this basic common idea, the two fixation systems have been realized with different architectures, since they are subjected to different requisites. The tibia fixation system has been developed in order to be compact since spaces are reduced and adjustments are expected to be smaller. Wider regulations is 6 DOF are required to the femur and wider space are available, so the femur fixation system has been designed with a different architecture, and in order to be integrated in the portal. Both the system have been developed on the anterior side of the joint, in order to leave the posterior side free. This feature guarantees high flexion angles (150°).

From the design and functional points of view, the integration of the femur fixation system and the portal represents an important feature of the machine. A reduced

---

number of members have to be rotated during flexion, i.e. reduced weights and inertia components have to be compensated by the rotary stepper motor. Smaller volumes are occupied by the integrated rotation and fixation systems, thus a wide accessibility to the knee is obtained. The possibility to unmount the crossbar, indeed, provides the chance of operating directly on the knee through the access on its anterior side.

The architecture of the overall rig has been developed in order to permit the measurement of the relative bone motion via an optoelectronic system. Trackers can be fixed directly to the bones (or to the platforms fixed to the bones) and a system of cameras can be used to record the movement. Wide visibility is guaranteed in the area around the knee and just under it, for recording patella and tibia movements from the anterior point of view. Visibility is guaranteed at the head of the femur, to measure its motion from the posterior point of view. Furthermore, a future development can see the integration of the tibia motion measurement with the platform kinematic analysis performed during control. The inaccuracies due to backlash in joints and resolver measurement errors on the kinematic analysis are lower than the inaccuracies due to the optoelectronic system (for example, Vicon Motion System guarantees an accuracy of 0.5 mm/0.5°).

The test rig proves to be versatile: all possible loading conditions within a certain range can be applied and can be modified as a function of the flexion angle, thus simulating different loading tasks. Furthermore if no external loads are applied to the tibia other than the weight compensation, the unloaded motion can be analysed too. In addition, the dimension of the clamping devices do not impose particular constraints on the specimen size. With some simple modifications also other human joints, for instance the ankle and the elbow, can be tested.

## REFERENCES

- [1] Frank C. Anderson and Marcus G. Pandy, "Dynamic optimization of human walking," *Journal of biomechanical engineering*, vol. 123, no. 5, pp. 381-390, 2001.
- [2] N. Sancisi, D. Zannoli, V., Belvedere, C Parenti-Castelli, and A Leardini, "A one-degree-of-freedom spherical mechanism for human knee joint modelling," *Proceedings of the Institution of Mechanical Engineers, Part H: Journal of Engineering in Medicine*, vol. 8, no. 725-735, p. 225, 2011.
- [3] J.C. Loh et al., "Knee stability and graft function following anterior cruciate ligament reconstruction: Comparison between 11 o'clock and 10 o'clock femoral tunnel placement," *Arthroscopy: The Journal of Arthroscopic and Related Surgery*, vol. 19, no. 3, pp. 297-304, 2003.
- [4] M. Wünschel et al., "Differences in knee joint kinematics and forces after posterior cruciate retaining and stabilized total knee arthroplasty," *The Knee*, vol. 20, no. 6, pp. 416-421, 2013.
- [5] T. J. Withrow, L. J. Huston, E. M. Wojtys, and J. A. Ashton-Miller, "Effect of varying hamstring tension on anterior cruciate ligament strain during in vitro impulsive knee flexion and compression loading," *The Journal of Bone and Joint Surgery*, vol. 90, no. 4, pp. 815-823, The Journal of Bone and Joint Surgery, Inc.
- [6] A.B. Zavatsky, "A kinematic-freedom analysis of a flexed-knee-stance testing rig," *Journal of biomechanics*, vol. 30, no. 3, pp. 277-280, 1997.
- [7] K. M. Varadarajan, R. E. Harry, T. Johnson, and G. Li, "Can in vitro systems capture the characteristic differences between the flexion-extension kinematics of the healthy and TKA knee?," *Medical engineering and physics*, vol. 31, no. 8, pp.

899-906, 2009.

- [8] G. Yildirim, P.S. Walker, and J. Boyer, "Total knees designed for normal kinematics evaluated in an up-and-down crouching machine," *Journal of Orthopaedic Research*, vol. 27, no. 8, pp. 1022-1027, 2009.
- [9] L.P. Maletsky and B.M. Hillberry, "Simulating dynamic activities using a five-axis knee simulator," *Journal of biomechanical engineering*, vol. 127, no. 1, pp. 123-133, 2005.
- [10] H. Fujie et al., "The use of robotics technology to study human joint kinematics: a new methodology," *Journal of biomechanical engineering*, vol. 115, no. 3, pp. 211-217, 1993.
- [11] H. Fujie, T. Sekito, and A. Orita, "A novel robotic system for joint biomechanical tests: application to the human knee joint," *Journal of biomechanical engineering*, vol. 126, no. 1, pp. 54-61, 2004.
- [12] B. Ding, R. M. Stanley, B. S. Cazzolato, and J. J. Costi, "Real-time FPGA control of a hexapod robot for 6-dof biomechanical testing," in *IECON 2011-37th Annual Conference on IEEE Industrial Electronics Society*, 2011, November, pp. 252-257.
- [13] M. Forlani, N. Sancisi, M. Conconi, and V. Parenti-Castelli, "A new test rig for static and dynamic evaluation of knee motion based on a cable-driven parallel manipulator loading system," *Meccanica*, pp. 1-11, 2015.
- [14] I.A. Kapandji, *Fisiologia Articolare, II parte: Arto Inferiore.*: Moduzzi Editore, 2007.
- [15] I. Hilal, S. Van Sint Jan, A. Leardini, and U. Della Croce, "Virtual Animation of the Kinematics of the Human for Industrial, Education and Research Purposes. D3.2. Technical Report on Data Collection Procedure ANNEX I," 1999.

- 
- [16] R. O'Rahilly, F. Müller, S. Carpenter, and R. Swenson, *Basic Human Anatomy*: Dartmouth Medical School, 2008.
- [17] H.M. Karakas and A. Harma, "Femoral shaft bowing with age: a digital radiological study of Anatolian Caucasian adults," *Diagn Interv Radiol*, vol. 14, no. 1, pp. 29-32, 2008.
- [18] Yan-Xi Chen et al., "Three-dimensional morphological characteristics measurement of ankle joint based on computed tomography image post-processing.," *Chinese medical journal*, vol. 124, no. 23, pp. 3912-3918, 2011.
- [19] M. Giladi et al., "Stress fractures and tibial bone width. A risk factor," *Journal of Bone l& Joint Surgery, British Volume*, vol. 69, no. 2, pp. 326--329, 1987.
- [20] H. Gray, *Anatomy of the Human Body*, 40th ed. New York, 2008.
- [21] F.H. Netter, *Atlas of Human Anatomy*, 6th ed.: Elsevier, 2014.
- [22] E. S. Grood and W. J. Suntay, "A joint coordinate system for the clinical description of three-dimensional motions: application to the knee," *Journal of biomechanical engineering*, vol. 105, no. 2, pp. 136-144, 1983.
- [23] M. Nordin and V.H. Frankel, *Basic biomechanics of the musculoskeletal system*: Lippincott Williams and Wilkins, 2001.
- [24] C. Belvedere et al., "Does medio-lateral motion occur in the normal knee? An in-vitro study in passive motion," *Journal of biomechanics*, vol. 44, no. 5, pp. 877-884, 2011.
- [25] B.D. Beynnon and A.A. Amis, "In vitro testing protocols for the cruciate ligaments
-

- 
- and ligament reconstructions," *Knee Surgery, Sports Traumatology, Arthroscopy*, vol. 6, no. 1, pp. S70-S76, 1998.
- [26] T. M. Guess and A. Stylianou, "Simulation of anterior cruciate ligament deficiency in a musculoskeletal model with anatomical knees," *The open biomedical engineering journal*, vol. 6, pp. 23-32, 2012.
- [27] H. Hirschfeld, M. Thorsteinsdottir, and E. Olsson, "Coordinated ground forces exerted by buttocks and feet are adequately programmed for weight transfer during sit-to-stand," *Journal of neurophysiology*, vol. 82, no. 6, pp. 3921-3029, 1999.
- [28] J.W. Xerogeanes et al., "Effect of knee flexion on the in situ force distribution in the human anterior cruciate ligament," *Knee Surgery, Sports Traumatology, Arthroscopy*, vol. 3, no. 1, pp. 9-13, 1995.
- [29] B.D. Beynnon et al., "The Relationship Between Anterior-Posterior Knee Laxity and the Structural Properties of the Patellar Tendon Graft A Study in Canines," *The American journal of sports medicine*, vol. 22, no. 6, pp. 812-820, 1994.
- [30] T.W. Rudy, G.A. Livesay, S.L.-Y. Woo, and F.H. Fu, "A combined robotic/universal force sensor approach to determine in situ forces of knee ligaments," *Journal of biomechanics*, vol. 29, no. 10, pp. 1357-1360, 1996.
- [31] G. Li et al., "The importance of quadriceps and hamstring muscle loading on knee kinematics and in-situ forces in the ACL," *Journal of biomechanics*, vol. 32, no. 4, pp. 395-400, 1999.
- [32] G. Li et al., "Kinematics of the knee at high flexion angles: an in vitro investigation.," *Journal of Orthopaedic Research*, vol. 22, no. 1, pp. 90-95, 2004.
- [33] P.M. Aubin, M.S. Cowley, and W.R. Ledoux, "Gait simulation via a 6-DOF parallel
-

- robot with iterative learning control," *Biomedical Engineering, IEEE Transactions on*, vol. 55, no. 3, pp. 1237-1240, 2008.
- [34] R. A. Howard et al., "Reproduction of in vivo motion using a parallel robot," *Journal of biomechanical engineering*, vol. 129, no. 5, pp. 743-749, 2007.
- [35] M. A. Pilambaraee, E. J. O. O'Brien, C. B. Frank, and N. G. Shrive, "There is significant load sharing and physical interaction between the anteromedial and posterolateral bundles of the ovine ACL under anterior tibial loads," *The Knee*, vol. 19, no. 6, pp. 797-803, 2012.
- [36] W. K. Barsoum et al., "Robotic testing of proximal tibio-fibular joint kinematics for measuring instability following total knee arthroplasty," *Journal of Orthopaedic Research*, vol. 29, no. 1, pp. 47-52, 2011.
- [37] I. M. Lawless, B. Ding, B. S. Cazzolato, and J. J. Costi, "Adaptive velocity-based six degree of freedom load control for real-time unconstrained biomechanical testing," *Journal of biomechanics*, vol. 47, no. 12, pp. 3241-3247, 2014.
- [38] E. Grood, S.F. Stowers, and F.R. Noyes, "Limits of movement in the human knee. Effect of sectioning the posterior cruciate ligament and posterolateral structures.," *The journal of bone and joint surgery*, vol. 70, no. 1, pp. 88-97, 1988.

# ANNEX 1.

## TECHNICAL CHARACTERISTICS OF THE BALLSCREW ACTUATOR

Extract from Parker Catalogue

ETH - Electro Cylinder  
Technical Characteristics

### Technical Characteristics

Cylinder size type	Unit	ETH032			ETH050			ETH080		
		M05	M10	M16 <sup>1)</sup>	M05	M10	M20 <sup>2)</sup>	M05	M10	M32 <sup>2)</sup>
Screw lead	[mm]	5	10	16	5	10	20	5	10	32
Screw diameter	[mm]	16			20			32		
<b>Travels, speeds and accelerations</b>										
Available strokes <sup>1)</sup>	[mm]	continuous from 50-1000 & standard strokes			continuous from 50-1200 & standard strokes			continuous from 50-1600 & standard strokes		
Max. permissible speed at stroke →										
50-400 mm	[mm/s]	333	667	1067	333	667	1333	267	533	1707
600 mm	[mm/s]	266	540	855	333	666	1318	267	533	1707
800 mm	[mm/s]	198	373	592	238	462	917	267	533	1707
1000 mm	[mm/s]	148	277	440	177	345	684	264	501	1561
1200 mm	[mm/s]	-	-	-	139	270	536	207	394	1233
1400 mm	[mm/s]	-	-	-	-	-	-	168	320	1006
1600 mm	[mm/s]	-	-	-	-	-	-	140	267	841
Max. Acceleration	[m/s <sup>2</sup> ]	4	8	12	4	8	15	4	8	15
<b>Forces</b>										
Max. axial traction/thrust force motor inline	[N]		3700	2400		7000	4400		25100	10600
Max. axial traction/thrust force depending on the motor speed n	[N]		3280	2050	9300	4920	2460			
Motor parallel	[N]	3600	2620	1640	7870	3930	1960	17800	11620	3630
Equivalent dynamic axial force at a lifetime of 2500 km	[N]	1130	1700	1610	2910	3250	2740	3140	7500	6050
<b>Max. transmissible torque / force constant</b>										
Max. transmissible torque inline motor	[Nm]	3.2	6.5	6.8	8.2	12.4	15.6	15.7	44.4	60.0
Max. transmissible torque depending on the motor speed n	[Nm]	3.5	6.4		9.1	9.3		17.5	22.8	
Motor parallel	[Nm]	3.5	5.2		7.7	7.7		17.5	22.8	
Force constant motor inline <sup>3)</sup>	[N/Nm]	1131	565	353	1131	565	283	1131	565	177
Force constant motor parallel <sup>3)</sup>	[N/Nm]	1018	509	318	1018	509	254	1018	509	159
<b>Mass</b>										
Mass of base Unit with zero stroke (incl. Cylinder rod)	[kg]	1.2	1.2	1.3	2.2	2.3	2.5	6.9	7.6	8.7
Mass of additional stroke (incl. Cylinder rod)	[kg/m]		4.8			8.6			16.7	
Weight of cylinder rod with zero stroke	[kg]		0.06			0.15			0.59	
Weight of cylinder rod - additional length	[kg/m]		0.99			1.85			4.93	
<b>Mass moments of inertia</b>										
Motor parallel without stroke	[kgmm <sup>2</sup> ]	8.3	8.8	14.1	30.3	30.6	38.0	215.2	213.6	301.9
Motor inline without stroke	[kgmm <sup>2</sup> ]	7.1	7.6	12.9	25.3	25.7	33.1	166.2	164.5	252.9
Parallel/Inline motor per meter	[kgmm <sup>2</sup> /m]	41.3	37.6	41.5	97.7	92.4	106.4	527.7	470.0	585.4
<b>Accuracy: Bidirectional Repeatability (ISO230-2)</b>										
Motor inline	[mm]								±0.03	
Motor parallel	[mm]								±0.05	
<b>Efficiency</b>										
Motor inline	[%]								90	
Motor parallel	[%]								81	
<b>Ambient conditions</b>										
Operating temperature	[°C]								-10...+70	
Ambient temperature	[°C]								-10...+40	
Storage temperature	[°C]								-20...+40	
Humidity	[%]								0...95 % (non-condensing)	
Location height range	[m]								max. 3000	

<sup>1)</sup> "Order Code" (page 52), <sup>2)</sup> Intermediate stroke lengths may be interpolated.

<sup>3)</sup> ATEX on request

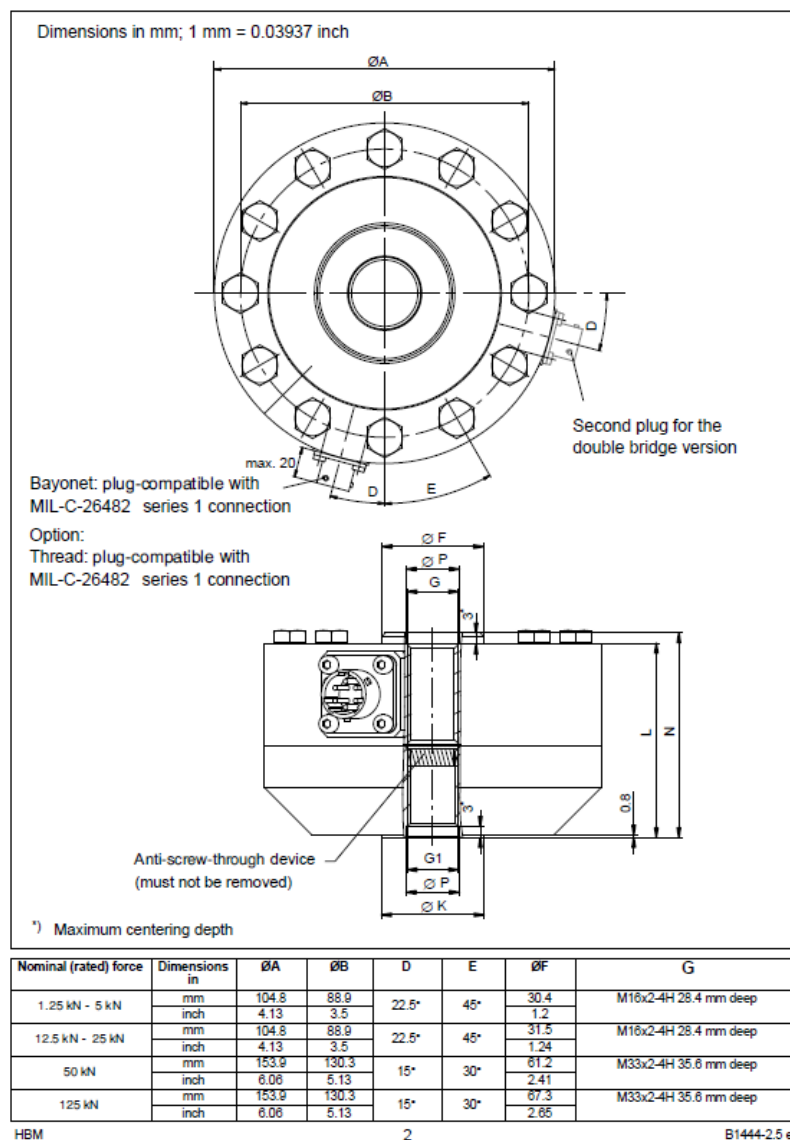
<sup>4)</sup> ATEX not available, <sup>5)</sup> The efficiency factors are included in the force constants.

## ANNEX 2.

### DIMENSIONAL AND TECHNICAL CHARACTERISTICS OF LOAD CELLS

Extract from technical sheet

#### U10M dimensions with foot adapter



## Specifications (VDI/VE 2638)

Nominal (rated) force	$F_{nom}$	kN	1.25	2.5	5	12.5	25	50	125	250	500
Nominal (rated) sensitivity	$C_{nom}$	mV/V	1 ... 1.5 <sup>1)</sup>			2 ... 2.5 <sup>1)</sup>					
Accuracy class			0.03			0.04			0.05	0.06	
Relative repeatability error in an unmodified mounting position	$b_{rg}$	%	0.025								
Relative zero signal error	$d_{s,0}$	%	1								
Relative reversibility error <sup>2)</sup> (at $0.4 \cdot F_{nom}$ )	$v_{0.4}$	%vl %vvc	< 0.075 0.03			< 0.1 0.04		< 0.125 0.05		< 0.125 0.05	
Relative linearity error	$d_{ln}$	%	< $\pm 0.03$			< $\pm 0.04$					< $\pm 0.06$
Relative creep over 30min	$d_{cr+E}$	%	< $\pm 0.04$			< $\pm 0.025$					
Effect of temperature on sensitivity/10K	$TK_C$	%	< $\pm 0.015$								
Temperature effect on the zero signal/10K	$TK_0$	%	< $\pm 0.015$								
Bending moment influence (at $10\% \cdot F_{nom} \cdot 10$ mm)	$d_Q$	%	< 0.01								
Output resistance	$R_O$	$\Omega$	280 ... 380								
Input resistance	$R_I$	$\Omega$	> 345								
Insulation resistance	$R_{is}$	G $\Omega$	> 2								
Reference excitation voltage	$U_{ref}$	V	5								
Operating range of excitation voltage	$B_{U,0}$	V	0.5 to 12								
Reference temperature	$T_{ref}$		+23 [73.4]								
Nominal (rated) temperature range	$B_{T,nom}$	°C [°F]	-10 ... +45 [+14 ... +113]								
Operating temperature range	$B_{T,0}$		-30 ... +85 [-22 ... +185]								
Storage temperature range	$B_{T,S}$		-30 ... +85 [-22 ... +185]								
Max. operating force	$(F_Q)$		240								
Breaking force	$(F_B)$	% v. $F_{nom}$	> 400								
Static lateral limit force <sup>3)</sup>	$(F_Q)$		100								
Bending limit moment	$M_{b,perm}$	N·m	30	60	125	315	635	1270	3175	5715	11430
Limit torque	$M_L$	N·m	30	60	125	315	635 <sup>4)</sup>	1270	3175	5715	11430
Nominal (rated) displacement	$s_{nom}$	mm	0.02			0.03			0.04	0.05	0.06
Fundamental resonance frequency	$f_G$	kHz	4.5	5.9	9.3	6.6	9.2	6.5	8.1	6.6	6.1
Rigidity	$F/S$	10 <sup>5</sup> N/mm	0.625	1.25	2.5	4.17	8.33	16.7	31.3	50.0	83.3
Permissible vibrational stress (Vibration bandwidth per DIN 50100)	$F_{vb}$	% v. $F_{nom}$	200								
Weight (without cable)											
With adapter		kg	1.2			3			10	23	60
Without adapter		lbs	2.65			6.61			22.05	50.71	132.28
		kg	0.6			1.3			5	11	28
		lbs	1.1			2.87			11.02	24.25	61.73
Immunity from interference (EN 61326-1, Table A.1)			Industrial environment								
Electromagnetic field (AM)		V/m	10								
Magnetic field		A/m	30								
Electrostatic discharge (ESD)											
Contact discharge		kV	4								
Air discharge		kV	8								
Burst (rapid transients)		kV	1								
Surge (impulse voltages)		kV	1								
Grid-bound interferences (AM)		V	3								

## ANNEX 3.

## FORCES REQUIRED AT THE 6-3 GOUGH-STEWART PLATFORM

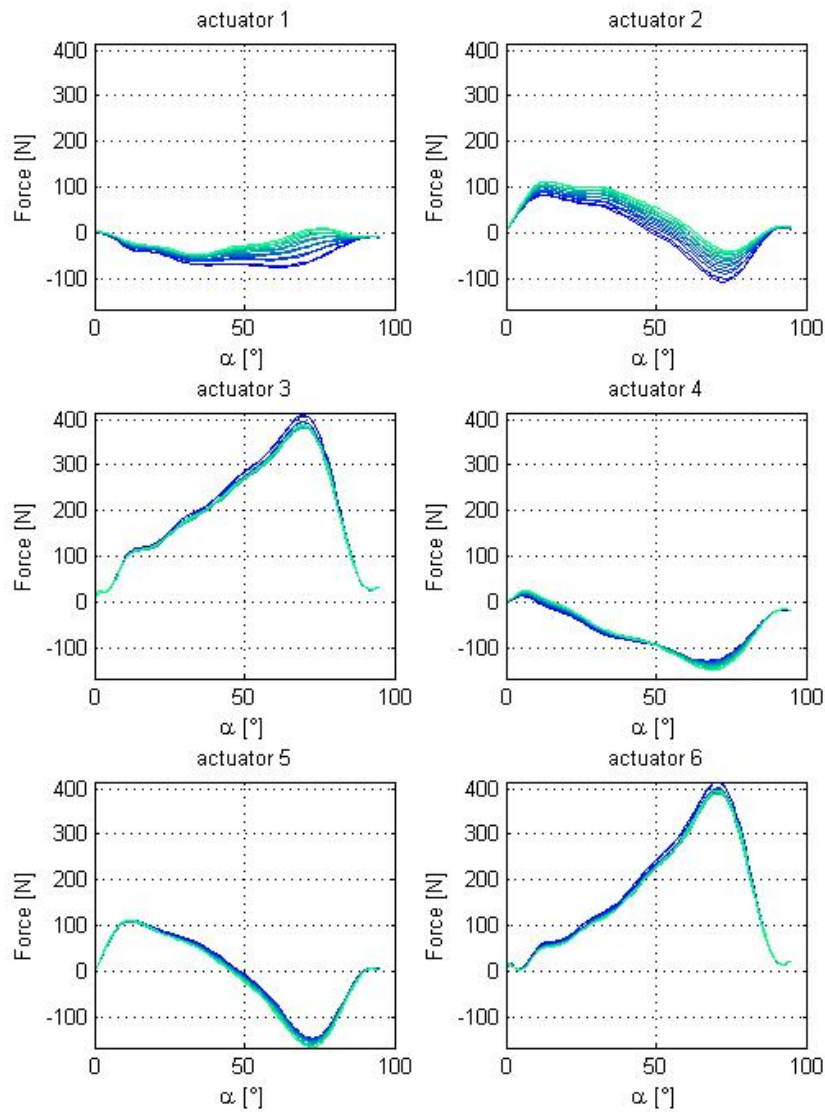


Figure A3.1 Trend of the forces required during sit to stand at the actuators of the 6-3 Gough-Stewart architecture as a function of the flexion angle  $\alpha$  at various diameter of the base: smallest diameters in blue color, larger diameters in light blue.

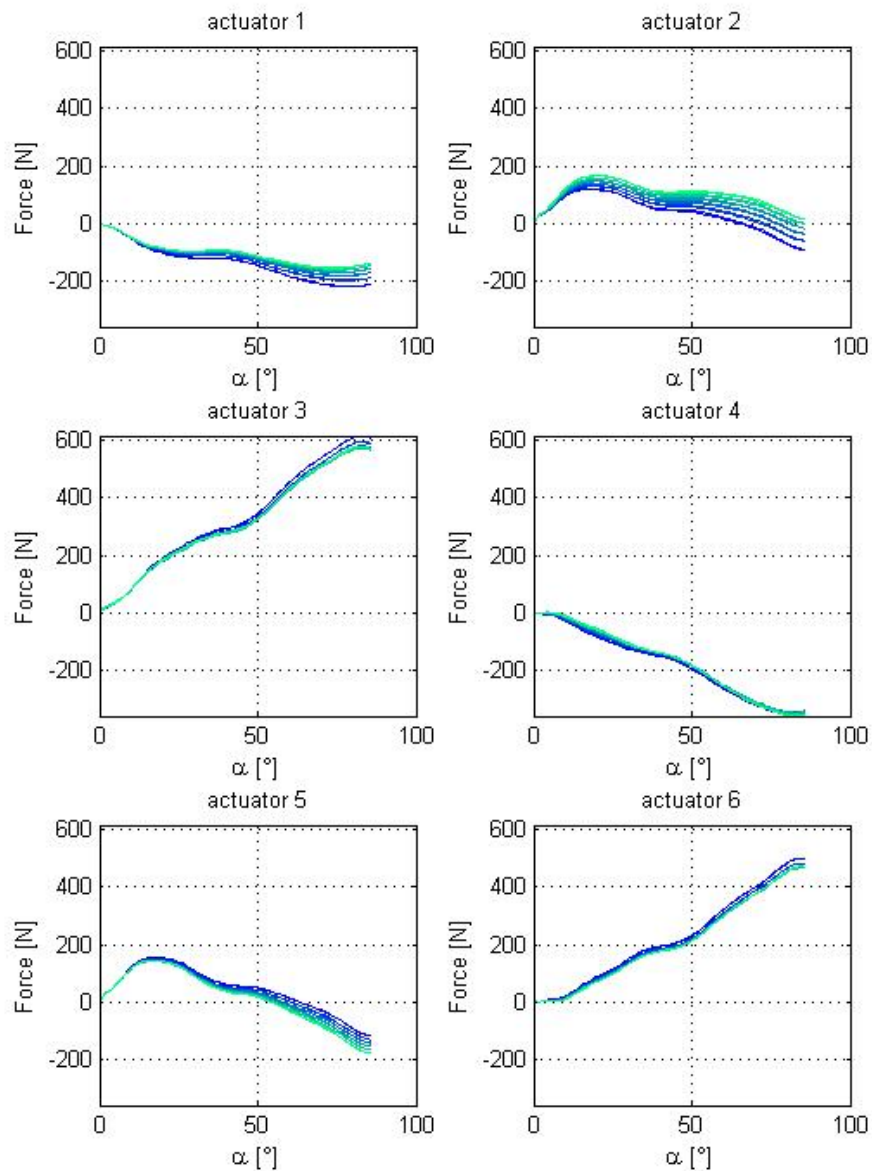


Figure A3.2 Trend of the forces required during squat at the actuators of the 6-3 Gough-Stewart architecture as a function of the flexion angle  $\alpha$  at various diameter of the base: smallest diameters in blue color, larger diameters in light blue.

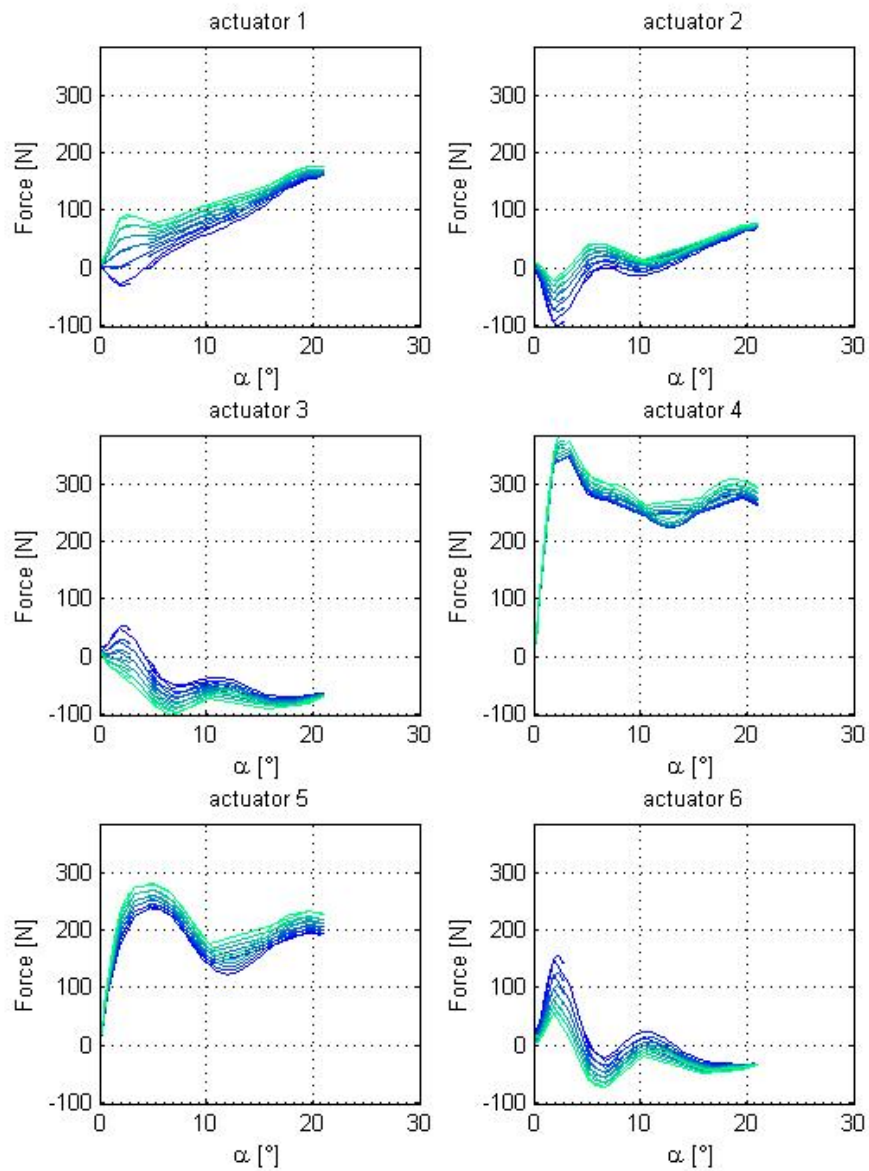


Figure A3.3 Trend of the forces required during walking part A at the actuators of the 6-3 Gough-Stewart architecture as a function of the flexion angle  $\alpha$  at various diameter of the base: smallest diameters in blue color, larger diameters in light blue.

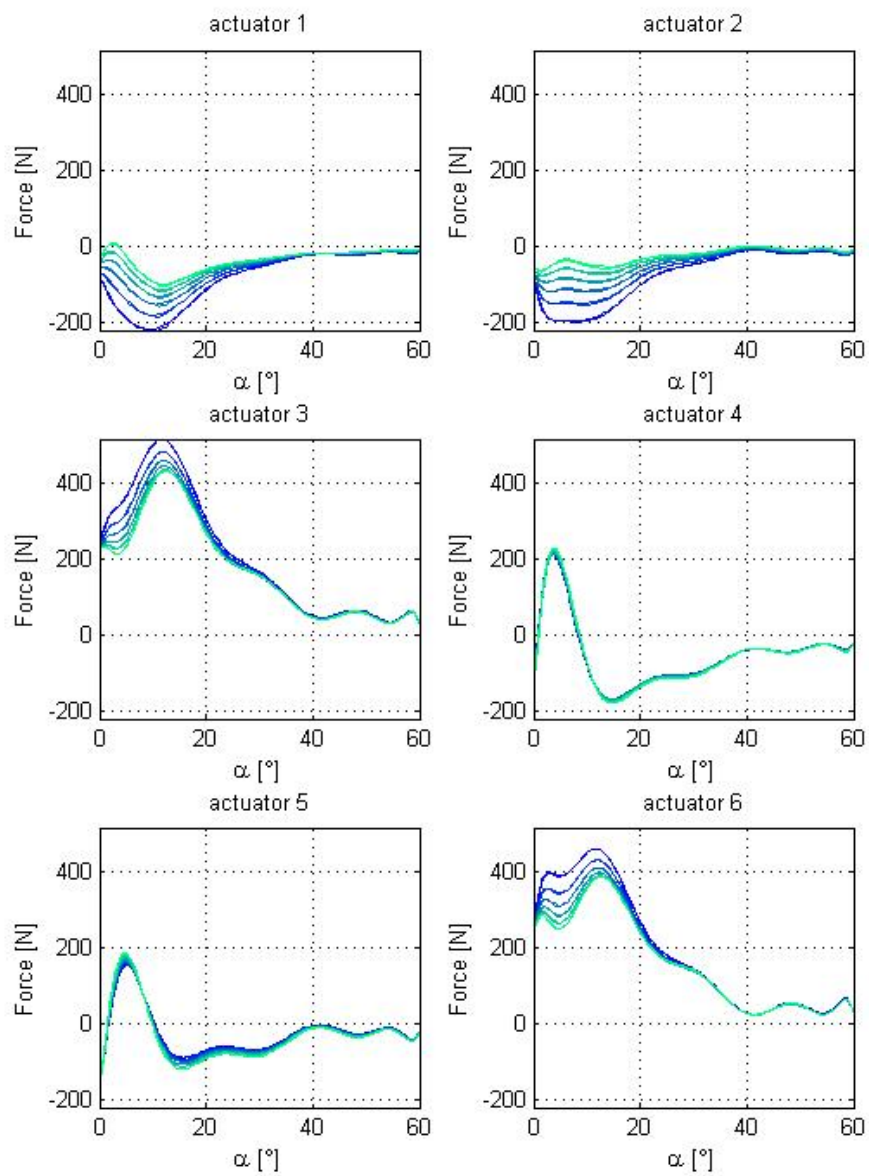


Figure A3.4 Trend of the forces required during walking part B at the actuators of the 6-3 Gough-Stewart architecture as a function of the flexion angle  $\alpha$  at various diameter of the base: smallest diameters in blue color, larger diameters in light blue.

## FORCES REQUIRED AT THE 6-6 GOUGH-STEWART PLATFORM

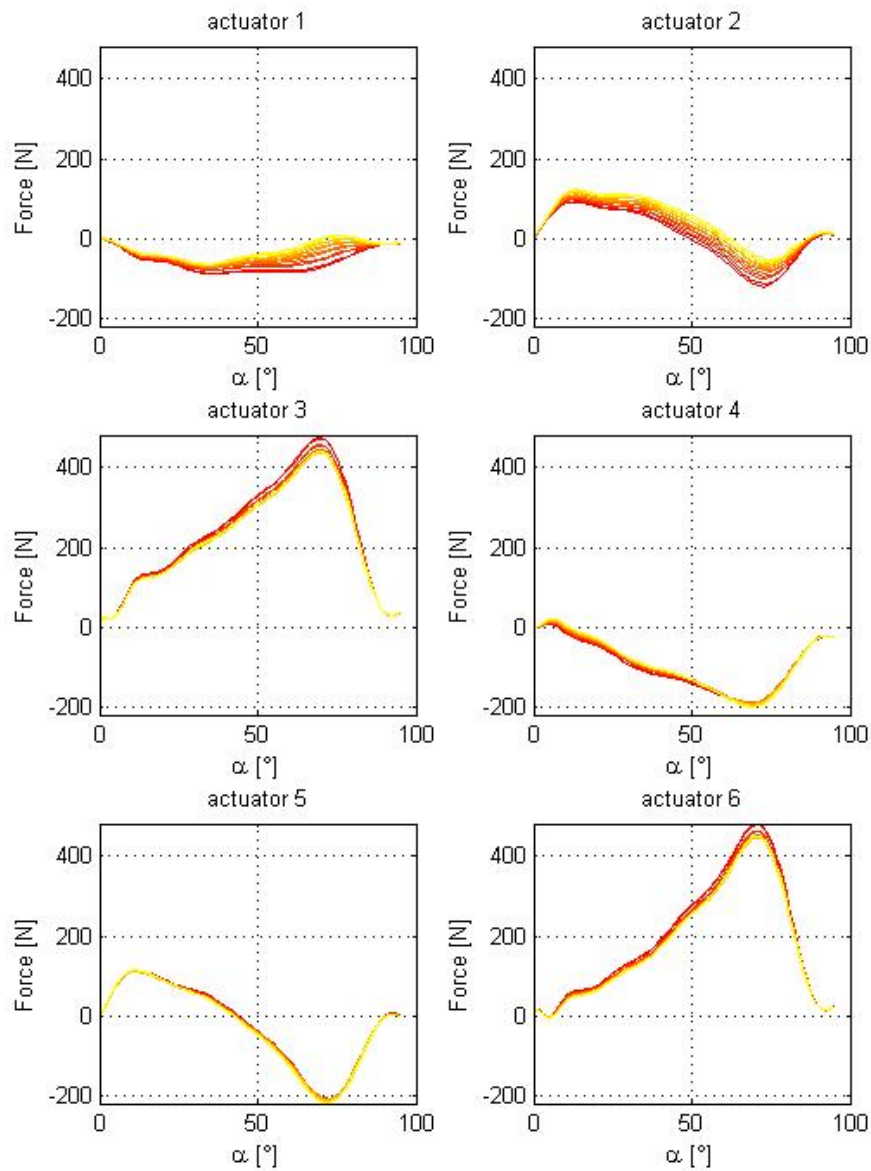


Figure A3.5 Trend of the forces required during sit to stand at the actuators of the 6-6 Gough-Stewart architecture as a function of the flexion angle  $\alpha$  at various diameter of the base: smallest diameters in red color, larger diameters in yellow.

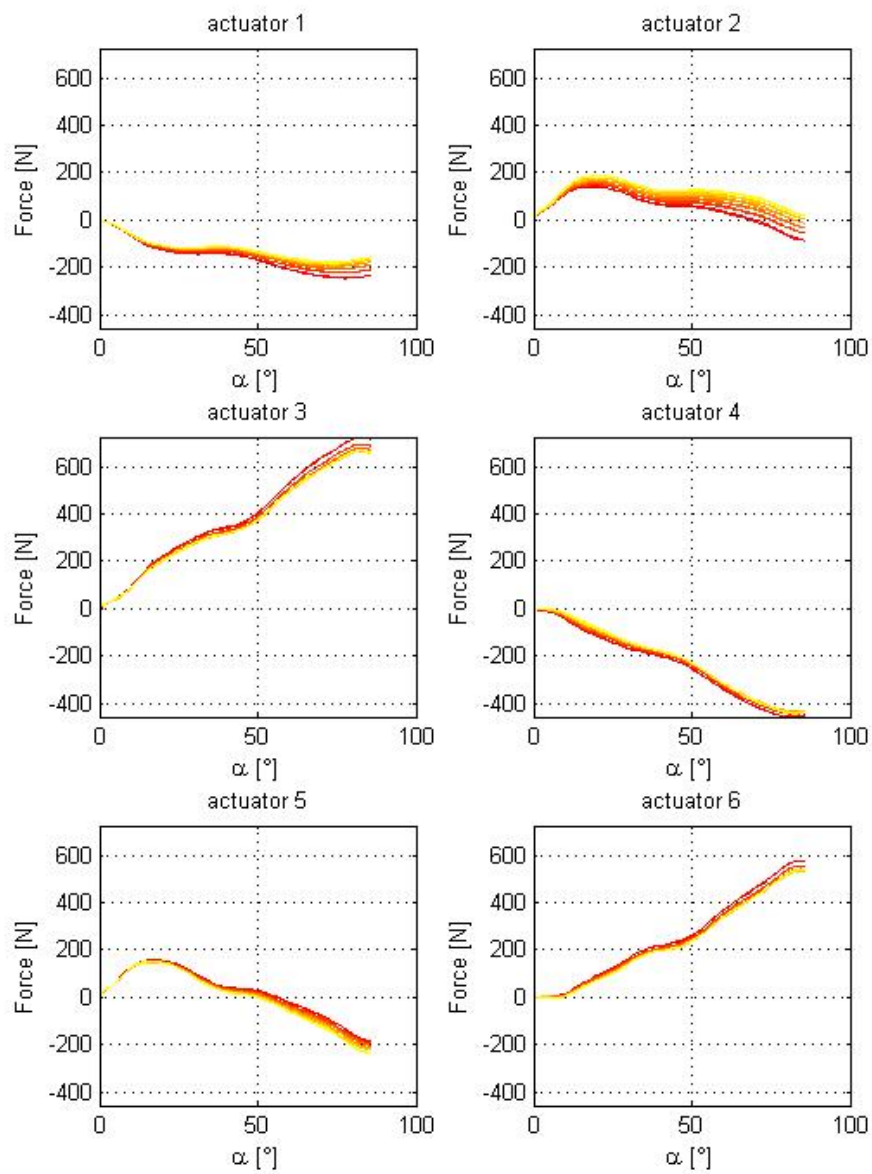


Figure A3.6 Trend of the forces required during squat at the actuators of the 6-6 Gough-Stewart architecture as a function of the flexion angle  $\alpha$  at various diameter of the base: smallest diameters in red color, larger diameters in yellow.

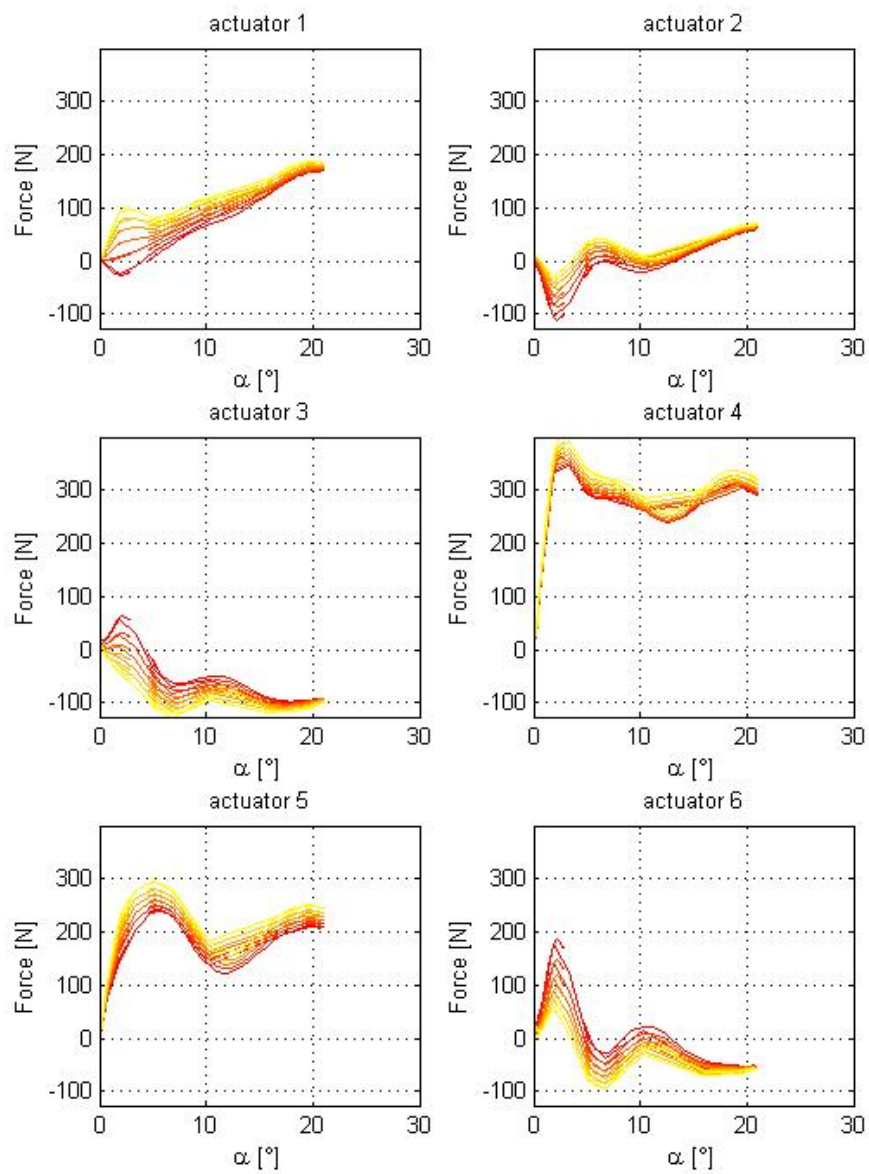


Figure A3.7 Trend of the forces required during walking A at the actuators of the 6-6 Gough-Stewart architecture as a function of the flexion angle  $\alpha$  at various diameter of the base: smallest diameters in red color, larger diameters in yellow.

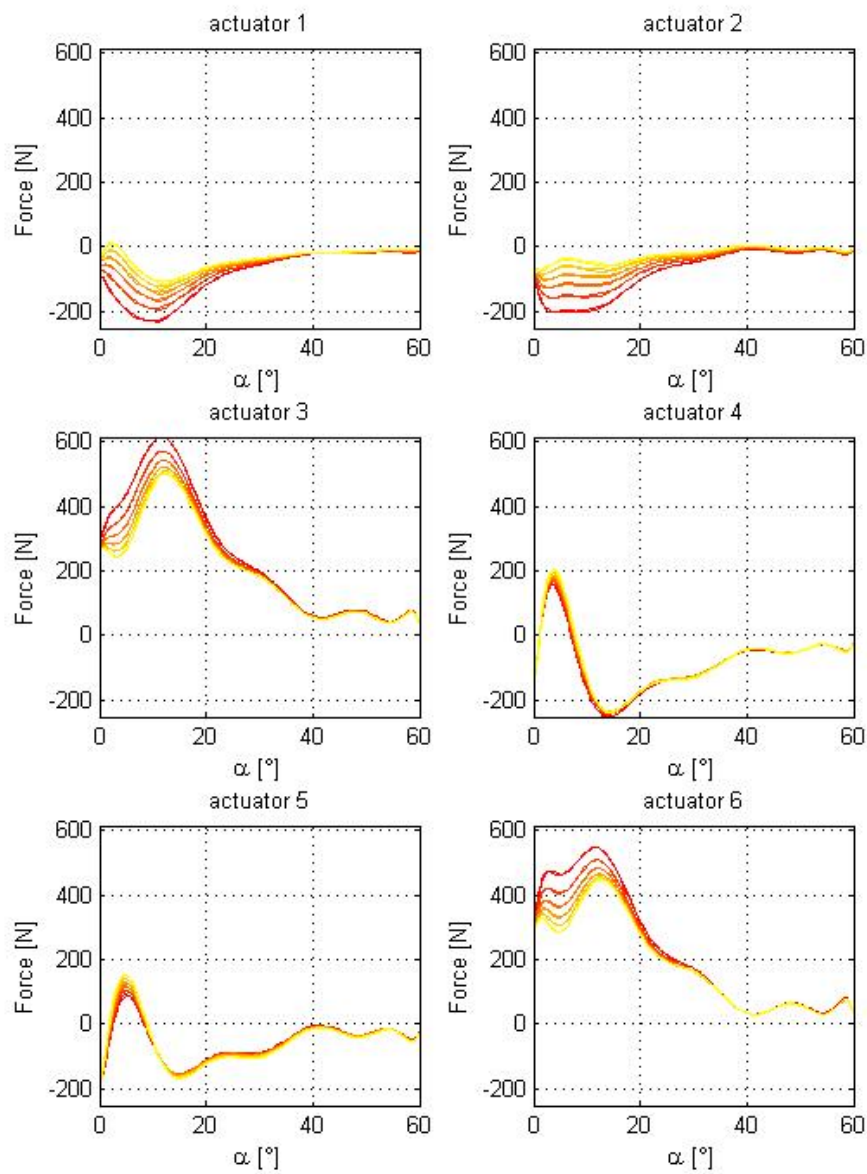


Figure A3.8 Trend of the forces required during walking B at the actuators of the 6-6 Gough-Stewart architecture as a function of the flexion angle  $\alpha$  at various diameter of the base: smallest diameters in red color, larger diameters in yellow.

## FORCES REQUIRED AT THE DECOUPLED PLATFORM

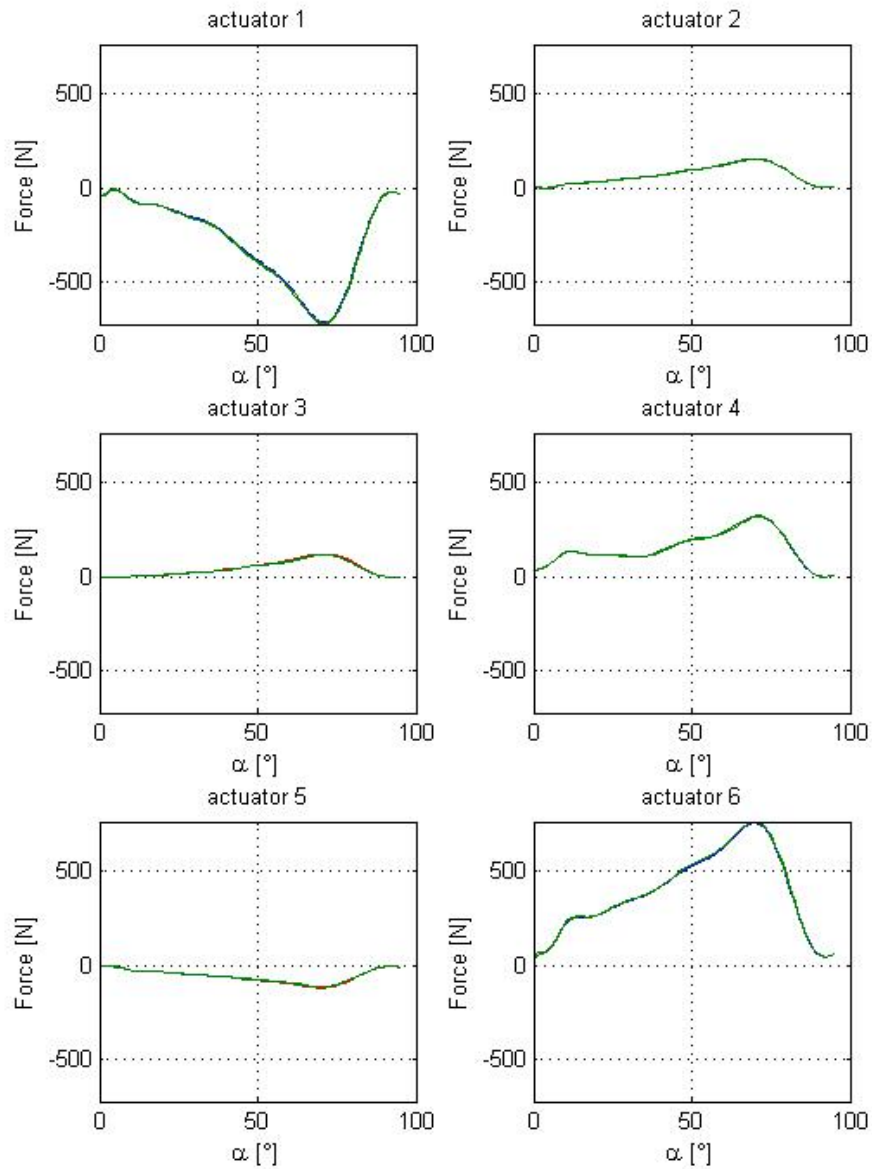


Figure A3.9 Trend of the forces required during sit to stand at the actuators of the decoupled architecture as a function of the flexion angle  $\alpha$ .

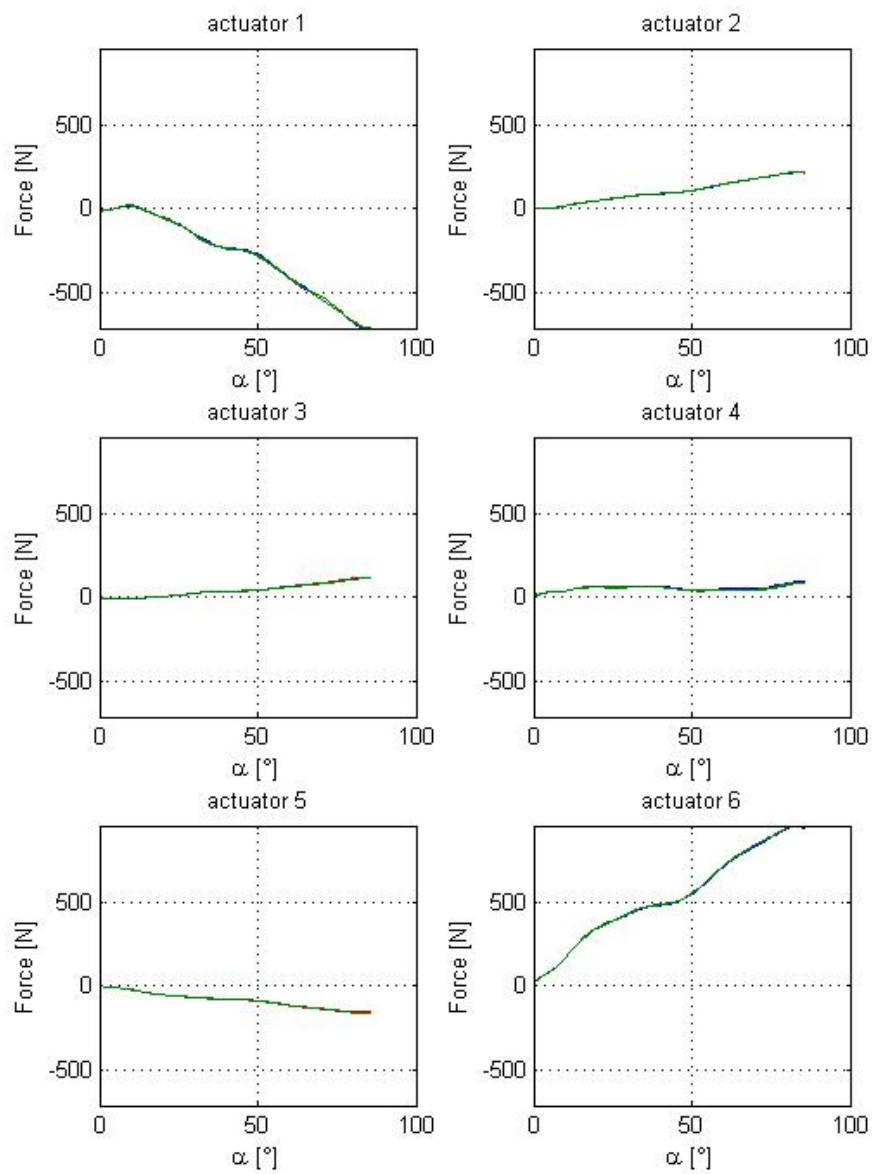


Figure A3.10 Trend of the forces required during squat at the actuators of the decoupled architecture as a function of the flexion angle  $\alpha$ .

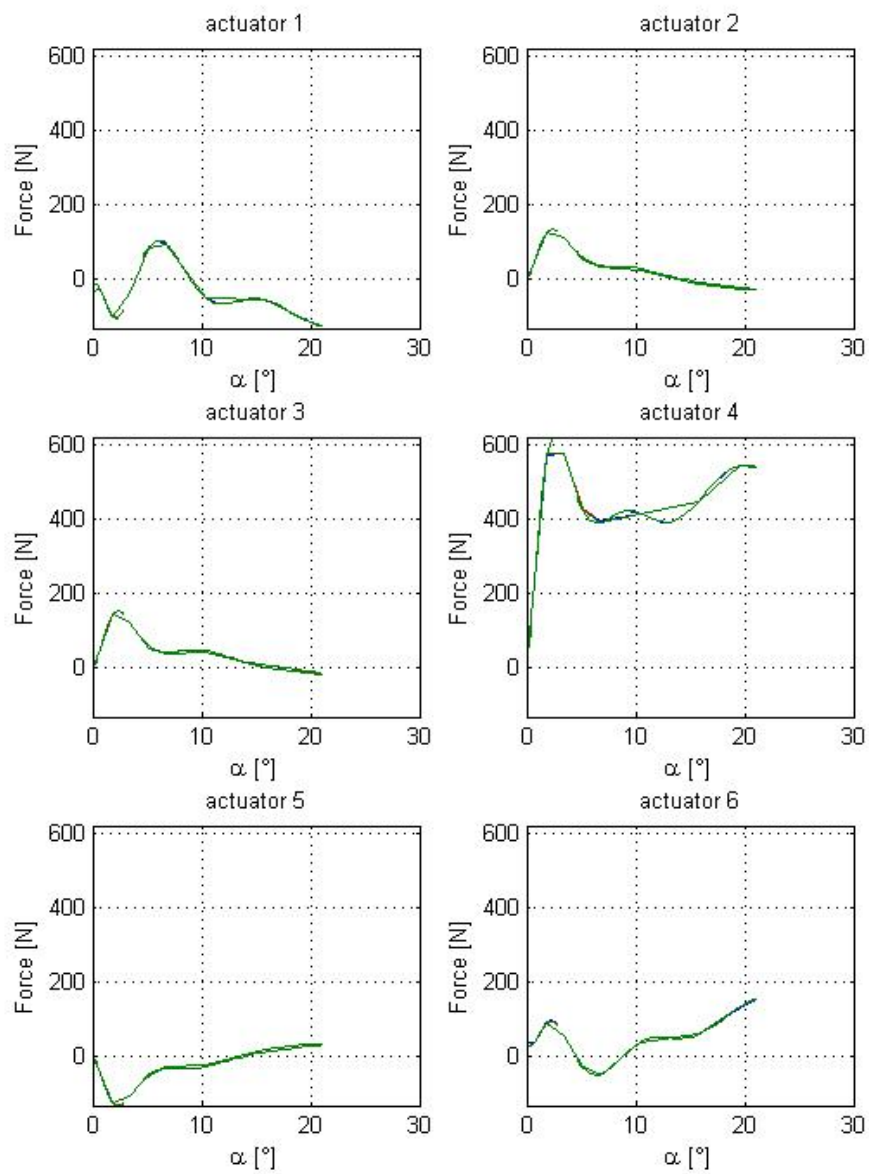


Figure A3.11 Trend of the forces required during walking A at the actuators of the decoupled architecture as a function of the flexion angle  $\alpha$ .

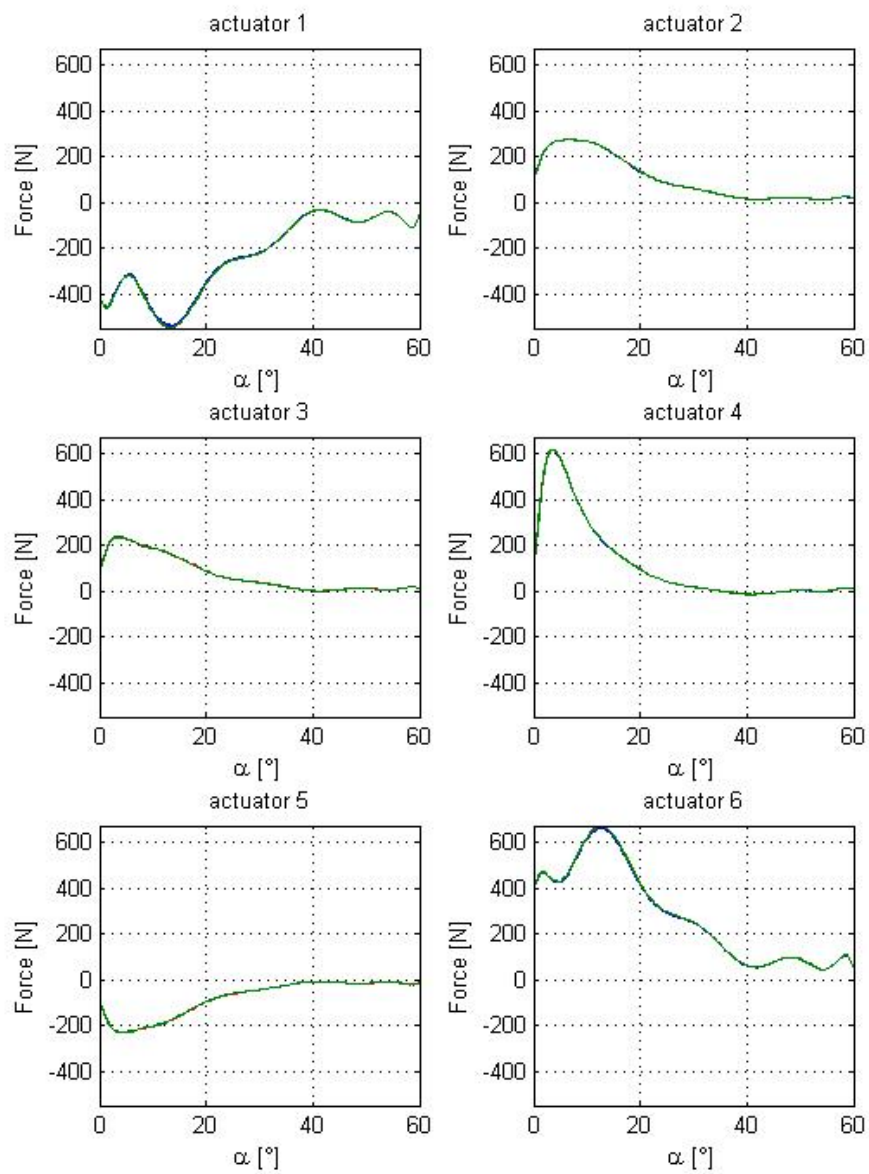


Figure A3.12 Trend of the forces required during walking B at the actuators of the decoupled architecture as a function of the flexion angle  $\alpha$ .